

# NASA Conference Publication 2043

## STRATCOM VIII

(NASA-CP-2043) STRATCOM 8 DATA WORKSHOP AND  
SUPPLEMENT (NASA) 137 p HC A07/MF A01  
CSSL 04A

N79-23461  
THRU  
N79-23475  
Unclas

G3/42 -25359

**Data Workshop April 13-14, 1978**

**Compiled by**

**Edith I. Reed**



**NASA**  
National Aeronautics and  
Space Administration

Conference Publicat  
CP-2043

STRATCOM-VIII

Data Workshop

April 13-14, 1978

Compiled by

Edith I. Reed

Stratospheric Physics and Chemistry Branch  
NASA/Goddard Space Flight Center  
Greenbelt, Maryland 20771

April 1978

## TABLE OF CONTENTS

ABSTRACT. . . . .	1
INTRODUCTION . . . . .	2
Table 1. Platforms . . . . .	4
Table 2. Parameters to be observed . . . . .	5
Table 3. Instruments and systems . . . . .	6
Table 4. Organizational acronyms . . . . .	10
INDIVIDUAL REPORTS	
Stratospheric Composition Balloon, Aircraft and Rocket- Borne Experiments . . . . .	12
Summary of System State-of-Health Measurements . . . . .	24
Air Temperature Measurement . . . . .	32
Air Pressure Measurement . . . . .	36
Ozone Measurements . . . . .	40
Electrochemical Concentration Cell Ozonesonde . . . . .	44
Measurement of the Ozone Profile in Support of STRATCOM-VIII . . . . .	49
Measurement of 200-400 nm Solar UV Fluxes on the STRATCOM-VIII Balloon Flight . . . . .	56
Measurement of Ultraviolet Fluxes . . . . .	63
Measurements of Solar UV Flux in the Stratosphere . . . . .	64
Measurements of Radiative Energy Transfer . . . . .	68
Apex Plate Payload . . . . .	75
Measurement of Infra-red Spectra, Nitrogen Oxides and Aerosols . . . . .	90
Measurement of D-region Electron Density by Partial Reflections . . . . .	91
Electrical Conductivity Measurements from the STRATCOM-VIII Experiment . . . . .	96
Electrical Structure & Ionizable Constituent Measurements. . .	103

## STRATCOM-VIII Data Workshop

### ABSTRACT

The STRATCOM-VIII effort took place at Holloman Air Force Base and White Sands Missile Range, New Mexico, on September 28-30, 1977. The prime emphasis was on the study of stratospheric photochemistry involving ozone, with secondary objectives including a study of the balloon environment, comparison of independent techniques for the measurement of  $O_3$  and NO, and the development of new sensor systems. More than forty sensors were included on the two large balloons, a U-2 aircraft, and several rockets and small balloons, in addition to meteorological balloons and rockets. Most of the systems performed as expected. This report consists of material available at a Data Workshop held April 13-14, 1978, and serves both to distribute information among the experimenters and to give some indication as to the extent to which the original objectives can be realized.

## INTRODUCTION

Although the stratosphere has been studied for a number of years, interest in that region has recently intensified. Man's activities on the surface of the earth and in the stratosphere itself may result in long-term changes in the stratosphere, which, in turn, may have an effect at the earth's surface. The problems are varied and may be posed in terms of aerosol content, carbon dioxide content, or NO and chlorine content, but the real concern is about any resultant changes in the ozone content and the temperature profiles.

Because of the great variability in the distribution of many of the trace species in the stratosphere, and our less-than-complete understanding of the photochemistry and transport, a definitive and detailed characterization of the stratosphere has proven difficult. One of the several possible approaches to this problem is to obtain vertical profiles of many parameters simultaneously at a particular place. From an engineering and operational viewpoint this is a difficult task. However, it was partly for the purpose of finding ways of overcoming such difficulties that the STRATCOM (STRATospheric COMposition) series of operations has been established.

The STRATCOM program has been a long-term multipurpose program for integrated and correlated measurements of stratospheric parameters related to composition, thermodynamics, and radiative balance. The emphasis has been on balloon-borne sensors, both in-situ and remote. The number of parameters for which flight-proven systems are available has increased over the years so that for the 1977 effort it was possible to include sensors for a broad spectrum of trace species and related parameters. As a major step in evaluating currently available ozone data and systems, sensors for the detection of ozone by several in situ and several remote techniques were included. A number of other related instruments were included consistent with the secondary objectives of instrument development and definition of features of the balloon environment.

The current effort, the eighth in the STRATCOM series, was held on September 28-30, 1977, at the Holloman Air Force Base (HAFB) and the White Sands Missile Range (WSMR) in New Mexico. It was managed by Dr. Harold N. Ballard of the Atmospheric Sciences Laboratory at WSMR with the assistance of Dr. Frank P. Hudson (now with Department of Energy, Headquarters, and with the cooperation of NASA's Upper Atmospheric Research Program. The effort included the flight of two large balloons, one dedicated mostly to an infrared solar absorption spectrometer and the second for a number of in situ and ultraviolet instruments. Three packages were dropped by parachute from the largest balloon. The U-2 aircraft with an infrared spectrometer and aerosol samplers made two flights in the vicinity. In addition, a number of small rocket and balloon-borne systems were flown.

By mid-February, all experimenters had received telemetry data and radar trajectories for their sensors. By the time of this Workshop, mid-April, it is anticipated that all experimenters will be able to describe the extent of their data and to note anomalies; some may even have completed the data reduction to the point of having final data in geophysical units.

The purpose of the Workshop is to enable experimenters to exchange information: to note which anomalies are peculiar to a single sensor and which are observed by several sensors. The fundamental data from meteorological sondes and from on-board temperature and pressure sensors are included. Experimenters are encouraged to make use of all the available data in the interpretation of the results.

This report includes an outline of the instrument complement for each of the platforms, both in terms of the instrument, the experimenter and his organization, and in terms of the parameters to be measured. A more complete discussion of the overall objectives of the STRATCOM-VIII effort and of the objectives of each experimenter are found in the report "STRATCOM-VIII Scientific Objectives and Mission Organization: (GSFC X-624-77-261, Edith Reed, October 1977, 104 pp.). Each experimenter was asked to provide camera-ready copy regarding his results so that they could be distributed to the participants and to other interested people. This report represents the result of that request and includes the copy as provided, adding only page numbers and these introductory materials.

In view of the preliminary nature of many of these sets of data, this Conference Publication should not be referenced as a source of such data without the express permission of the experimenter. Those desiring to make use of these data should contact the responsible experimenter directly.

Table 1. Platforms

Balloon VIII-a (in-situ and remote sensors)	21.7x10 <sup>6</sup> ft <sup>3</sup>
Parachute drops from Balloon VIII-a (three)	
Balloon VIII-b (remote sensors)	11.6x10 <sup>6</sup> ft <sup>3</sup>
U-2 Aircraft (remote and in-situ sensors)	
Rocket flights (four different payloads)	
Meteorological rocket flights (11)	
Meteorological balloon flights	
Rawinsondes (16)	
Ozonesondes (2 types)	
Ground measurements	
Meteorological	
Ozone	
Ionospheric	
Tracking and telemetry	

Parameter	Observation Point	Instrument/Agency
O <sub>3</sub> overburden	X	Balloon VIII-a
O <sub>3</sub> in-situ	X	Package temperatures San
H <sub>2</sub> O	X	Levelness indicator San
CO <sub>2</sub>	X	Magnetometers San
CO	X	UV filter photometer Pan
NO	X	UV spectrometer San/GSFC
NO <sub>2</sub>	X	UV spectr. skylight USU
HNO <sub>3</sub>	X	Filter photometers USU
N <sub>2</sub> O	X	UV filter photo. O <sub>3</sub> CSU/GSFC/Sen
N <sub>2</sub> O <sub>5</sub>	X	Chemilum. O <sub>3</sub> ASL
CFCl <sub>3</sub>	X	Dasibi O <sub>3</sub> GSFC
CF <sub>2</sub> Cl <sub>2</sub>	X	Cryogenic sampler NCAR
ClONO <sub>2</sub>	X	Gas chromatograph San/NCAR
CCl <sub>4</sub>	X	Water vapor-Al <sub>2</sub> O <sub>3</sub> Pan
CH <sub>3</sub> Cl	X	Air temp. thermistor ASL
CHCl <sub>3</sub> , CH <sub>3</sub> CCl <sub>3</sub>	X	Air pressure ASL
CH <sub>4</sub>	X	IR/visible pyranom. ASL
H <sub>2</sub>	X	Nikon camera UTEP/ASL
Sky flux	X	Blunt probe UTEP/Penn
Earth flux	X	Gerdien Condenser UTEP/Penn
Lyman alpha	X	Kr lamp Penn/UTEP
solar UV	X	Apex plate:
air temp.	X	Air temp. thermistor UTEP
air pressure	X	Balloon skin temp. UTEP
aerosols	X	Pyranometer ASL
conductivity,	X	Lyman-alpha UTEP
ion mobility,	X	Humidity, resistance UTEP
attitude	X	Water vapor, Al <sub>2</sub> O <sub>3</sub> Pan
status param.	X	Parachute drops:
	X	Chemiluminescent NO USU
	X	Chemiluminescent O <sub>3</sub> ASL
	X	Filter photometers USU
	X	Kr lamp Gerdien Penn
	X	Water vapor, Al <sub>2</sub> O <sub>3</sub> Pan
	X	Balloon VIII-b
	X	IR spectrometer UDen
	X	IR radiometers UDen/ASL/AFGL
	X	U-2 aircraft: ARC
	X	IR spectrometer UDen
	X	Aerosol collector ARC
	X	SAS-II ARC
	X	Rockets:
	X	UV filter photo. O <sub>3</sub> CSU/GSFC/Sen
	X	Chemiluminescent O <sub>3</sub> ASL
	X	Gerdien UTEP
	X	Blunt probe UTEP
	X	Small balloons:
	X	MAST O <sub>3</sub> ASL
	X	ECC O <sub>3</sub> WFC
	X	Ground:
	X	Dobson O <sub>3</sub> ASL
	X	Partial refl. ionos. ASL
	X	C-3 ionosonde ASL
	X	UV filter photo. O <sub>3</sub> Sen

Table 2. Parameters to be observed.



Table 3. Instruments and Systems

<u>Platform</u>	<u>Instrument/System</u>	<u>Person</u>	<u>Organization</u>
VIII-a Basic System	Balloon Design Flight Control	Arthur Korn, Code LCB Duke Gildenberg	AFGL AFGL/HAFB
	Balloon Launch support	Joseph Koehly	AFGL/HAFB
	Mechanical structure	Hector Carrasco Gustavo Cordova John Whitacre	UTEP
	Payload integration	Miguel Izquierdo Svi Salpeter Preston Herrington	UTEP Sandia
	Control and telemetry	Miguel Izquierdo Preston Herrington	UTEP Sandia
	Power Supply	Claude Tate	ASL
	State of Health Instruments Package temperatures Levelness indicator Magnetometers Other payload monitors	Preston Herrington	Sandia
	Experiments	UV filter photometer	Bach Sellers
UV spectrometer		Bernard Zak James Mentall, Code 624	Sandia NASA/GSFC
UV spectrometer (skylight)		Rex Megill K. D. Baker Larry Jensen Jagir Randhawa	USU ASL
Filter photometers (2)		Rex Megill	USU
UV filter photometer ozone sonde		Arlin Krueger David Wright, Code 912 Peter Simeth	CSU NASA/GSFC SenTran
Chemiluminescent ozone sonde (2)		Jagir Randhawa	ASL

<u>Platform</u>	<u>Instrument/System</u>	<u>Person</u>	
	Dasibi ozone monitor	John Ainsworth,	Code 62
	Cryogenic sampler	Richard Lueb Leroy Heidt	
	Gas chromatograph	Robert Woods Leroy Heidt Richard Lueb	Sandia NCAR
	Water vapor sensors( $Al_2O_3$ )	Philip Goodman	Pan
	Air temperature sensors	Harold Ballard	ASL
	Air pressure sensors	Harold Ballard	ASL
	IR Pyranometer (nadir)	Robert Rubio	ASL
	Visible Pyranometer (nadir)	Robert Rubio	ASL
	Nikon camera (nadir)	Robert Rubio Claude Tate	ASL
	Blunt Probe	Jack Mitchell	UTEP
	Kr Lamp	Les Hale	Penn
	Gerdien Condenser		
	Wind Anemometer	Carlos McDonald	UTEP
	Apex plate payload:	Carlos McDonald	UTEP
	Air Temperature sensor		
	Balloon skin temperature		
	Pyranometer, IR and visible	Robert Rubio	
	Lyman-alpha intensity		
	Levelness indicator		
	Humidity sensor		
	Water vapor sensor ( $Al_2O_3$ )	Philip Goodman	
	Parachute drop no. 1	Rex Megill	
	Chemiluminescent NO sonde	Alan Shaw	
	Filter photometers, $O_3$ and albedo	Rex Megill	
	Chemiluminescent ozone detector	Jagir Randhawa	
	Parachute drop no. 2:		
	Krypton lamp-Gerdien Condenser	Leslie Hale Charles Croskey	Penn
	Parachute drop no. 3:		
	$Al_2O_3$ water vapor sensor	Philip Goodman	Pan

<u>Platform</u>	<u>Instrument/System</u>	<u>Person</u>	<u>Organization</u>
VIII-b	IR spectrometer	David Murcraý John Williams	U. Denver
	IR radiometers(air temp)	David Murcraý Don Snider Robert McClatchey	U. Denver ASL AFGL
	Air temperature sensors	Harold Ballard	ASL
	Structure, telemetry, integration, power	David Murcraý	U. Denver
U-2 Aircraft	Senior contact	Leo Poppoff	NASA/ARC
	IR spectrometer	David Murcraý	U. Denver
	Aerosol impact collector	Neil Farlow Guy Ferry Ken Snetsinger	NASA/ARC
	SAS-II (NO, NO <sub>2</sub> , O <sub>3</sub> )	Max Loewenstein Walter Starr	NASA/ARC
Super Loki rocket	UV filter photometer ozone sonde	Arlin Krueger David Wright Charles Manion	CSU NASA/GSFC NASA/WFC
Arcas rocket	Chemiluminescent ozone sonde	Jagir Randhawa	ASL
Arcas rocket	Gerdien condenser	Jack Mitchell	UTEP
Super Loki rocket	Blunt probe	Jack Mitchell	UTEP
Data sonde rocket	Meteorological data	Stan Kubinski	ASL
Radiosonde balloon	Meteorological data	Stan Kubinski	ASL
Small balloon	MAST ozone sonde	Jagir Randhawa	ASL
Small balloon	ECC ozone sonde	Charles Manion	NASA/WFC
Ground	Dobson ozone spectrophotometer	Jagir Randhawa	ASL
	Filter UV photometer	Peter Simeth	SenTran
	Pyrometer-visible	Robert Rubio	ASL
	Partial reflection ionosonde C-3 Ionosonde	Robert Olsen	ASL

<u>Platform</u>	<u>Instrument/System</u>	<u>Person</u>	<u>Organization</u>
	Meteorology, forecasting	Duke Gildenberg	AFGL/HAFB
	Meteorology, post flight analysis	John Bujnach	UST
	Tracking	Alton Duff Tillman Powell	ASL
	Data acquisition and reduction	Miguel Izquierdo Edward Avila George Holmack	UTEP WSMR
	Missile Range support	Robert Jones Leland Robertson	WSMR ASL
	Photochemical modeling	Frank Hudson Jose Serna	DOE PSL
	Model, balloon environment	Richard Davis, M/S 474	NASA/LaRC
	Scientific publications	Edith Reed, Code 624	NASA/GSFC
	Overall management	Harold Ballard	ASL

Table 4. Organizational Acronyms

AFGL	Air Force Geophysics Laboratory Hanscom Air Force Base, Massachusetts 01731
AFGL/HAFB	Detachment 1, Balloon Branch Air Force Geophysics Laboratory (AFCS) Holloman Air Force Base, New Mexico 88330
ASE	Atmospheric Sciences Laboratory US Army Electronics Command White Sands Missile Range, New Mexico 88002
CSU	Department of Atmospheric Sciences Colorado State University Fort Collins, Colorado 80523
DOE	Environmental Research Department of Energy Washington, D. C. 20545
NASA/ARC	Space Sciences Division Ames Research Center Moffett Field, California 94035
NASA/GSFC	Goddard Space Flight Center Greenbelt, Maryland 20771
NASA/LaRC	Langley Research Center Hampton, Virginia 23665
NASA/WFC	DO-PMOB-PMS (ASRP) Wallops Flight Center Wallops Island, Virginia 23337
NCAR	National Center for Atmospheric Research P. O. Box 3000 Boulder, Colorado 80303
Pan	Panametrics, Inc. 221 Crescent Street Waltham, Massachusetts 02154
Penn	Ionosphere Research Laboratory Pennsylvania State University University Park, Pennsylvania 16802

PSL Physical Sciences Laboratory  
New Mexico State University  
Las Cruces, New Mexico 88001

Sandia Division 9226  
Sandia Laboratories  
Albuquerque, New Mexico 87115

SenTran SenTran Company  
2705 de la Vina Street  
Santa Barbara, California 93105

UDenver Department of Physics and Astronomy  
University of Denver  
Denver, Colorado 80208

UTEP Electrical Engineering Department  
University of Texas at El Paso  
El Paso, Texas 79968

UST Institute for Storm Research  
University of St. Thomas  
Houston, Texas 77006

USU Center for Research in Aeronomy  
Utah State University  
Logan, Utah 84322

WSMR White Sands Missile Range  
New Mexico 88002

D7  
N 79-23462

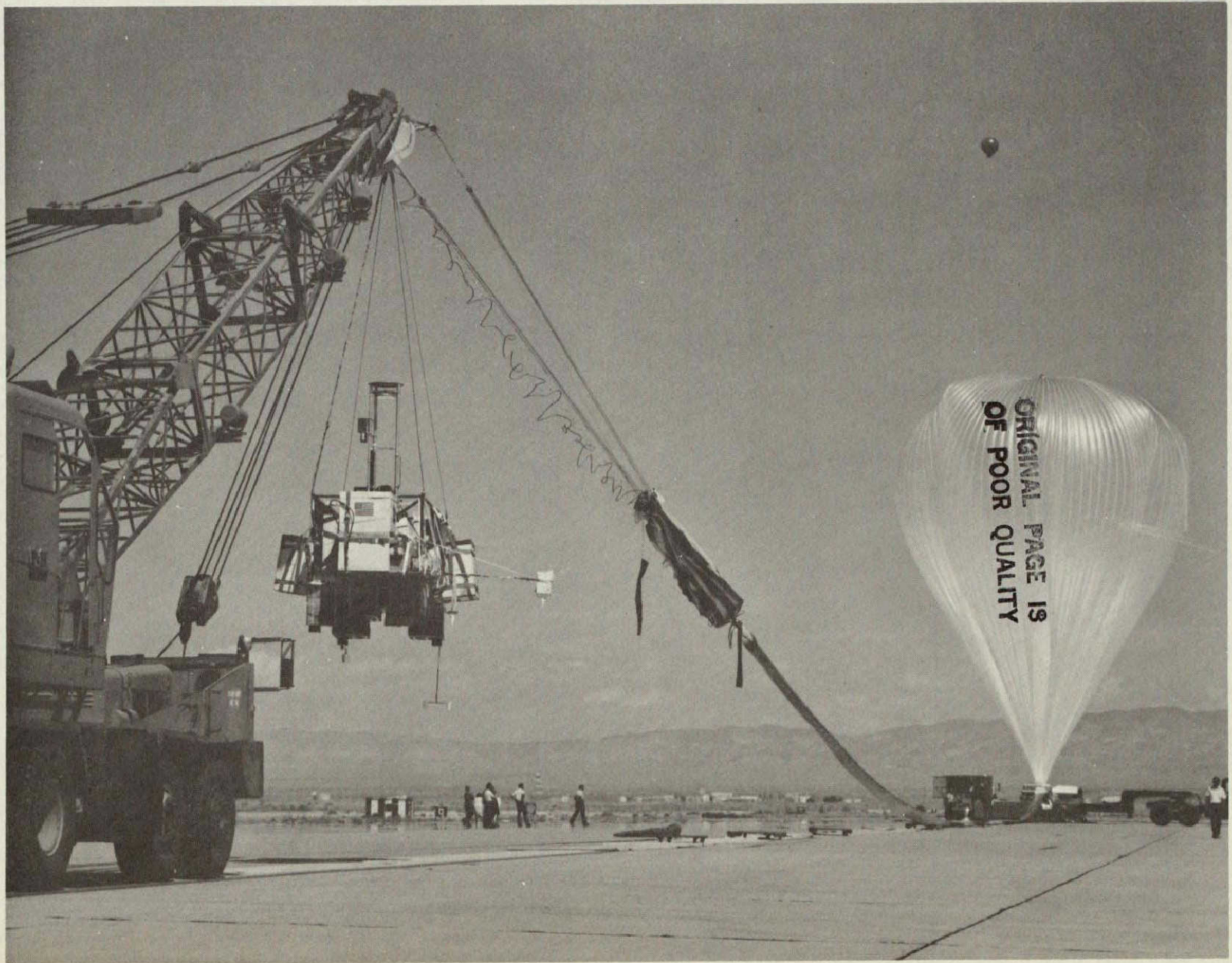
STRATOSPHERIC COMPOSITION BALLOON, AIRCRAFT AND ROCKET-BORNE  
EXPERIMENTS 28-30 September 1977

(SYSTEMS, INSTRUMENTS, TRAJECTORIES, SUPPORTING MEASUREMENTS)

Harold N. Ballard, USA Atmospheric Sciences Laboratory, WSMR, NM  
M. Izquierdo, EE Dept, University of Texas at El Paso, El Paso, TX  
A. Korn, Air Force Geophysics Laboratory, Bedford, MA  
D. Murcay, Physics Department, University of Denver, Denver, CO  
W. Page, NASA Ames Research Center, Moffett Field, CA

STRATCOM (STRATospheric COMposition) is a long term multi-purpose program for integrated, correlated measurements of stratospheric parameters related to composition, thermodynamics and radiative balance. The eighth experiment in the series, dating back to the first in 1968, was conducted in the period 28-30 September 1977. Balloon VIII-b ( $11.6 \times 10^6 \text{ft}^3$ ), carrying a solar-pointing grating infrared spectrometer, two  $\text{CO}_2$  thermal emission radiometers and two in-situ air temperature sensors was launched at 1251 MST on 28 September 1977 from Holloman AFB ( $32^\circ\text{N}$ ) to float at an altitude of 39 km from 1521 MST with the instruments making measurements at that altitude through the time of sunset at 1822 MST. Balloon VIII-a ( $21.6 \times 10^6 \text{ft}^3$ ) lifted a payload consisting of four UV filter photometers, two UV spectrometers, two chemiluminescent ozonesondes, dasibi ozone monitor, 14 tube cryogenic sampler, two aluminum oxide  $\text{H}_2\text{O}$  sensors, four air temperature sensors, atmospheric pressure sensor, infrared and visible pyranometers, downward-looking camera, blunt-krypton lamp-Gerdien condenser probe, three component anemometer, balloon apex-plate payload and three parachute-borne dropsondes. These dropsondes were for measurement of profiles of NO and  $\text{H}_2\text{O}$  after release from the balloon principal payload. It was launched at 0607 MST from Holloman AFB and reached a maximum altitude of 41 km near 0900 MST, with measurements being made by the various instruments from the time of launching, and subsequently in the 41-30 km interval until shortly after the time of sunrise (0540 MDT) on 30 September. The three dropsondes were released successfully in the 0815-0945 interval, 29 September. A NASA U-2 aircraft flew two missions near an altitude of 20 km, one on 28 September and one on 29 September, each one in support of the corresponding balloon-borne experiments. The U-2 carried an infrared spectrometer, NO,  $\text{O}_3$  sensor and aerosol impact collector. Radiosonde and rocketsonde measurements of winds, temperature and density were made daily in the period 22-30 September so as to study atmospheric transport phenomena in association with the balloon trajectories. MAST and ECC ozonesondes, chemiluminescent and filter photometer ozonesondes, blunt and Gerdien condenser probes and atmospheric temperature sensors were launched on small balloons and rockets on 29<sup>v</sup> and 30 September at the same times as measurements were being made by similar sensors aboard balloon VIII-a.

# STRATCOM VIII-B





I-477-57

EAST

GMD — ○ —

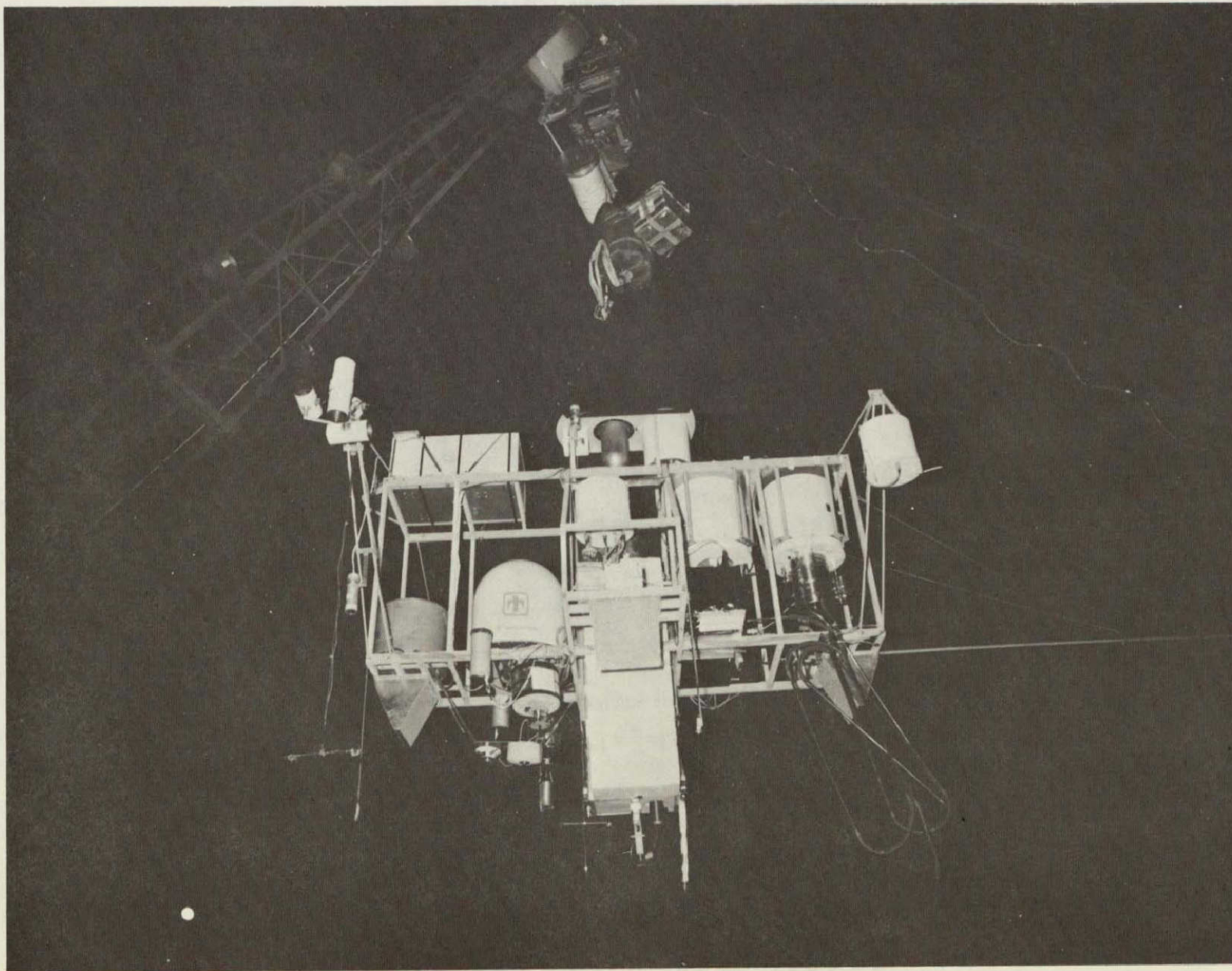
FAI — △ —

ARCFT — □ —

RADAR — \* —



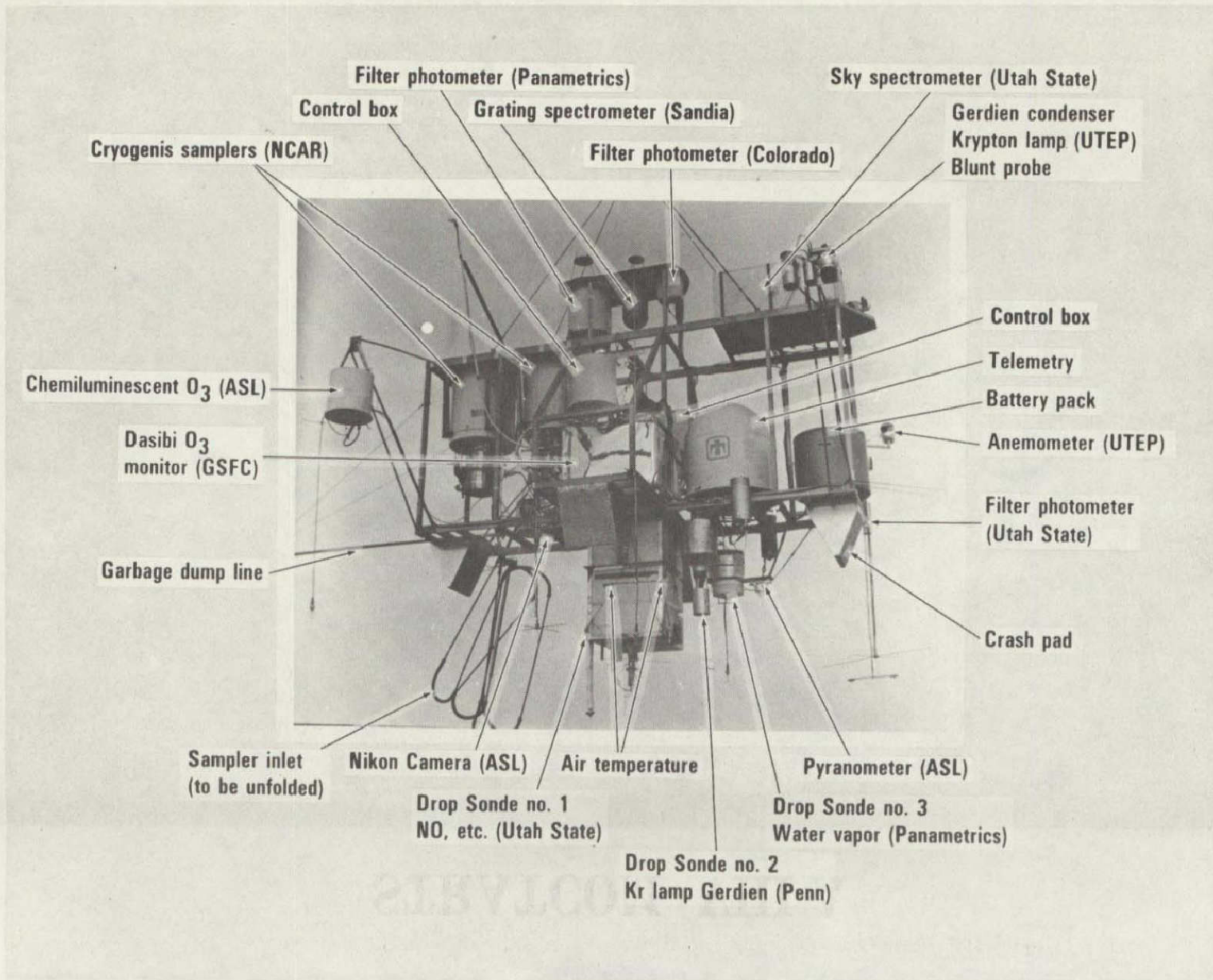
# STRATCOM VIII-A



-15-

ORIGINAL PAGE 19  
OF POOR QUALITY

# STRATCOM VIII-A INSTRUMENTS



-16-

ORIGINAL PAGE IS  
OF POOR QUALITY



STRATCOM VIII-A - APEX PLATE PACKAGE

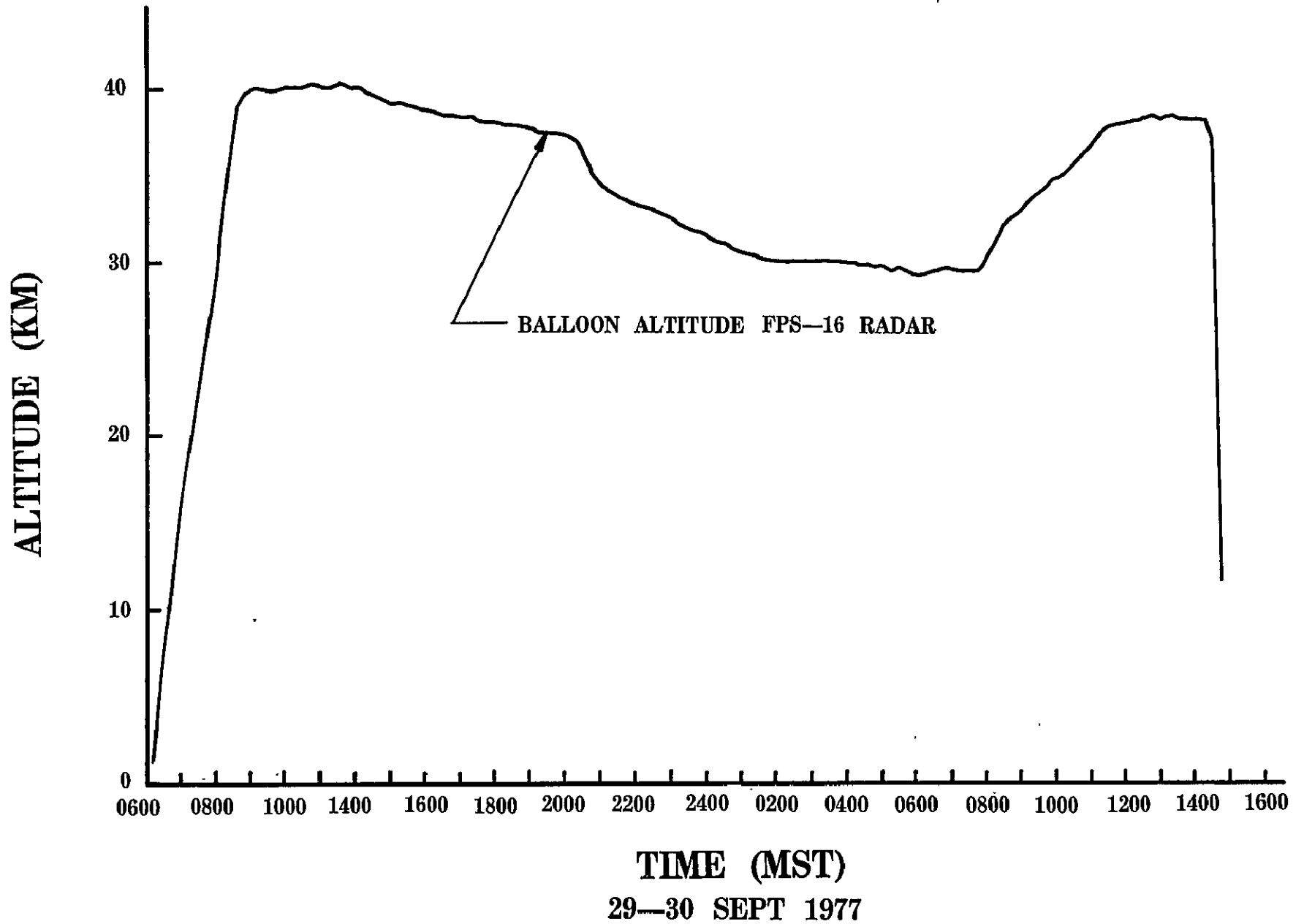
# STRATCOM BALLOON VIII—A HORIZONTAL TRAJECTORY



ORIGINAL PAGE IS  
OF POOR QUALITY

# STRATCOM VIII-A

-6T-



SUPPORTING MEASUREMENTS FOR STRATCOM VIII

<u>Platform</u>	<u>Time (MDT)</u>	<u>Date (1977)</u>	<u>Location</u>
Balloon radio sonde	0700	Sep 22	HAFB
Loki data sonde	1215*	" 22	SMR
Loki data sonde	1200*	" 23	SMR
Balloon radio sonde	0030	" 24	HAFB
Balloon radio sonde	0635	" 24	HAFB
Loki Data Sonde	1100*	" 24	SMR
Balloon radio sonde	0001	" 25	HAFB
Balloon radio sonde	0600	" 25	HAFB
Loki data sonde	1100*	" 25	SMR
Balloon radio sonde	0001	" 26	HAFB
Balloon radio sonde	0700	" 26	HAFB
Loki data sonde	1000*	" 26	SMR
Balloon radio sonde	1200	" 27	HAFB
Loki data sonde	1205*	" 27	SMR
Balloon radio sonde	0900	" 28	HAFB
Balloon radio sonde	1300	" 28	HAFB
Balloon VIII-b	1351	" 28	HAFB
Super-loki data sonde	1427*	" 28	SMR
U-2 aircraft in vicinity	1845	" 28	
Termination of Balloon VIII-b		" 28	
Balloon radio sonde	2100	" 28	HAFB
Balloon radio sonde	0200	" 29	HAFB
Mast ozone sonde	0230	" 29	SMR
Balloon radio sonde	0615	" 29	HAFB
Balloon VIII-a	0707	" 29	HAFB
Parachute drop no. 1 #	0915	" 29	
Parachute drop no. 2	0932	" 29	
ECC ozone sonde	1025	" 29	SMR
U-2 aircraft in vicinity	1045	" 29	
Parachute drop no. 3	1045	" 29	
Balloon radio sonde	1200	" 29	HAFB
ARCAS ozone sonde (ASL) #	1207*	" 29	SMR
Super-loki ROCOZ	1222*	" 29	SMR
Mast ozone sonde #	1230	" 29	SMR
Super-loki data sonde	1330	" 29	SMR
Super-loki blunt probe	1445*	" 29	SMR
ARCAS Gerdien condenser #	1519*	" 29	SMR
ARCAS ozone sonde (ASL)	1620*	" 29	SMR
Balloon radio sonde	1800	" 29	HAFB
Loki data sonde	2010*	" 29	SMR
Balloon radio sonde	0600	" 30	HAFB
Loki data sonde	0702*	" 30	SMR
Mast ozone sonde	0800	" 30	SMR
Loki data sonde	1200*	" 30	SMR
Termination of Balloon VIII-a	1330	" 30	

*NOTES:*

*\*A balloon radio.sonde was simultaneously launched at the SMR.*

*#Performance of vehicle or payload was seriously substandard,*

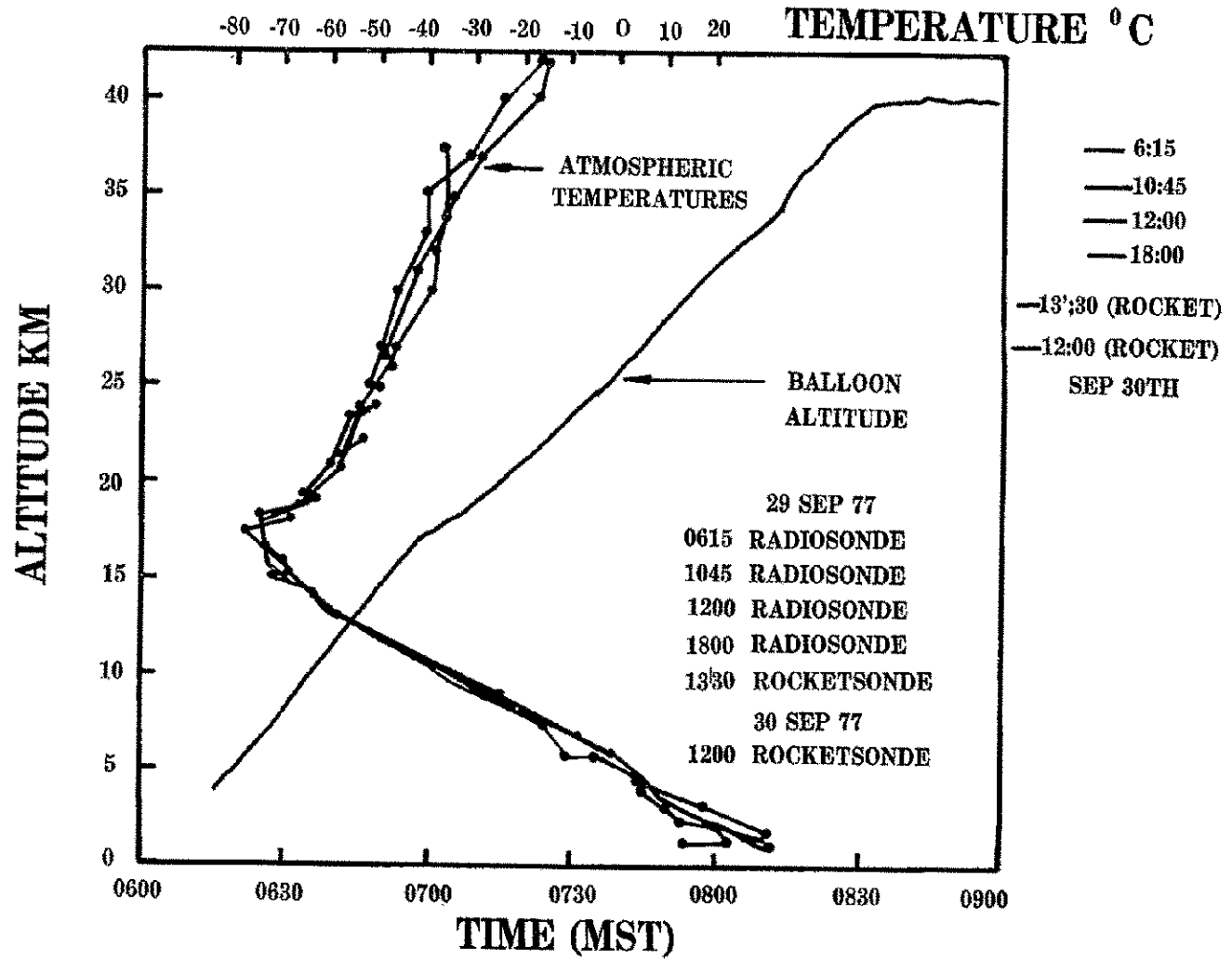
*HAFB - Holloman Air Force Base*

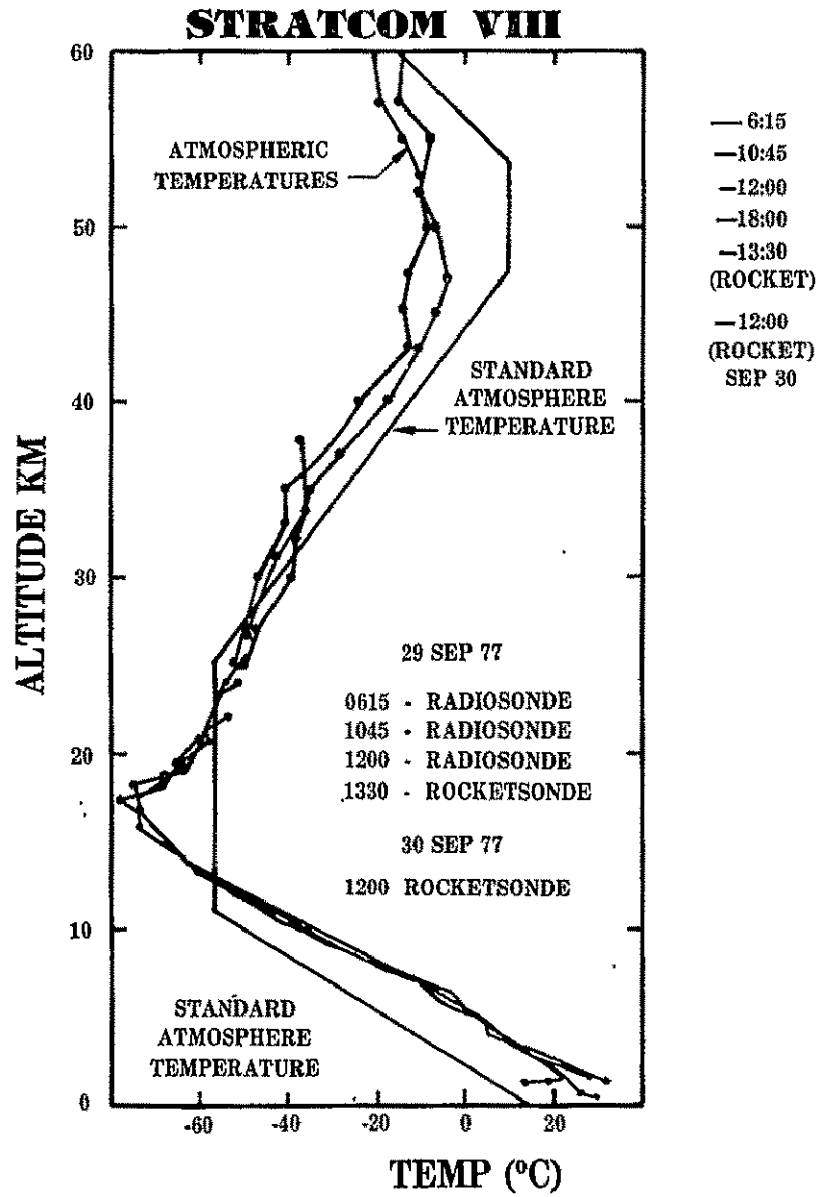
*SMR -- Small Missile Range*

*The balloon radio sondes and the Loki/Super-loki data sondes are for meteorological data.*



# STRATCOM VIII





SUMMARY OF SYSTEM STATE-OF-HEALTH MEASUREMENTS  
STRATCOM VIII-A Balloon Experiment

by

P. B. Herrington    Sandia Laboratories

Various measurements were made to determine the temperature and attitude of the gondola and the status of primary power and control equipment. Bead thermistors were used to measure temperatures at selected points throughout the gondola. A two-axis magnetometer and a two-axis pendulum were used to measure gondola attitude. Voltage and current measurements indicated the status of the primary power sources and associated power converters.

Temperature Measurements

Five temperature measurements were made in order to monitor system status. The locations of the thermistors were as follows:

<u>Sensor Number</u>	<u>Location</u>
1	TM Can (top)
2	TM can (near bottom)
3	UV Spectrometer (Inside can)
4	Battery #1 Container
5	Frame

All thermistors had an effective measurement range of  $-50^{\circ}\text{C}$  to  $+50^{\circ}\text{C}$ . Sensor Numbers 1 and 2 were located inside the main electronics housing (TM can) which was located on the gondola. The top and sides of the TM can (which was pressurized to 15 psia) were aluminum painted

on the outside surfaces with EPO-LUX No. 100 white epoxy paint.

Approximately 1-1/2 inch of styrofoam insulation was used around the inside of the top and sides of the can. The bottom of the TM can was alodyne (conductive chromate) aluminum which was approximately half covered with 1 inch styrofoam.

Sensor Number 3 was mounted inside the UV Spectrometer housing.

Sensor Number 4 was mounted inside the Battery #1 container which was mounted on the gondola. This container housed 18 Yardney LR-100 cells which were insulated from the walls of the container by 2-1/2 inches of styrofoam. All surfaces of the container were alodyne aluminum.

The Battery #1 container was heated (with heating tapes wrapped around the exterior) prior to launch to a sensor reading of 28°C. Very little power (700 milliwatts peak) was dissipated inside the battery container during the flight.

Sensor Number 5 was mounted to the instrument mounting frame (gondola).

Figure 1 shows the variation in frame temperature throughout the experiment. The minimum temperature recorded was -50°C, and the maximum temperature recorded was +35°C.

Figure 2 shows the variation in temperature inside the uv spectrometer housing. The maximum temperature measured was + 40°C. The minimum temperature measured was -50°C. However, -50°C was the minimum temperature which could be measured by the system and the actual minimum temperature may have been outside the effective measuring range of the thermistor.

The temperature inside the Battery #1 container varied from a maximum of 40°C to a minimum of 15°C.

The temperature inside the TM can varied from a maximum of 37.5°C to a minimum of 10°C.

#### ATTITUDE MEASUREMENTS

##### Pendulum

A two axis potentiometric pendulum was used to determine the levelness of the instrument frame.

The following table shows the initial offsets and changes which occurred

	X-AXIS offset in degrees	Y-AXIS offset in degrees
Launch	0.23	0.15
Drop #1 (0915)	0.55	0.60
Drop #2 (0932)	0.37	0.90
Drop #3 (1045)	0.24	Momentary change to 0.6
(2010-2300)	Varied linearly to 0.60	no change
Loss of power	0.60	.90

##### Magnetometers

Two Heliflux RAM-5C magnetometers were mounted orthogonally to determine the direction of pointing relative to magnetic north.

Attempts have been made on earlier experiments (STRATCOM V-VII) to correlate the gondola's rate of oscillation with rate of change of altitude. (In this discussion, a rotation is an oscillation, but the converse is not necessarily true.)

Figure 3 shows both the rate and magnitude of oscillations measured. These data were averaged over 30 minute periods. Comparing Figure 3 with the altitude trajectory can lead to the conclusion that the rate of altitude change affects both the magnitude and rate of oscillations. However, both magnitude and rate may change considerably with no apparent change in rate of ascent or descent. For example, consider the changes at approximately 1500.

During the early hours of September 30 (0130-0530), approximately 4 hours was required for a complete rotation.

The usefulness of this data is doubtful, but it continues to be interesting.

#### Power Supply Monitors

Primary power for the experiments was supplied by three battery packages. Battery Number 1 was made up of 18 Yardney LR-100 silver-zinc cells, and Battery Numbers 2 and 3 were made up of 18 Yardney LR-20 silver zinc cells. Each LR-100 cell has an average voltage of 1.5 volts and a capacity of 100 ampere-hours. Each LR-20 cell has an average voltage of 1.5 volts and a capacity of 20 ampere-hours.

The system 28-volt monitor shows that the voltage varied from 32 volts at launch to 24 volts at 0636 on September 30. The power failed shortly after 0636 because of inability to change battery packages by remote command.

## Other Monitors

The command receiver signal strength monitor, and two other monitors showed intermittent and unusual results fro periods of the experiment. Analysis of these results will continue.

Figure 1.  
Frame Temperature  
(Effective temperature ~~is~~ measurement  
range:  $-50^{\circ}\text{C}$  to  $+50^{\circ}\text{C}$ ).

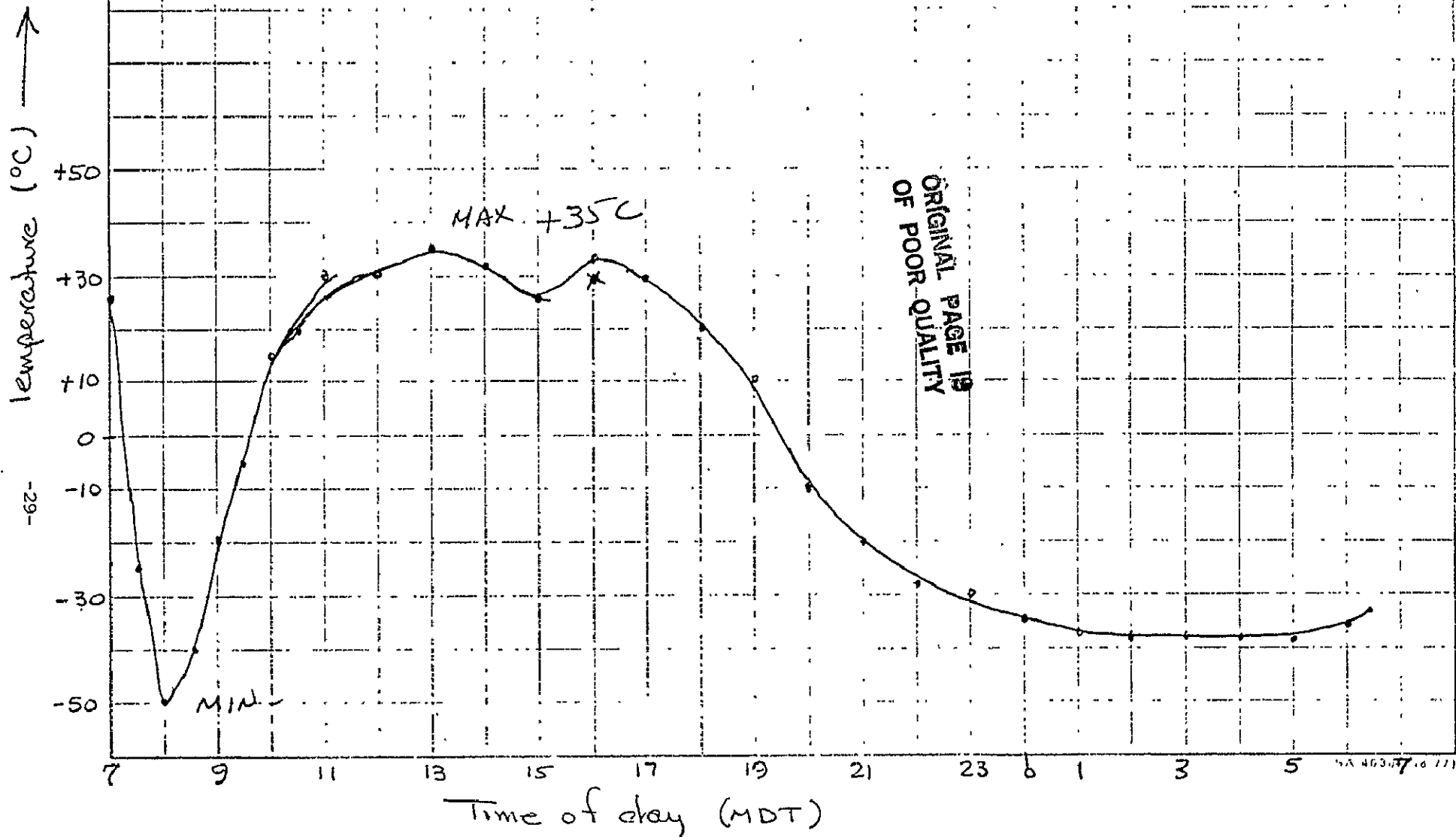
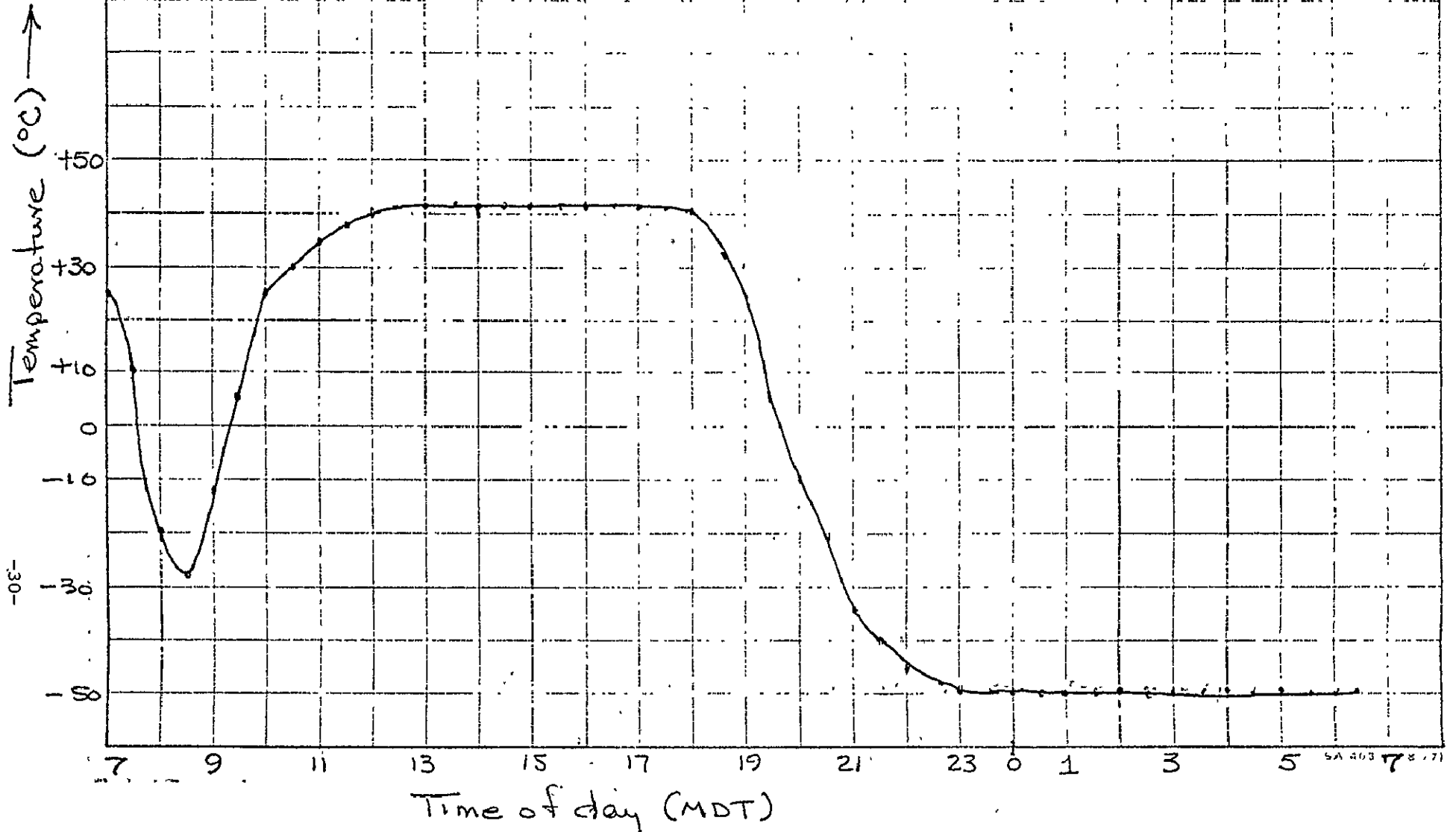


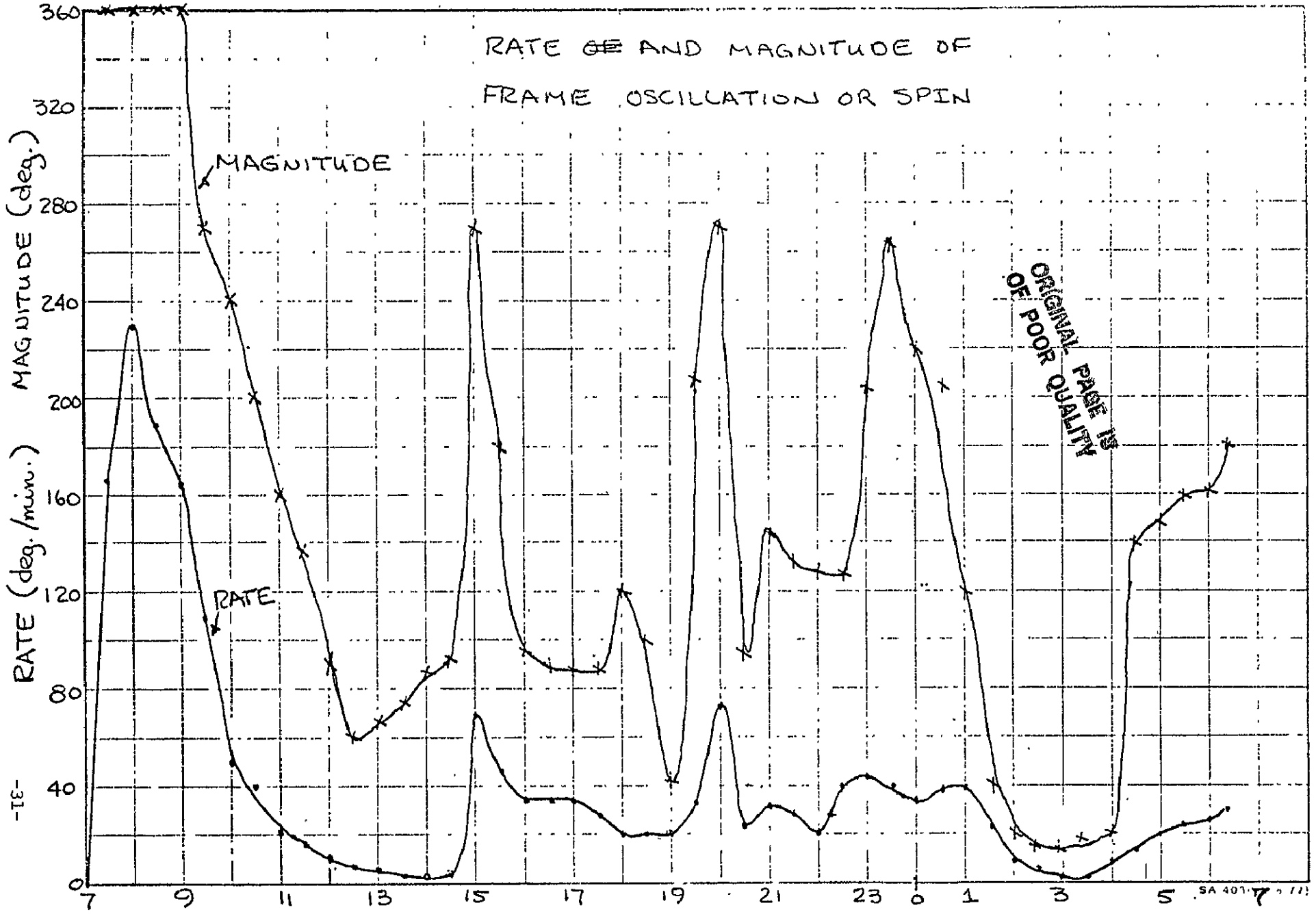


Figure 2.

UV Spectrometer Temperature  
(Effective temperature measurement,  
range:  $-50^{\circ}\text{C}$  to  $+50^{\circ}\text{C}$ )



RATE ~~OF~~ AND MAGNITUDE OF  
FRAME OSCILLATION OR SPIN



ORIGINAL PAGE IS  
OF POOR QUALITY

Air Temperature Sensor

Balloon VIII-a

Balloon VIII-b

## AIR TEMPERATURE MEASUREMENT

Harold N. Ballard, USA Atmospheric Sciences Laboratory, WSMR, NM

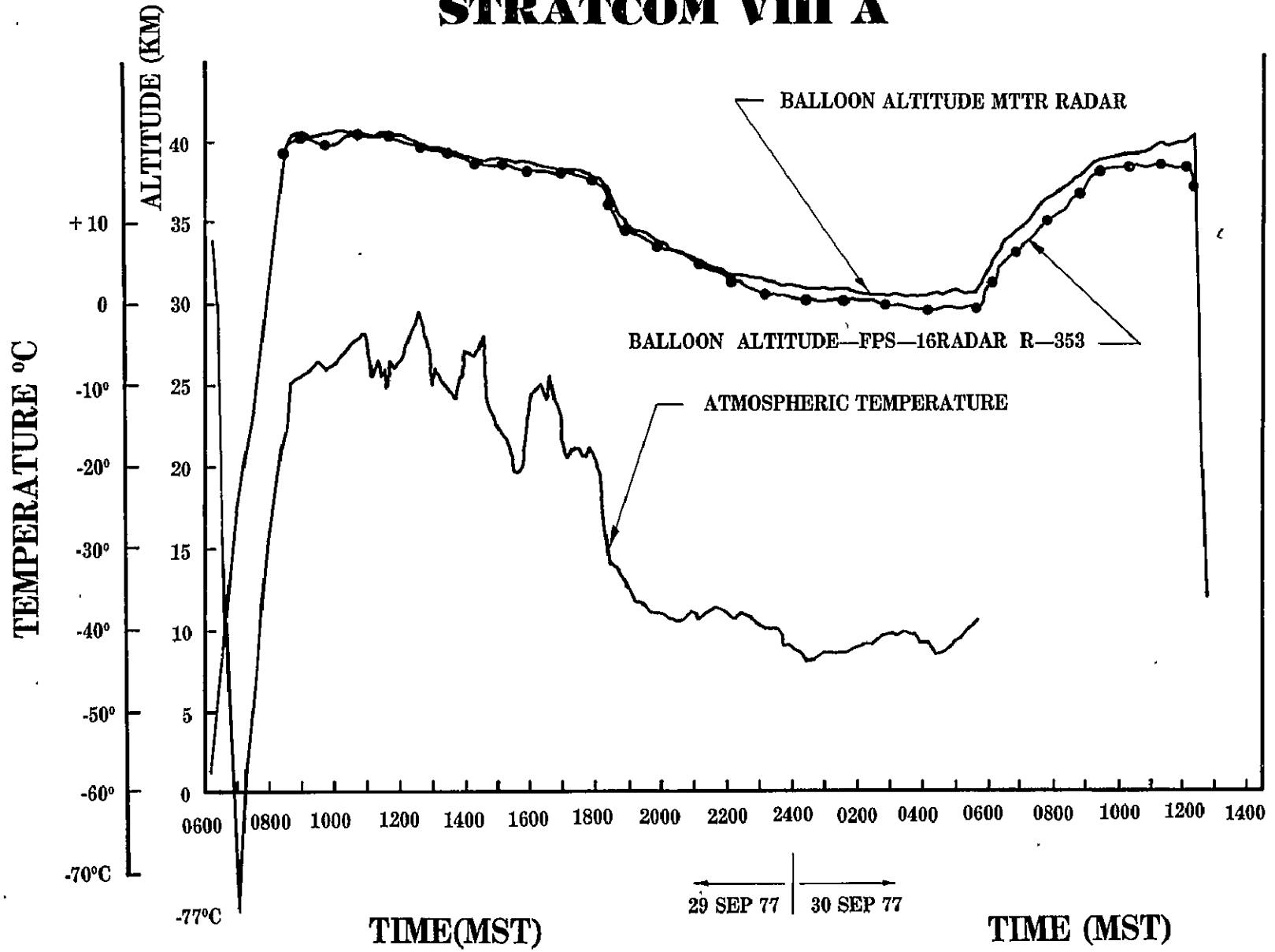
## INSTRUMENT

A coupled pair of identical film-mounted spherical bead thermistors serve as air temperature sensors aboard both Balloons VIII-a and VIII-b. The VIII-a payload will be reeled downward approximately 200 m beneath the balloon. The thermistor mounts are arranged in such a way so that when solar radiation is incident in a direction which is perpendicular to one film, then the direction of the incident solar ray is parallel to the second film. As the payload rotates during the flight (its rotation rate relative to the earth's magnetic field is sensed by a magnetometer), the temperature of each sensor will vary depending on the orientation of the film surfaces with respect to the sun. The maximum difference in the temperatures recorded by the two identical sensors is given an experimental determination of the maximum solar radiation correction to the two temperatures recorded by the film-mounted thermistors; the lesser of the two temperatures is taken to represent the atmospheric temperature (all other corrections being negligible). During the times of the flight when the thermistors and film mounts are totally shaded from directly incident solar radiation, and during the night, no correction need be applied to the recorded temperatures. Thus accurate ( $\pm 1^{\circ}\text{C}$ ) measurements of the atmospheric temperature can be made throughout the course of the flight without recourse to theoretical corrections to the observed temperatures.

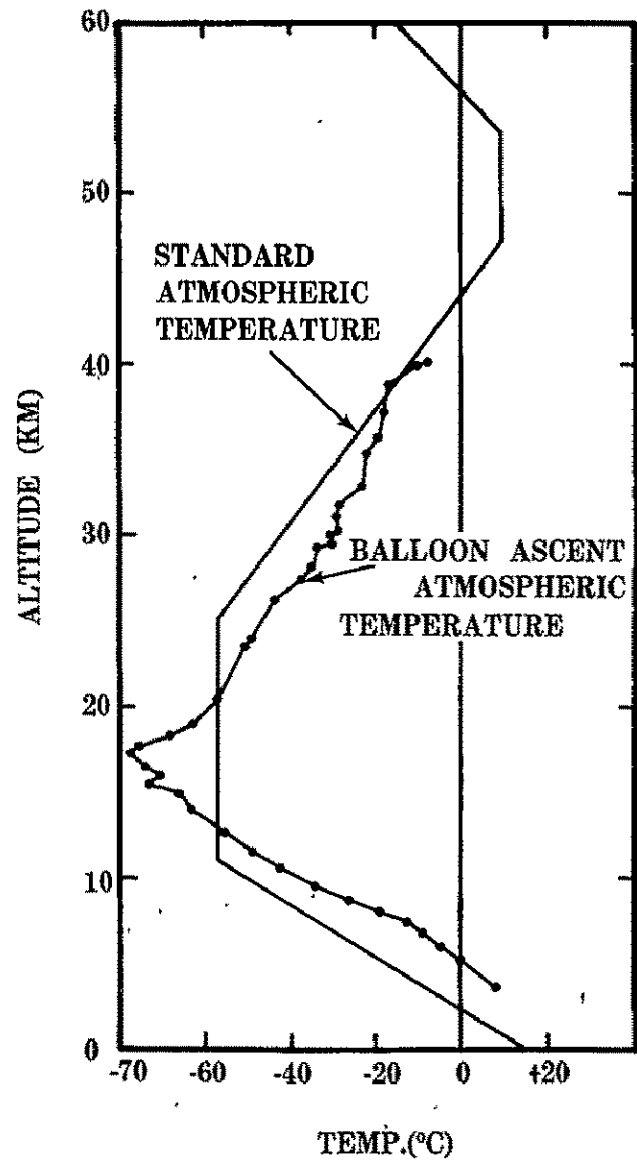
## OBJECTIVES

1. To measure the detailed temporal and spacial variations in the meteorological parameters of temperature, pressure, and density (derived) at times of darkness, sunrise, and daylight, the daylight variations to be related to the measured uv solar flux. Implicit in this objective is the determination of the diurnal tidal temperature variations at altitudes above 30 km.
2. To serve as a tool for obtaining detailed information concerning the balloon and payload behavior.
3. To provide background data for temperature-dependent experiments.

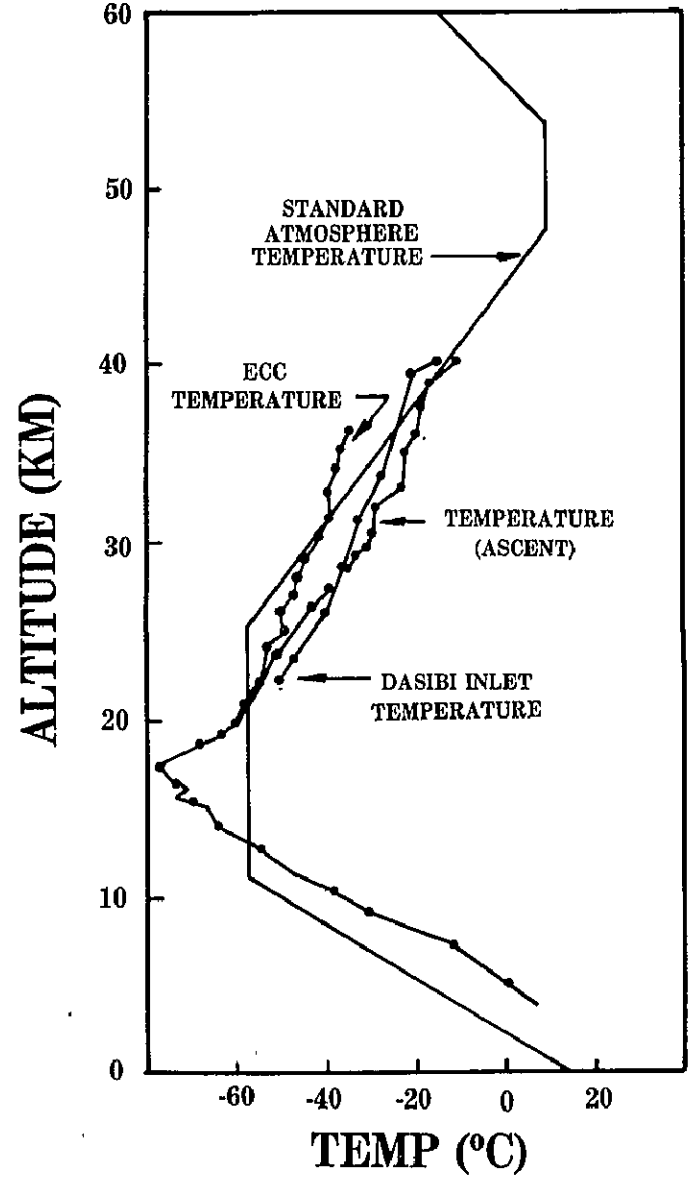
# STRATCOM VIII A



# STRATCOM VIII A



# STRATCOM VIII A



DA  
N79-23465

Air Pressure Sensor

Balloon

AIR PRESSURE MEASUREMENT

Harold N. Ballard, USA Atmospheric Sciences Laboratory, W:

INSTRUMENT

The pressure measurement is made by a Model 830J Rosemont sensor which utilizes the principle of a changing pressure to change correspondingly the capacitance of the pressure sensitive element. The sensor's range is stated to be from zero to 100 Torr (14 km); however, the sensor will not be activated until an altitude of 20 km (41 Torr) is reached during the balloon ascent. The resolution of the sensor is specified by the manufacturer as infinitesimal; however, associated electronic and pressure read-out systems limit the resolution to  $4.4 \times 10^{-2}$  Torr. Thus in the vicinity of an altitude of 30 km the pressure resolution corresponds to an altitude resolution of approximately 33 meters.

OBJECTIVE

To provide data for use in conjunction with the air temperature data for study of atmospheric structure.

# **STRATCOM VIII-A**

## **PRESSURE SENSOR**

**MANUFACTURER**

**ROSEMOUNT, INC.**

**MODEL**

**830J**

**METHOD**

**CAPACITIVE DIAPHRAGM**

**RANGE**

**0 to 100 mm Hg**

**RESPONSE TIME**

**0.25 SEC**

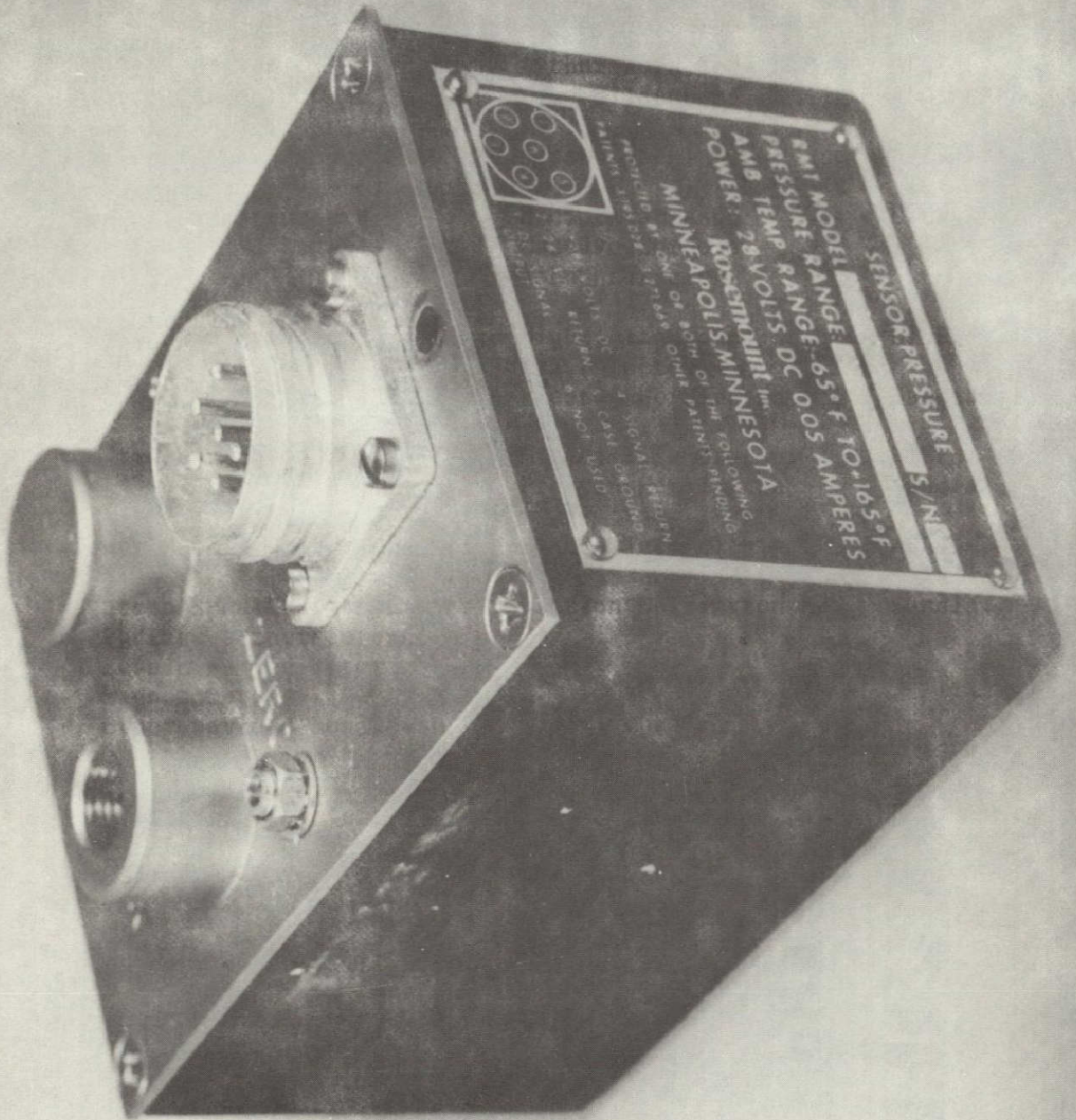
**TEMPERATURE COMPENSATED**

**-55 TO 70°C**

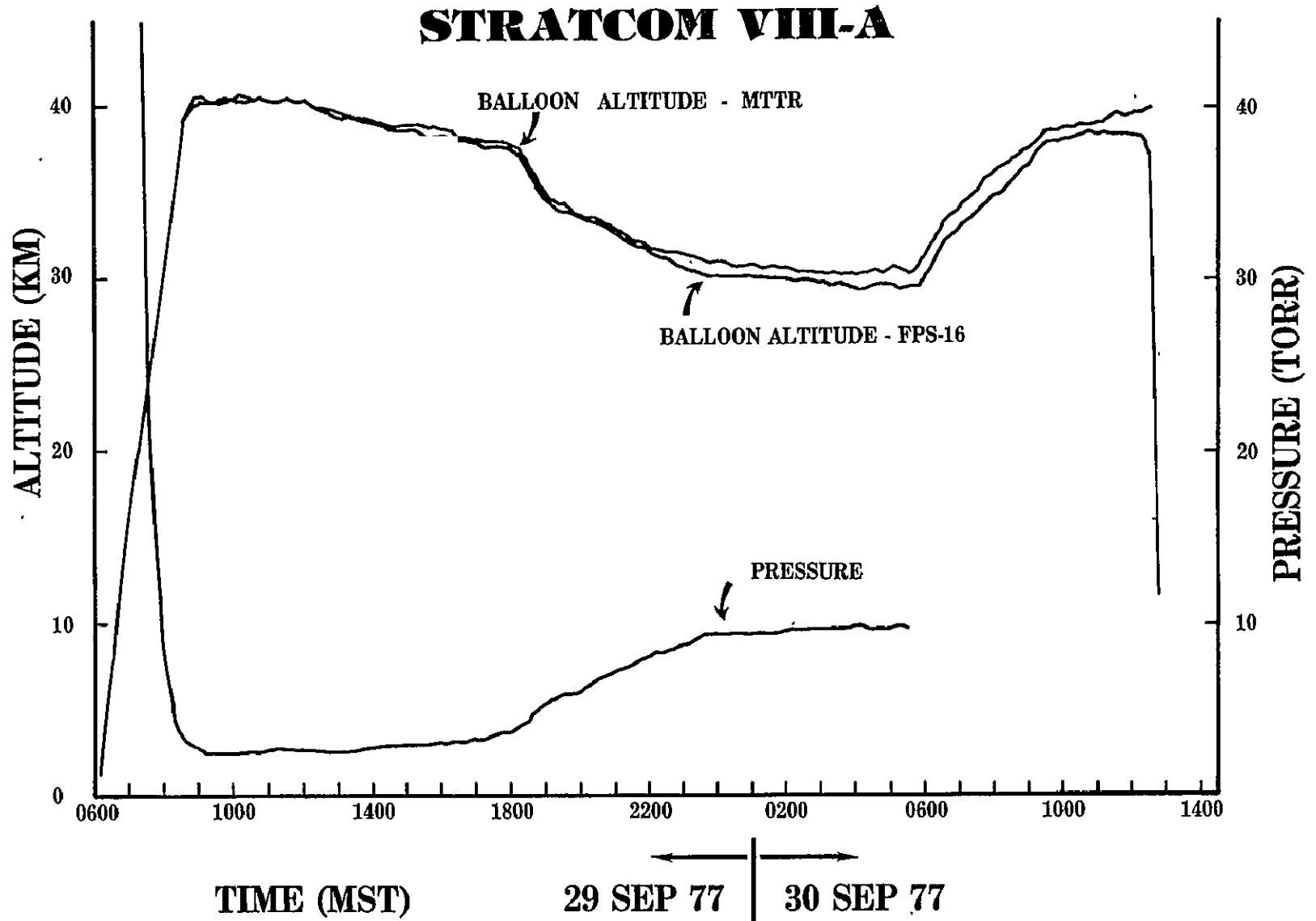
**EXPERIMENTAL ACCURACY**

**2.5%**





**ORIGINAL PAGE IS  
OF POOR QUALITY**



DB  
N79-23466

Chemiluminescent Ozonesonde

Balloon VIII-a  
Arcas Rocket Dropsonde  
MAST Balloonsonde  
Dobson Spectrophotometer

#### OZONE MEASUREMENTS

Jagir Randhawa, USA Atmospheric Sciences Laboratory, WSMR, NM

#### INSTRUMENTS

1. The chemiluminescent ozonesonde to be flown with the STRATCOM balloon flight consists of two main parts:

a. A constant-volume sampling pump made from TEFLON is used for the intake of the air sample. Sample is drawn at a rate of 200 millimeters per minute.

b. Ozone is detected by the chemiluminescent process (Rhodamine - B). Ozone molecules in the air sample flow over the detector and the photons produced by the destruction of ozone molecules on the chemiluminescent material are monitored by the photomultiplier tube, the output signal from which is transmitted to the ground receiver.

2. The instrument is calibrated under simulated flight conditions in the laboratory and is capable of measuring ozone concentration with an uncertainty of  $\pm 10\%$  of the actual concentration.

In addition to the two ozonesondes on the main payload and an experimental unit in dropsonde no. 1, the following experiments will be performed during the day of the balloon launch:

1. A rocket-borne chemiluminescent ozonesonde will be deployed to measure ozone profile from 60 to 15 km.

2. A chemical ozonesonde (Mast) will be launched on a small balloon to measure ozone concentration up to 30 km.

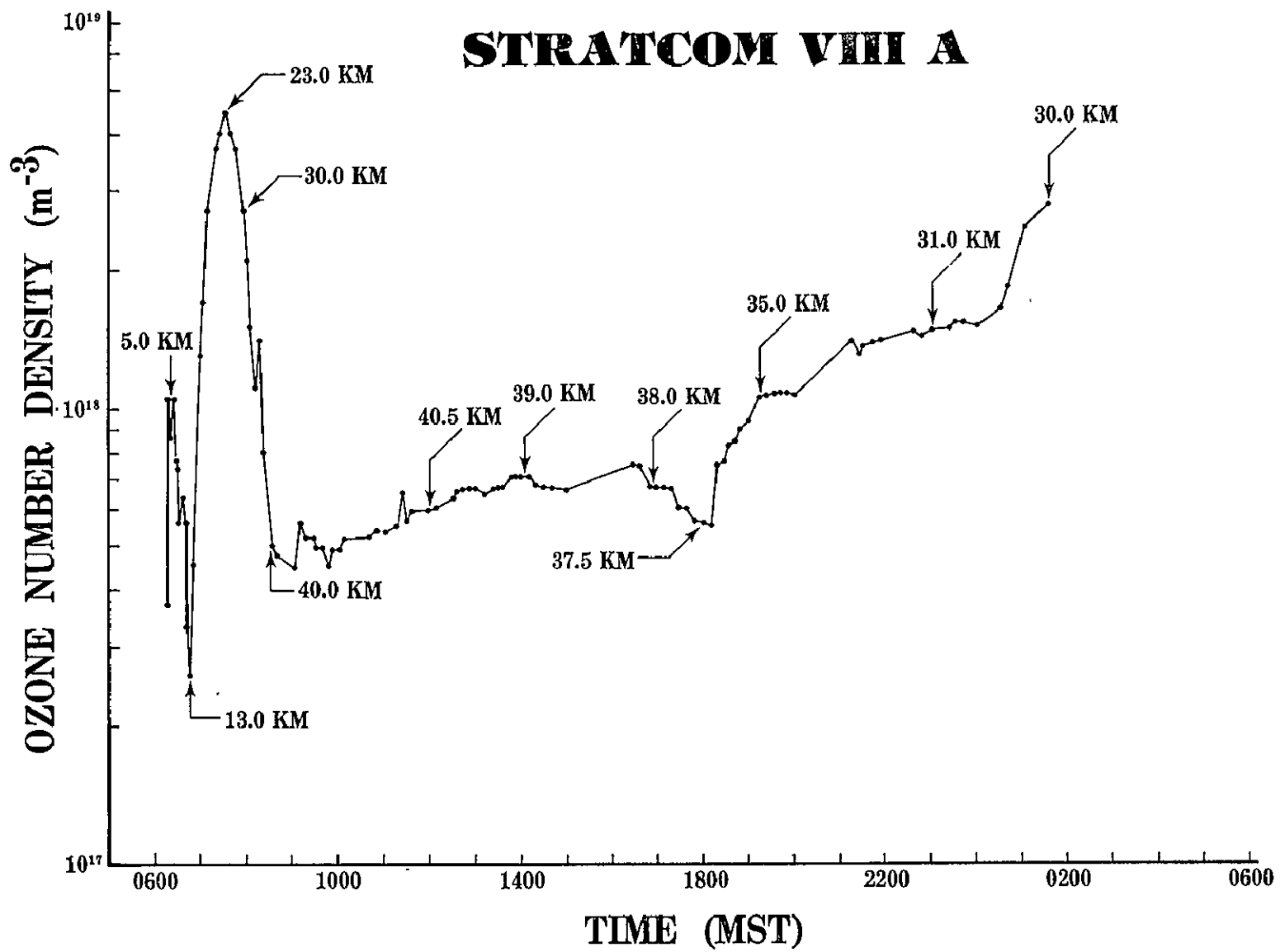
3. Dobson spectrophotometer will be in operation during the day of the balloon flight and will measure the total ozone present in the atmosphere.

#### OBJECTIVES

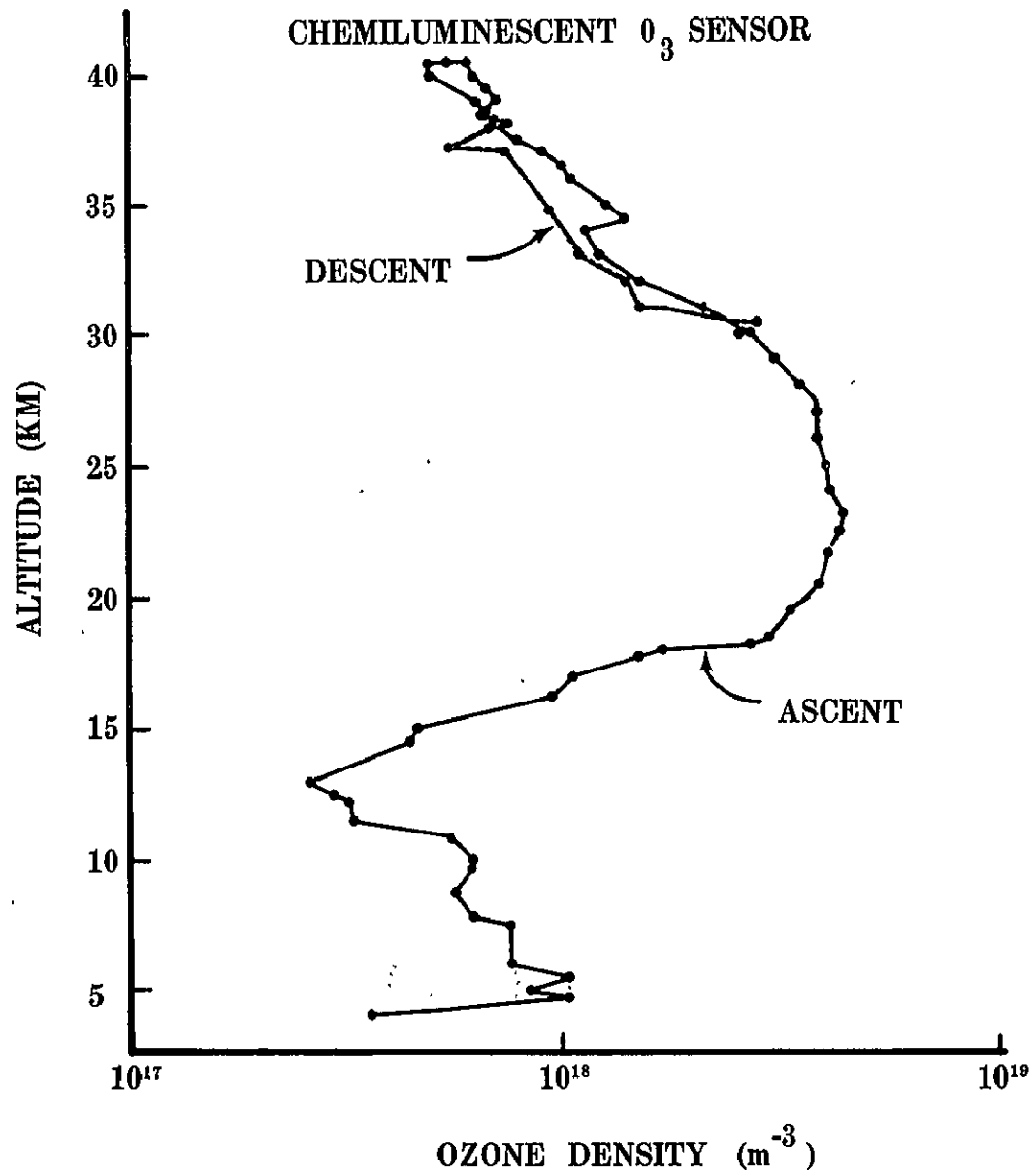
1. Determination of ozone concentration in the tropopause and stratosphere.

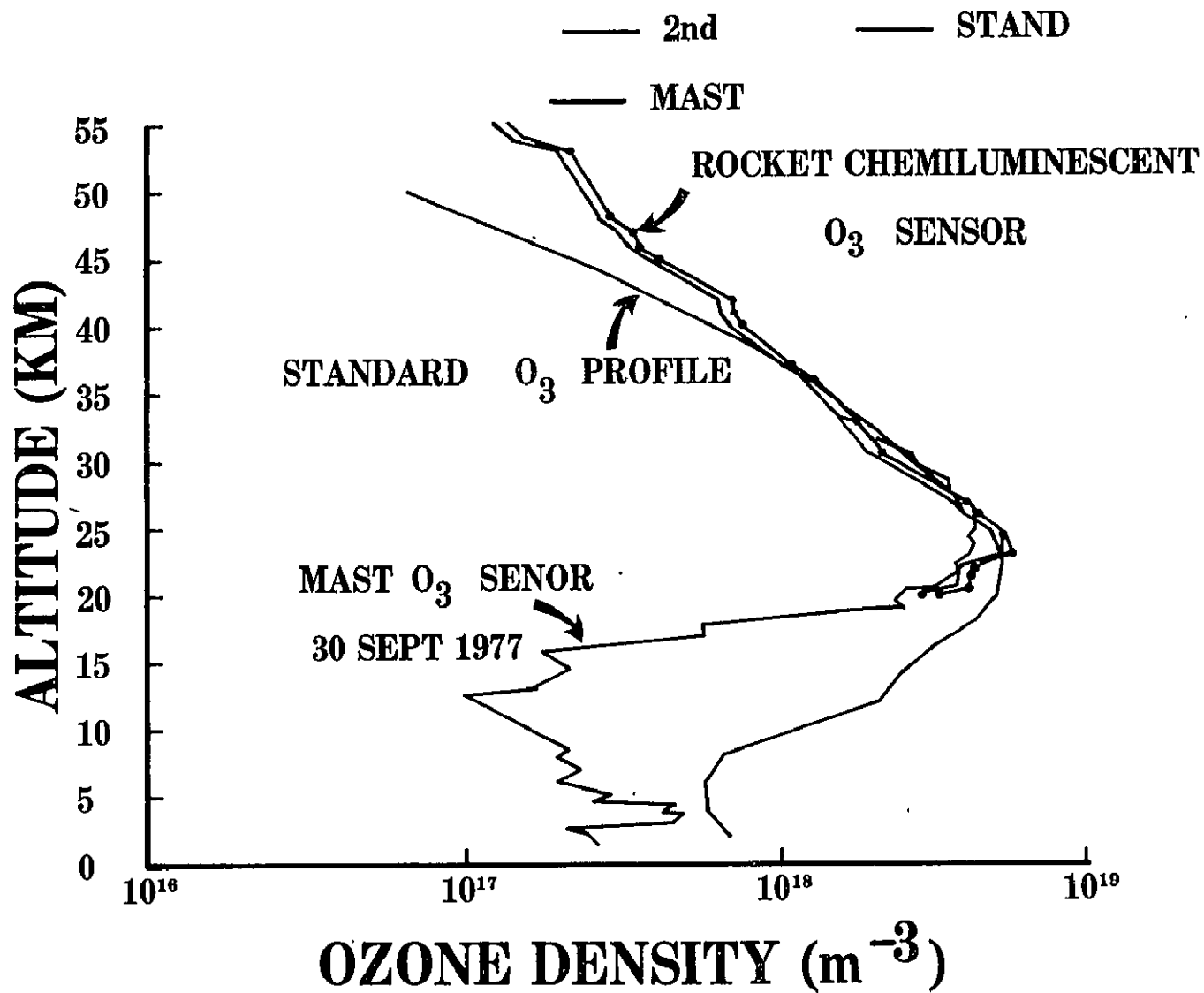
2. Measurement of diurnal variation of the ozone density in the stratosphere and its importance to ozone photochemistry.

3. Comparison of ozone concentrations measured with other techniques on the same balloon.



CHEMILUMINESCENT O<sub>3</sub> SENSOR





STATION WHITE SAND LAUNCH DATE 92977 LAUNCH ZULU 1625 ECC SONDE 3A-205X  
 SURFACE CONDITIONS PRESS 878,5 MB TEMP 299,4 DEG K HUMIDITY 45,0 PRCNT  
 TB CAL 30,0 DEG C AT 74,2 ORD OOS= 37,4 OIZ= 36,3 OZO= 64,5 IO=0,204 PS= 27,6  
 BASELINE CAL TEMP 30,0 DEG C AT 74,0 DIV HUMIDITY 62,2 PRCNT AT 46,0 ORD

ELECTROCHEMICAL CONCENTRATION CELL  
 OZONESONDE  
 Charles Manion  
 Wallops Flight Center  
 Wallops Island, Virginia 23337

VODS= 132' A0= 0; A1= 1,000

TIME	ALT	OZONE	OZDEN	TOTOZ	PRESS	TEMP	HUMTY	DEWPT	LOG	PTEMP	MIXRT	SPD	DIR	NS	EW	TV	SPECIF	UNC
MIN	GP	MT	MICMB	GAMMA	ATMCM	MB	DEG K	DEG K	PRESS	DEG K	MICGG	MPS	DEG	MPS	MPS	DEG K	HUMTY	P3
0	1219	20,1	50,6	0	878,5	297,5	62,3	259,9	2,9437	308,7	0,05	2,0	60,0	-1,0	-1,7	299,88	0,0133	26,1
1,0	1445	27,4	53,9	0,00055	856,0	294,2	52,3	284,2	2,9325	307,6	0,05	0,4	143,5	0,3	-0,2	295,91	0,0094	27,4
1,2	1506	27,5	53,8	0,00070	850,0	295,0	52,0	284,8	2,9294	309,0	0,05	0,9	172,3	0,3	0,4	296,78	0,0103	
2,0	1703	27,6	53,6	0,00119	831,0	297,5	51,2	286,8	2,9196	313,6	0,06	2,4	265,0	0,2	2,4	299,56	0,0116	27,6
3,0	1980	29,0	56,8	0,00190	805,0	295,4	52,2	285,2	2,9058	314,2	0,06	4,8	266,3	0,3	4,8	297,29	0,0107	29,0
4,2	2033	28,8	56,4	0,00204	800,0	294,8	53,3	285,0	2,9031	314,3	0,06	5,2	265,2	0,5	5,2	296,77	0,0106	
4,0	2264	27,7	54,7	0,00264	779,0	292,7	58,0	284,3	2,8915	314,3	0,06	6,9	260,4	1,2	6,8	294,53	0,0104	27,7
5,0	2544	27,0	53,7	0,00334	754,0	290,1	61,8	282,8	2,8774	314,5	0,06	9,4	253,6	2,6	9,0	291,83	0,0098	27,0
6,0	2842	25,6	51,2	0,00407	728,0	288,0	57,9	279,9	2,8621	315,4	0,06	10,7	253,2	3,1	10,2	289,50	0,0083	25,6
7,0	3124	25,8	52,2	0,00475	704,0	285,7	47,6	274,8	2,8476	315,8	0,06	12,2	257,6	2,6	11,9	286,71	0,0060	25,8
7,2	3171	26,4	53,3	0,00487	700,0	285,5	45,1	273,9	2,8451	316,1	0,06	12,3	258,7	2,4	12,1	286,49	0,0054	
8,0	3402	29,1	59,0	0,00547	681,0	284,7	53,2	269,1	2,8331	317,7	0,07	13,0	264,1	1,3	12,9	285,41	0,0041	29,1
9,0	3687	24,5	50,2	0,00619	658,0	281,9	55,0	267,2	2,8182	317,7	0,06	17,9	269,5	0,1	12,9	282,52	0,0037	24,5
10,0	3967	26,2	54,0	0,00688	636,0	280,8	20,2	259,3	2,8035	319,5	0,07	12,2	271,7	-0,4	12,2	281,14	0,0021	26,2
11,0	4256	32,6	67,1	0,00769	614,0	280,2			2,7882	322,2	0,09	8,6	276,2	-0,9	8,6	280,25	0	32,6
11,7	4444	32,4	67,1	0,00828	600,0	279,0			2,7782	322,8	0,09	7,0	278,2	-1,0	6,9	278,96	0	
12,0	4540	32,4	67,1	0,00858	593,0	278,3			2,7731	323,1	0,09	6,2	279,2	-1,0	6,1	278,31	0	32,4
13,0	4847	28,2	58,6	0,00949	571,0	277,8			2,7566	326,0	0,08	5,9	287,9	-1,8	5,6	277,79	0	28,2
14,0	5164	32,3	67,8	0,01042	549,0	274,7			2,7396	326,1	0,10	6,4	306,3	-3,8	5,2	274,74	0	32,3
15,0	5491	27,0	57,3	0,01138	527,0	272,1	4,5	256,2	2,7218	326,8	0,08	8,4	318,2	-6,3	5,6	272,19	0,0003	27,0
16,0	5829	28,0	59,9	0,01231	505,0	269,8	4,0	253,3	2,7033	327,9	0,09	9,1	324,7	-7,4	5,3	269,81	0,0002	28,0
16,2	5907	27,6	59,1	0,01292	500,0	269,2	3,9	252,5	2,6990	328,1	0,09	9,2	324,8	-7,5	5,3	269,20	0,0002	
17,0	6146	26,3	56,8	0,01317	485,0	267,3	3,5	250,3	2,6857	328,7	0,09	9,5	324,9	-7,8	5,5	267,35	0,0002	26,3
18,0	6475	25,9	56,1	0,01404	465,0	266,3	3,7	229,9	2,6675	331,4	0,09	11,1	320,0	-8,5	7,1	266,30	0,0002	25,9
19,0	6781	23,6	51,6	0,01481	447,0	263,9	11,5	249,2	2,6503	332,2	0,09	8,2	291,7	-3,0	7,6	263,98	0,0005	23,6
20,0	7061	23,5	51,8	0,01548	431,0	261,5	7,5	253,0	2,6345	332,5	0,09	8,7	332,3	-7,7	4,1	261,50	0,0003	23,5
21,0	7385	22,3	49,8	0,01625	413,0	258,6	8,6	252,2	2,6160	333,0	0,09	13,7	352,3	-13,6	1,8	258,68	0,0003	22,3
21,8	7625	21,3	48,2	0,01680	400,0	255,6	11,8	252,7	2,6021	332,1	0,09	11,9	341,6	-11,2	3,7	255,68	0,0003	

STATION WHITE SAND LAUNCH DATE 92977 LAUNCH ZULU 1625 ECC SONDE 7A-205X

22,0	7682	21,1	47,8	0,01693	397,0	254,9	12,6	232,8	2,5988	331,9	0,09	11,4	339,1	-10,7	4,1	254,97	0,0003	21,1
23,0	8027	21,9	50,1	0,01772	379,0	252,8	13,5	231,7	2,5786	333,5	0,10	14,8	331,8	-13,0	7,0	252,81	0,0003	21,9
24,0	8364	21,9	50,7	0,01851	362,0	249,7	14,5	229,9	2,5587	333,8	0,10	17,6	326,7	-14,7	9,7	249,74	0,0002	21,9
24,7	8678	20,5	47,7	0,01907	350,0	247,4	15,3	228,4	2,5441	333,9	0,10	20,3	321,5	-15,8	12,7	247,38	0,0002	
25,0	8734	19,7	46,2	0,01935	344,0	246,1	15,7	227,6	2,5366	333,9	0,09	21,7	318,8	-16,3	14,3	246,18	0,0002	19,7
26,0	9119	20,1	47,6	0,02019	326,0	243,4	17,8	226,5	2,5132	335,3	0,10	25,5	315,7	-18,3	17,8	243,43	0,0002	20,1
27,0	9498	18,9	45,4	0,02102	309,0	240,5	19,3	224,7	2,4900	336,4	0,10	25,1	312,6	-17,7	19,2	240,54	0,0002	18,9
27,6	9705	17,7	42,7	0,02144	300,0	239,6	19,2	223,9	2,4771	338,0	0,10	23,5	308,0	-14,6	18,4	239,61	0,0001	
28,0	9847	16,9	40,8	0,02172	294,0	238,9	19,1	223,3	2,4683	339,0	0,10	21,8	304,8	-12,5	17,9	238,97	0,0001	16,9
29,0	10186	19,7	48,2	0,02243	280,0	235,9	19,3	220,7	2,4472	339,4	0,12	18,3	303,7	-10,2	15,2	235,93	0,0001	19,7
30,0	10538	17,1	42,5	0,02317	266,0	232,7			2,4249	339,7	0,11	15,4	311,4	-10,2	11,5	232,70	0,0001	17,1
31,0	10877	16,5	41,4	0,02384	253,0	230,1			2,4031	340,8	0,11	17,8	312,2	-11,9	13,1	230,12	0,0001	16,5
31,2	10956	16,3	41,1	0,02399	250,0	229,5			2,3979	341,0	0,11	18,3	311,2	-12,0	13,7	229,50	0,0001	
32,0	11202	15,8	40,1	0,02446	241,0	227,6			2,3820	341,8	0,11	19,8	308,1	-12,2	15,6	227,62	0,0001	15,8
33,0	11511	16,5	42,2	0,02505	230,0	225,1			2,3617	342,5	0,12	17,2	294,4	-7,1	15,7	225,06	0,0001	16,5
34,0	11832	16,5	42,8	0,02569	219,0	223,0			2,3404	344,2	0,12	22,8	283,0	-5,1	22,3	223,02	0,0001	16,5
35,0	12166	14,5	38,0	0,02632	208,0	220,6			2,3181	345,5	0,12	27,5	284,5	-6,9	26,6	220,62	0,0001	14,5
35,8	12418	14,9	39,3	0,02678	200,0	219,4			2,3010	347,5	0,12	25,3	284,7	-6,7	25,4	219,40	0,0001	
36,0	12483	15,1	39,7	0,02690	198,0	219,1			2,2967	348,0	0,13	26,0	284,7	-6,6	25,1	219,08	0,0001	15,1
37,0	12814	14,8	39,3	0,02751	188,0	217,5			2,2742	350,6	0,13	20,5	276,2	-2,2	20,3	217,51	0,0001	14,8
38,0	13124	15,4	41,3	0,02809	179,0	215,2			2,2529	351,9	0,14	23,5	269,5	-0,2	23,5	215,23	0,0001	15,4
39,0	13447	15,9	43,2	0,02873	170,0	213,0			2,2304	353,4	0,16	28,9	272,3	-1,1	28,8	213,03	0,0001	15,9
40,0	13784	16,6	45,4	0,02943	161,0	210,7			2,2068	355,1	0,17	23,6	271,7	-0,7	23,6	210,73	0,0001	16,6
41,0	14097	18,2	50,2	0,03013	153,0	209,4			2,1847	358,1	0,20	28,2	278,8	-4,3	27,9	209,45	0,0001	18,2
41,3	14217	18,3	50,5	0,03041	150,0	208,9			2,1761	359,2	0,20	28,1	278,6	-4,2	27,8	208,89	0,0001	
42,0	14467	18,4	51,2	0,03100	144,0	207,7			2,1584	361,4	0,21	27,7	278,1	-3,9	27,5	207,75	0,0001	18,4
43,0	14768	19,6	54,9	0,03175	137,0	206,0			2,1367	363,5	0,24	20,7	265,4	1,7	20,6	205,97	0,0001	19,6
44,0	15129	21,9	61,7	0,03273	129,0	204,5			2,1106	367,2	0,28	18,5	269,7	0,1	18,5	204,54	0,0001	21,9
44,6	15316	22,9	64,9	0,03330	125,0	203,5			2,0969	368,5	0,30	19,6	277,7	-2,7	19,2	203,46	0,0001	
45,0	15461	23,6	67,4	0,03373	122,0	202,6			2,0864	369,6	0,32	20,4	283,8	-4,9	19,8	202,62	0,0001	23,6
46,0	15862	27,6	78,9	0,03511	114,0	202,0			2,0569	375,6	0,40	18,6	286,6	-5,3	17,8	201,96	0,0001	27,6
47,0	16235	32,1	92,3	0,03660	107,0	200,8			2,0294	380,3	0,50	3,2	245,4	1,3	2,9	200,83	0,0001	32,1
48,0	16515	34,8	100,7	0,03786	102,0	199,7			2,0086	383,3	0,57	4,4	211,2	3,8	2,3	199,66	0,0001	34,8
48,3	16630	35,5	103,0	0,03842	100,0	199,2			2,0000	384,6	0,59	5,5	224,4	3,3	3,9	199,19	0,0001	
49,0	16868	36,9	107,6	0,03958	96,0	198,2			1,9823	387,2	0,64	7,7	251,5	2,4	7,3	198,21	0,0001	36,9
50,0	17240	42,6	125,3	0,04161	90,0	194,4			1,9542	390,8	0,78	2,5	235,5	1,4	2,0	196,43	0,0001	42,6
51,0	17502	48,2	141,2	0,04323	86,0	197,2			1,9345	397,5	0,93	0,7	198,5	0,7	0,2	197,20	0,0001	48,2
52,0	17851	62,2	178,1	0,04585	81,0	201,7			1,9085	413,7	1,27	11,2	288,6	-3,6	10,7	201,73	0,0001	62,2
52,2	17924	65,6	187,5	0,04652	80,0	202,0			1,9031	415,7	1,36	13,2	292,9	-5,5	11,8	202,00	0,0001	
53,0	18151	76,0	216,5	0,04861	77,0	202,8			1,8865	422,0	1,64	19,2	306,1	-11,3	15,5	202,84	0,0001	76,0

ORIGINAL PAGE 19  
OF POOR QUALITY



STATION WHITE SAND LAUNCH DATE 92977 LAUNCH ZULU 1625 ECC SONDE 3A-205X

54.0	18550	78.5	223.2	0.05270	72.0	203.1	1.8573	430.6	1.81	8.8	325.4	-7.2	5.0	203.05	0.	78.5
54.5	18719	88.5	248.9	0.05467	70.0	205.2	1.8451	438.7	2.10	8.4	214.5	-3.0	-1.3	205.18	0.	
55.0	18493	98.9	275.3	0.05670	68.0	207.4	1.8325	447.0	2.41	7.9	100.4	-1.4	-7.8	207.36	0.	98.9
56.0	19169	111.5	306.0	0.06045	65.0	210.4	1.8129	459.4	2.84	17.1	107.2	-5.0	-16.4	210.37	0.	111.5
57.0	19461	112.5	306.4	0.06462	62.0	212.0	1.7924	469.2	3.01	1.7	95.1	0.2	-1.7	211.98	0.	112.5
57.5	19665	113.6	308.2	0.06756	60.0	212.8	1.7782	475.5	3.14	5.4	183.0	-0.3	4.7	212.83	0.	
58.0	19676	114.8	310.1	0.07060	58.0	213.7	1.7634	482.1	3.28	11.2	273.9	-0.8	11.2	213.72	0.	114.8
59.0	20209	121.1	325.9	0.07555	55.0	214.6	1.7404	491.4	3.65	8.1	217.5	6.4	4.9	214.56	0.	121.1
60.0	20441	123.7	337.7	0.07915	53.0	214.9	1.7243	497.4	3.93	7.4	246.3	-3.0	-6.8	214.90	0.	123.7
61.0	20770	128.2	343.9	0.08439	50.3	215.2	1.7016	505.7	4.22	7.8	294.0	-3.2	-7.1	215.23	0.	128.2
61.1	20807	128.2	343.8	0.08500	50.4	215.3	1.6990	506.7	4.25	7.8	299.7	-3.6	6.5	215.29	0.	
62.0	21104	124.3	343.4	0.08976	47.7	215.7	1.6785	514.6	4.46	7.6	344.7	-7.3	2.0	215.73	0.	128.3
63.0	21431	129.8	345.3	0.09502	45.3	217.0	1.6561	525.4	4.75	7.0	30.7	-6.0	-3.6	217.03	0.	129.8
64.0	21763	130.4	345.2	0.10037	43.0	218.1	1.6335	536.0	5.03	7.3	89.2	-0.1	-7.3	218.14	0.	130.4
65.0	22083	122.2	341.1	0.10550	40.9	218.8	1.6117	545.3	5.24	5.2	96.7	0.6	-5.1	218.77	0.	129.2
65.4	22225	120.4	339.2	0.10775	40.0	218.6	1.6021	548.4	5.32	4.3	93.6	0.3	-4.3	218.63	0.	
66.0	22404	127.5	336.9	0.11058	38.9	218.5	1.5899	552.4	5.43	3.2	89.8	-0.0	-3.2	218.46	0.	127.5
67.0	22741	125.3	332.0	0.11584	36.9	217.8	1.5670	559.2	5.62	3.1	118.6	2.4	-4.5	217.83	0.	125.3
68.0	23078	123.5	327.7	0.12103	35.0	217.5	1.5441	566.8	5.85	6.9	144.0	5.6	-4.0	217.51	0.	123.5
69.0	23453	125.0	330.5	0.12679	33.0	218.3	1.5185	578.5	6.28	8.2	261.9	1.2	8.1	218.30	0.	125.0
70.0	23812	127.6	336.2	0.13238	31.2	219.1	1.4942	590.0	6.77	11.6	291.9	-4.3	10.8	219.08	0.	127.6
70.7	24064	129.1	337.2	0.13636	30.0	221.0	1.4771	601.9	7.13	9.5	139.9	-2.9	-2.6	221.01	0.	
71.0	24173	129.7	337.6	0.13807	29.5	221.8	1.4698	607.0	7.29	8.6	74.8	-2.2	-8.3	221.83	0.	129.7
72.0	24535	129.8	336.9	0.14378	27.9	222.4	1.4456	618.4	7.71	4.0	73.0	-1.2	-3.8	222.43	0.	129.8
73.0	24921	134.3	345.5	0.14993	26.3	224.3	1.4200	634.4	8.46	4.6	299.5	-2.3	4.0	224.34	0.	134.3
73.8	25252	134.5	346.9	0.15531	25.0	223.9	1.3979	642.3	8.92	4.0	80.0	-3.2	-0.7	223.87	0.	
74.0	25332	134.6	347.3	0.15659	24.7	223.8	1.3927	644.2	9.03	3.9	27.7	-3.4	-1.8	223.76	0.	134.6
75.0	25770	129.8	335.9	0.16358	23.1	223.2	1.3636	654.9	9.31	3.4	344.8	-3.3	0.9	223.17	0.	129.8
76.0	26089	127.3	328.9	0.16852	22.0	223.5	1.3424	665.0	9.59	9.7	348.1	-9.5	2.0	223.46	0.	127.3
77.0	26425	125.5	323.2	0.17364	20.9	224.2	1.3201	677.0	9.95	4.3	326.9	-3.6	2.4	224.19	0.	125.5
77.8	26714	123.5	317.3	0.17796	20.0	224.8	1.3010	687.4	10.23	16.0	172.8	10.6	-9.8	224.78	0.	
78.0	26780	123.1	315.9	0.17894	19.8	224.9	1.2967	689.7	10.38	15.7	137.6	13.8	-12.6	224.92	0.	123.1
79.0	27157	117.1	299.2	0.18436	18.7	226.1	1.2718	704.7	10.38	19.7	119.6	9.7	-17.1	226.06	0.	117.1
80.0	27447	110.9	281.1	0.18829	17.9	227.9	1.2529	719.3	10.27	5.7	87.1	-0.3	-6.7	227.90	0.	110.9
80.5	27597	110.2	278.5	0.19026	17.5	228.4	1.2430	725.5	10.43	7.7	74.3	-2.3	-7.2	228.38	0.	
81.0	27752	109.4	275.9	0.19227	17.1	228.9	1.2330	731.9	10.60	8.8	61.1	-4.2	-7.7	228.88	0.	109.4
82.0	28113	106.1	269.2	0.19686	16.2	227.5	1.2095	738.8	10.85	8.0	62.2	-3.8	-7.1	227.48	0.	106.1
83.0	28494	107.3	270.6	0.20167	15.3	228.9	1.1847	755.5	11.62	3.9	83.3	-0.5	-3.9	228.88	0.	107.3
83.5	28626	106.4	268.3	0.20333	15.0	228.9	1.1761	759.9	11.75	3.7	79.1	-0.6	-3.6	228.88	0.	
84.0	28947	104.2	262.9	0.20731	14.3	228.9	1.1553	770.3	12.08	3.1	68.9	-1.1	-2.9	228.88	0.	104.2

-46-

ORIGINAL PAGE IS OF POOR QUALITY

STATION WHITE SAND LAUNCH DATE 92977 LAUNCH ZULU 1625 ECC SONDE 3A-205Y

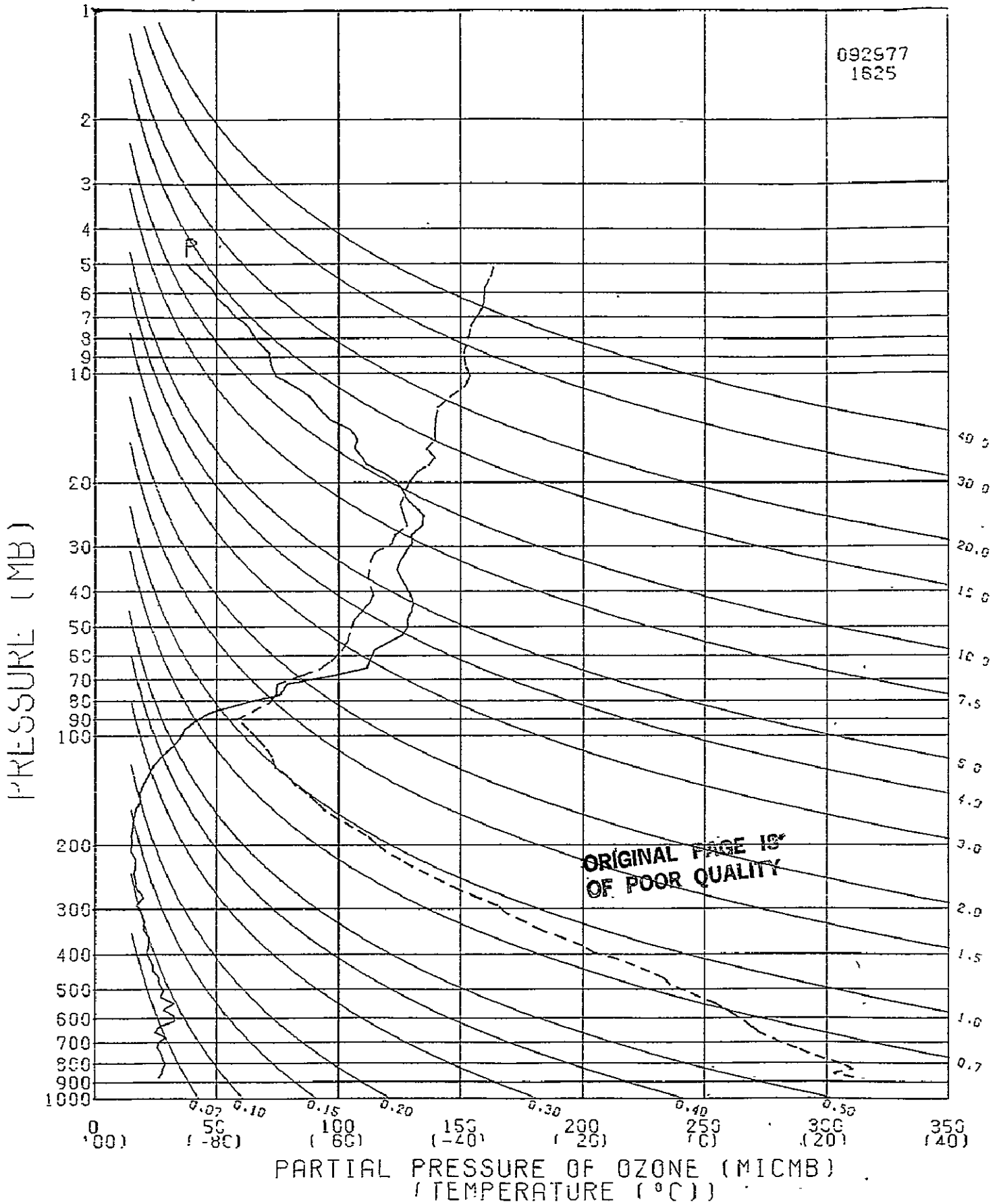
85,0	29382	95,6	241,1	0,21244	13,4	229,0	1,1271	785,2	11,83	3,3	64,0	-1,4	-3,0	229,01	0,	95,6
85,9	29648	91,4	230,1	0,21756	12,5	229,4	1,0969	802,3	12,12	3,9	56,2	-2,2	-3,2	229,39	0,	
86,0	29902	90,9	228,8	0,21815	12,4	229,4	1,0934	804,2	12,15	4,0	55,3	-2,3	-3,3	229,43	0,	90,9
87,0	30352	87,5	218,3	0,22284	11,6	231,5	1,0645	827,1	12,50	3,3	62,2	-1,5	-2,9	231,48	0,	87,5
88,0	30776	81,6	201,6	0,22700	10,9	233,8	1,0374	850,2	12,41	1,7	124,2	1,0	-1,4	233,78	0,	81,6
89,0	31231	73,8	181,7	0,23107	10,2	234,6	1,0086	869,5	12,00	3,9	124,7	2,2	-3,2	234,58	0,	73,8
89,3	31366	73,2	180,4	0,23221	10,0	234,4	1,0000	873,8	12,14	4,6	124,6	2,6	-3,8	234,39	0,	
90,0	31718	71,7	176,9	0,23515	9,5	233,9	0,9777	884,8	12,50	6,3	124,4	3,6	-5,2	233,91	0,	71,7
91,0	32242	71,0	175,6	0,23946	8,8	233,6	0,9445	903,3	13,39	0,9	114,8	-0,4	-0,8	233,64	0,	71,0
92,0	32895	65,1	160,4	0,24458	8,0	234,3	0,9031	930,9	13,48	1,3	233,7	0,8	1,1	234,31	0,	65,1
93,0	33430	62,3	153,3	0,24850	7,4	234,8	0,8692	954,1	13,96	8,7	144,2	7,1	-5,1	234,85	0,	62,3
94,0	33812	57,4	140,7	0,25113	7,0	235,8	0,8451	973,2	13,60	8,3	154,5	7,5	-3,6	235,78	0,	57,4
95,0	34219	54,2	132,3	0,25372	6,6	236,7	0,8195	993,6	13,62	6,6	158,8	6,1	-2,4	236,71	0,	54,2
96,0	34652	49,9	121,6	0,25629	6,2	237,0	0,7924	1012,6	13,54	9,9	148,6	8,5	-5,2	236,97	0,	49,9
96,3	34879	48,6	118,3	0,25754	6,0	237,0	0,7782	1022,5	13,41	8,8	142,2	7,0	-5,3	237,04	0,	
97,0	35115	47,2	114,9	0,25884	5,8	237,1	0,7634	1032,7	13,49	7,7	135,6	5,5	-5,4	237,10	0,	47,2
98,0	35612	42,3	102,6	0,26137	5,4	238,2	0,7324	1058,7	12,98	3,6	123,9	2,0	-3,0	238,16	0,	42,3
99,0	36149	37,2	90,0	0,26378	5,0	238,7	0,6990	1084,6	12,33	999,9	999,9	999,9	999,9	238,68	0,	37,2

INTEGRAL 0,26378  
 RESIDUAL 0,02303  
 TOTAL OZONE 0,28681

-47-

ORIGINAL PAGE IS  
 OF POOR QUALITY

092577  
1625



WHITE SAND

ECC

MEASUREMENT OF THE OZONE PROFILE  
IN SUPPORT OF STRATCOM VIIID/B  
N79-23467

A. J. Krueger, Goddard Space Flight Center, Greenbelt, MD 20771  
D.U. Wright, Goddard Space Flight Center, Greenbelt, MD 20771  
Peter Simeth, Sen Tran Co., Santa Barbara, CA 93102  
Staff, Wallops Flight Center, Wallops Island, VA 23337

## ABSTRACT

A rocket carrying an optical ozonesonde was launched at 1822 GMT on Sept. 29, 1977 from W.S.M.R. in support of the STRATCOM VIII balloon. The integral ozone amount above the balloon ceiling altitude of 40 km was measured as .0117 atm-cm with an uncertainty less than  $\pm 7\%$ . The ozone density at 40 km was  $6.77 \times 10^{17}$  mol/m<sup>3</sup>. Ozone densities in molecules/m<sup>3</sup> at higher altitudes were  $2.28 \times 10^{17}$  at 45 km,  $6.72 \times 10^{16}$  at 50 km,  $2.20 \times 10^{16}$  at 55 km, and  $7.26 \times 10^{15}$  at 60 km. In addition, the ozone distribution was measured at lower altitudes from the tropopause at 17 km to 40 km.

## INTRODUCTION

Several STRATCOM experiments require a determination of the ozone amount remaining above the balloon ceiling altitude for interpretation of results which depend on the incident solar flux in the middle ultraviolet. The present experiment determined that parameter with an optical ozone sensor carried aloft with a Super Loki-Dart rocket, launched from White Sands Missile Range at the time the STRATCOM VIII balloon was near its ceiling altitude of 40 km.

Sensor

The ROCOZ optical ozonesonde operates by measuring the attenuation of ultraviolet sunlight in atmospheric layers. The ozone density is directly computed from the attenuation per kilometer height interval given the ozone absorption coefficient for the wavelength band in use. The instrument used for this rocket observation is the standard unit in use for the past two years at Wallops Flight Center and Churchill Research Range. A description of the instrument may be found in Krueger, et al. (1978) (available in the summer) and in the "STRATCOM VIII Scientific Objectives and Mission Organization" document. The latter report contains a description of the balloon version of the instrument which is identical to the rocket instrument except for one filter center wavelength, telemetry, thermal control, and external packaging.

## Calibration and Data Analysis

The particular instrument (ROCOZ #250) used for this sounding (Flight #174) has the following calibration characteristics:

<u>Filter #</u>	<u>Center Wavelength, A</u>	<u>Half-width, A</u>	<u><math>x(\tau=0), \text{cm}^{-1}</math></u>
0	3194.3	38.7	0.674
1	3041.8	40.0	5.297
2	2836.0	38.4	76.83
3	2584.0	71.1	294.33

The half-width, given in Column 3, is the wavelength interval between the points where the filter transmission is 50% of the peak transmission. The parameter in Column 4 is the ozone absorption coefficient in  $\text{cm}^{-1}$  for an ozone optical depth of zero. A slight dependence of the absorption coefficient on ozone optical depth is included in the data reduction. The correction is generally less than 1% at unit optical depth. The temperature dependence of the ozone absorption spectrum is approximately accounted for by assuming  $-44^{\circ}\text{C}$  coefficients apply to the Filter #1 data, but  $+18^{\circ}\text{C}$  coefficients represent the Filter #2 and 3 data.

Filter #0 is a reference channel, while the other filters are used at overlapping altitude intervals as follows: Filter #1, 17-38 km, Filter #2, 38-49 km, and Filter #3, 44-64 km.

The flight data were processed manually in the same manner as other rocket flights.

### Flight Results

The ozone profile from the three active filters in this instrument is shown in Figure 1 and the composite data (from merging the results in overlap regions) are given in Table 1. The results from Filter #3 average 1% higher than the Filter #2 ozone densities from 44 to 49 km. In the single overlapping height between Filters #1 and 2, the Filter #2 results are 4% higher. (This value changes to -1% if the Filter #1 data are extended 5 km upwards beyond the limit of optimum accuracy.) The ozone profile exhibits only minor structural deviations from a constant scale height ( $H=4.3$  km) profile above 38 km. Below this the local scale height increases until the ozone density maximum (of  $5.2 \times 10^{18} \text{m}^{-3}$ ) near 25 km is reached.

The ozone mixing ratio profile is shown in Figure 2. This exhibits a peak of  $18.4 \mu\text{g/g}$  (11 ppm) near 33 km and a rather

featureless decay above and below, becoming less than 10  $\mu\text{g/g}$  at 25 and 44 km, and less than 5  $\mu\text{g/g}$  at 21.5 and 50 km.

The probable errors in the results are generally less than 10% between 21 and 50 km. Above 50 km the errors grow due to parachute pendulation and lower attenuation per unit height. Below 21 km the errors grow rapidly due to a small signal level. If 21 km is taken as the nominal base of this sounding, the total ozone amount above 20.5 km is 0.257 atm -cm. The total ozone observed with the WSMR Dobson Spectrophotometer at the time of this sounding was 0.284 atm -cm. The residual ozone of 0.027 atm -cm is quite low, perhaps due to the very low temperatures in the lower stratosphere. A conjunctive balloon sounding using an ECC ozonesonde finds a residual below 20.4 km of 0.079 atm -cm. Consequently, the sounding data must be considered as preliminary until a thorough examination is completed.

An initial inspection of the rocket data has shown that a completely unreasonable telemetry zero offset would be required to bring the rocket profile into agreement with the ECC data. Likewise, a filter temperature coefficient 10 times larger than the manufacturers specification would be required. The discrepancy could be accounted for by postulating interference in the 3042 Å band by another (unidentified) atmospheric constituent. This is, of course, highly speculative because the absorption would have to be comparable (30%) to the ozone attenuation per unit height between 25 and 35 km.

The residual ozone above the 40 km STRATCOM VIII ceiling altitude can be computed from the rocket profile. A value of 0.012 atm -cm with an uncertainty on the order of  $\pm 7\%$  is obtained. The error is estimated from the errors in the ozone density just above 40 km. The above numbers must also be treated with caution because of the problem noted in the total ozone discussion. It should be pointed out that the optical ozone data for heights above 38 km are internally consistent and that the usual test for validity of data, namely close correspondence in the regions of redundant data, is completely satisfied.

#### Acknowledgements

We sincerely appreciate the efforts of the Physical Sciences Laboratory, Las Cruces, New Mexico for telemetry fabrication; the Naval Weapons Center, China Lake, California and P & P Industries, College Park Maryland for payload calibrations; National Weather Service personnel at Wallops Flight Center, and the White Sands Missile Range personnel for flight operations; and Miss Carol Fry of P & P Industries for data processing.

## References

Krueger, A.J., P. Simeth, B. Ellefson, W.R. McBride, M. Hill, S. Flangan, W. Gammill and S.G. Park, 1978: "Design of an Optical Ozonesonde for the Super Loki-Dart Rocket", NASA Technical Report, Summer, 1978.

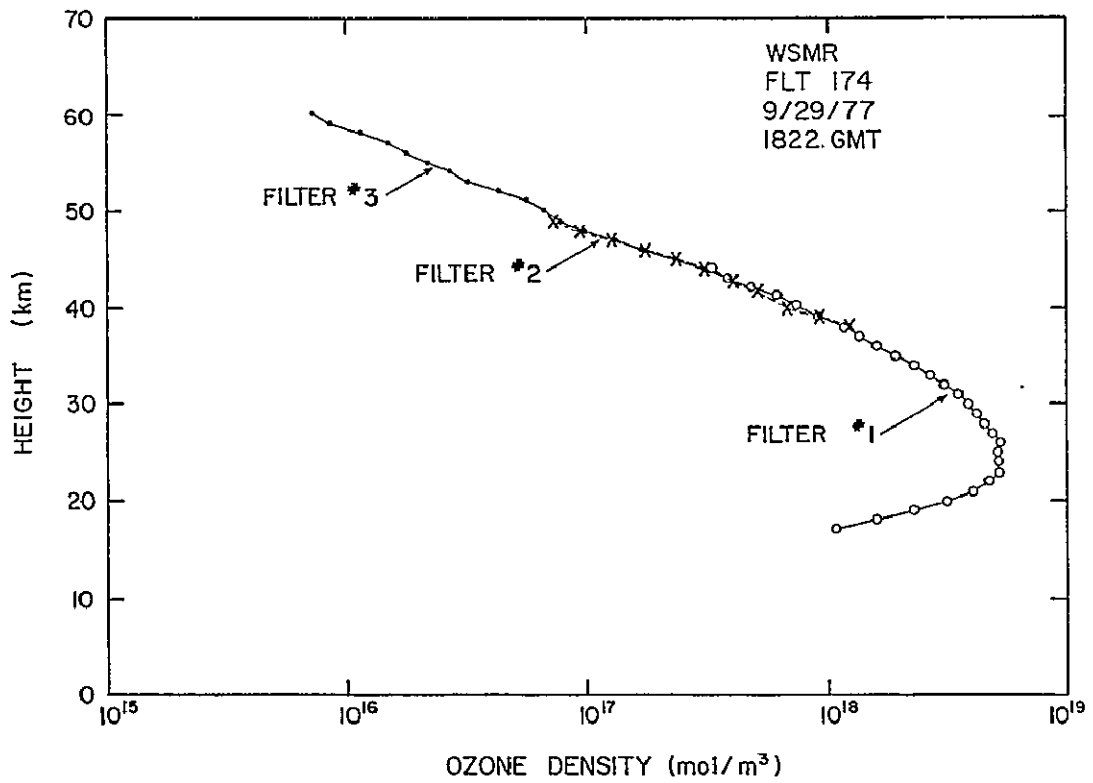


Figure 1. Ozone density profile observed with ROCOZ system in support of STRATCOM VIII project.



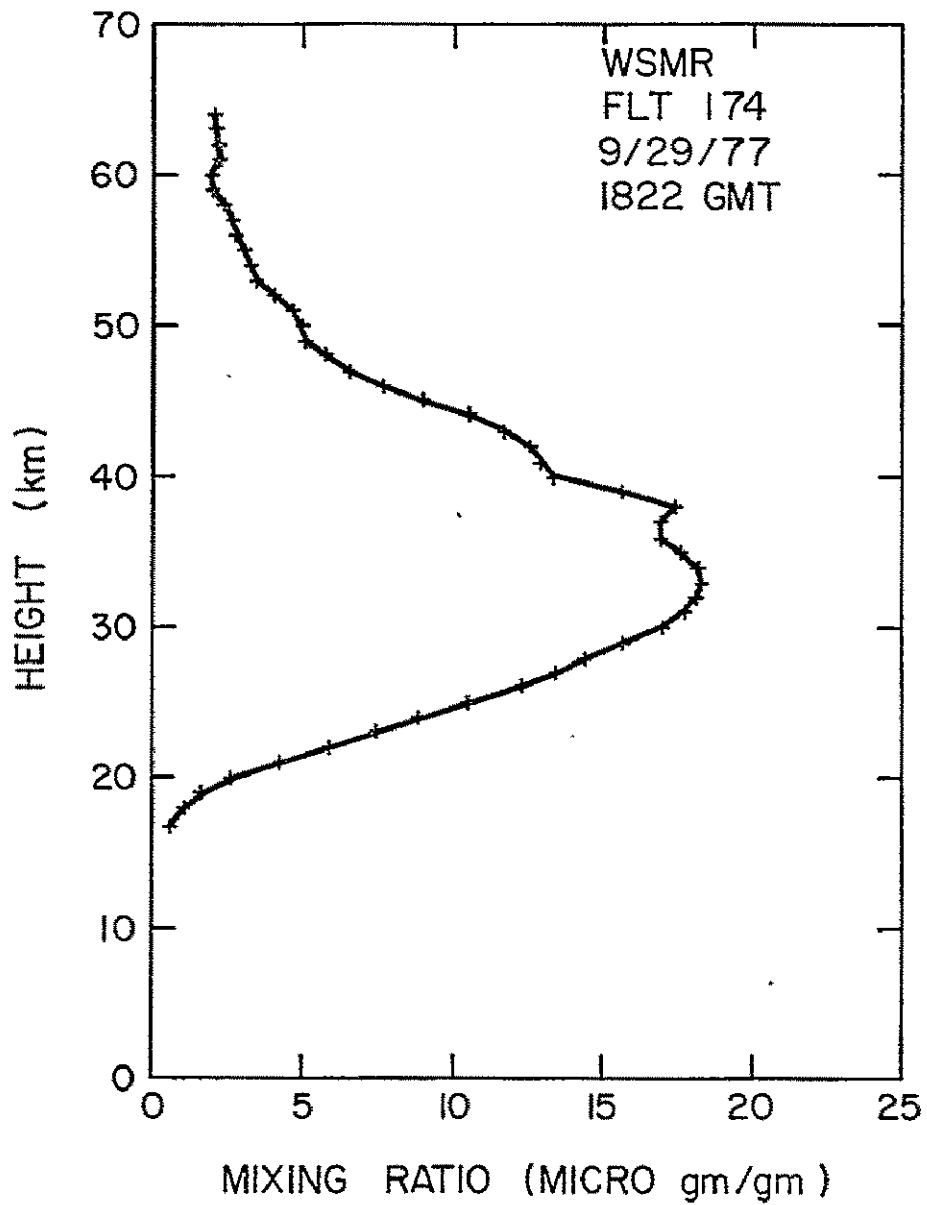


Figure 2. Ozone mixing ratio profile from ROCOZ data in support of STRATCOM VIII project.

DATA REPORT FOR ROCOZ FLIGHT NUMBER 174

FLIGHT LOCATION WHITE SANDS, NEW MEX. DATE 92977  
 LAUNCH TIME, GMT 1822

HEIGHT KM	O <sub>2</sub> DEN MOL/CM <sup>3</sup>	MIX RATIO		AIR DENSITY GM/CM <sup>3</sup>	AIR TEMP DEG C
		MASS	VOLUME		
60	7.2534E+09	1.895	1.112	.31	-14.6
59	8.5994E+09	1.91	1.15	.36	-16.8
58	1.1827E+10	2.29	1.38	.41	-18.0
57	1.5050E+10	2.59	1.56	.46	-15.0
56	1.7444E+10	2.88	1.68	.52	-11.2
55	2.0202E+10	3.20	1.82	.58	-8.0
54	2.6897E+10	3.20	1.93	.67	-11.5
53	3.2222E+10	3.43	2.07	.75	-7.0
52	4.3999E+10	3.98	2.40	.86	-10.6
51	5.6471E+10	4.61	2.78	.97	-9.6
50	6.7179E+10	4.88	2.95	1.10	-7.0
49	9.9411E+10	5.67	3.42	1.23	-4.5
48	1.1229E+11	6.49	3.92	1.40	-4.6
47	1.5999E+11	7.49	4.58	1.58	-4.6
46	2.2222E+11	8.60	5.58	1.78	-2.5
45	2.8888E+11	9.87	6.55	2.05	3.5
44	3.5555E+11	10.49	7.52	2.33	5.5
43	4.3333E+11	11.47	8.59	2.68	-1.0
42	5.3999E+11	12.51	9.55	3.11	-1.8
41	6.7222E+11	13.22	10.73	3.56	-16.6
40	8.7777E+11	13.22	11.99	4.08	-17.5
39	9.9166E+11	15.55	12.99	4.69	-20.0
38	1.1300E+12	17.41	14.39	5.50	-26.0
37	1.3555E+12	16.88	16.18	6.40	-29.0
36	1.5911E+12	16.33	18.18	7.44	-31.9
35	1.9133E+12	17.57	20.60	8.68	-35.4
34	2.2888E+12	18.22	23.00	10.06	-36.5
33	2.6777E+12	18.31	25.06	11.66	-37.6
32	3.2888E+12	18.88	27.88	13.53	-38.8
31	3.8444E+12	17.68	30.67	15.62	-39.9
30	4.4666E+12	15.99	33.24	18.05	-43.8
29	5.1999E+12	14.34	35.65	21.43	-45.4
28	6.0999E+12	13.34	38.08	24.95	-45.4
27	7.2999E+12	12.39	40.08	29.12	-46.9
26	8.8999E+12	10.24	42.34	34.12	-48.4
25	1.0888E+13	8.44	44.24	39.99	-50.0
24	1.3222E+13	7.37	45.50	47.33	-52.7
23	1.6000E+13	5.82	47.51	56.10	-55.0
22	1.9333E+13	4.17	50.51	65.17	-54.4
21	2.3333E+13	2.66	52.51	77.10	-57.5
20	2.8999E+13	1.11	56.60	94.62	-59.5
19	3.6333E+13	.47	59.97	114.31	-65.5
18	4.5555E+13	.55	55	138.08	-71.2
17	5.6666E+13	.2	.31	168.88	-75.0
STOP					

Table 1

D8

MEASUREMENT OF 200-400 nm SOLAR UV FLUXES  
ON THE STRATCOM 8A BALLOON FLIGHT

N 79 - 23468

Frederick A. Hanser, Bach Sellers, and Jean L. Hunerwadel  
Panametrics, Inc., Waltham, MA 02154

ABSTRACT

A filter wheel UV Spectroradiometer (UVS) was used to measure solar UV fluxes in 10 band-passes in the 200-400 nm region at altitudes up to 40 km on Stratcom 8A. Ozone layer thicknesses were derived from the balloon ascent measurements and an ozone density profile obtained. Measurements at the 39-40 km float altitude before and after local noon give a solar flux in the  $(220 \pm 5)$  nm  $O_2-O_3$  transmission window of  $4.53 \times 10^{-6} W/(cm^2 \cdot nm)$  at approximately 1 AU on 29 September 1977, when the sunspot number was about 63.

INTRODUCTION

The Panametrics' UV Spectroradiometer (UVS) operated properly for the entire first day of the Stratcom 8A balloon flight. Good solar UV flux data and derived ozone layer thicknesses were obtained for the balloon ascent and throughout the day at float altitude, through sunset. A vertical profile of ozone density has been obtained from the calculated ozone thicknesses. The 220 nm filter data at float altitude give a good measure of the solar UV flux at this wavelength on 29 September 1977.

INSTRUMENT DESCRIPTION

The UVS is a filter wheel irradiator, originally developed for high altitude aircraft use in the DOT-CIAP (Ref. 1). For the Stratcom 8A balloon flight the UVS had a cone diffuser and quartz shield to allow vertical mounting with no sun-pointing requirement. The UVS has flown in this configuration on Stratcoms 7A and 8A, while on 6A a flat diffuser and  $45^\circ$  aiming on a sun-oriented platform was used (Refs. 2, 3). A short description of the UVS as used on Stratcom 8A is given in Ref. 4.

The ten filter set wavelengths, bandpass widths, and calibration sensitivity with the UV photomultiplier are given in Table 1. The calibration is from a 200W quartz-iodine Standard of Irradiance (traceable to NBS), converted to the solar spectral shape.

## DATA ANALYSIS

The UVS signals are converted to downward going fluxes as described in Refs. 1, 2 and 3. For the Stratcom balloon flights the fluxes are also divided by  $\cos \theta_{\text{sun}}$ ,  $\theta_{\text{sun}}$  being the solar zenith angle, so that the high altitude response is the direct solar flux attenuated only by  $\text{O}_3$  and  $\text{O}_2$ . The ratios of the UV fluxes are used to calculate the vertical thickness of the ozone layer above the balloon altitude. Differences of ozone thicknesses calculated for different altitudes allows the vertical ozone density profile to be obtained.

At the highest altitudes the 220 nm filter results are used to obtain the unattenuated solar flux at (220+5) nm. This is done by plotting the logarithm of the measured flux against the pressure (at the UVS altitude)/ $\cos \theta_{\text{sun}}$ , which latter is proportional to the attenuation path length. The extrapolation of the straight line portion (high altitude, small  $\theta_{\text{sun}}$ ) of the data to zero pressure gives the solar flux unattenuated by  $\text{O}_3$  and  $\text{O}_2$ .

## RESULTS

Some results from the UVS on Stratcom 8A are given in Fig. 1, where the measured UV fluxes at four wavelengths are shown as a function of altitude. The solar zenith angle is also decreasing during ascent, so the solar fluxes increase partly because of the decreasing slant path through the ozone layer above the balloon. The major effect on the shorter wavelengths (292 and 307 nm) is the decrease in ozone attenuation as the balloon rises through the stratospheric ozone layer.

The ozone thicknesses calculated from the measured UV fluxes have been used to calculate the vertical ozone density profile, and this is plotted in Fig. 2. The altitude bars show the altitudes contributing to each density calculation, the ozone density being an/effective average over that altitude range. The density values are estimated to be accurate to about 10%.

The 220 nm solar flux measurements are shown in Fig. 3. Here the measurements at float altitude are plotted against

$P/\cos\theta_{\text{sun}}$  on a semilog scale. The straight line fit for  $P/\cos\theta_{\text{sun}} < 10 \text{ mb}$  gives  $4.53 \times 10^{-6} \text{ W}/(\text{cm}^2\text{-nm})$ , with the ascent-sunrise data and the sunset data both giving about the same result.

The present UVS derived 220 nm solar flux results are given below.

<u>Flight</u>	<u>Date</u>	<u>Diffuser Used</u>	<u>Sunspot #</u>	<u>Flux (W/(cm<sup>2</sup>-nm))</u>
6A	24-25/9/75	Flat	0	$4.19 \times 10^{-6}$
7A	29/9/76	Cone	18	$3.27 \times 10^{-6}$
8A	29/9/77	Cone	63	$4.53 \times 10^{-6}$

As discussed in Ref. 3, the 6A and 7A measurements, combined with other measurements, are consistent with solar 220 nm flux increasing with sunspot number. The 8A measurement further supports this finding. In particular, the 7A and 8A measurements, both made with the cone diffuser, indicate a substantial change with sunspot number. It is thus highly desirable to make additional 220 nm measurements with the UVS during the coming sunspot maximum, to provide more conclusive data on this variation.

#### References

1. F. A. Hanser, B. Sellers, and J. L. Hunerwadel, "Design, Fabrication, and Flight of a UV Spectrophotometer Aboard a WB57F High Altitude Aircraft for the CIAP Flight Series - Summary Report," Report PANA-UVS-7, Panametrics, Inc., Waltham, Mass. (Dec. 1975). (Available as ADA019745 from NTIS, Springfield, VA.)
2. F. A. Hanser, B. Sellers, and J. L. Hunerwadel, "Measurement of 200-400 nm Solar UV Fluxes at Altitudes up to 40 km," in "Stratospheric Composition Balloon-Borne Experiment 23-26 September 1975," Compiled by H. N. Ballard and F. P. Hudson, Report ECOM-5830 (Oct. 1977).
3. F. A. Hanser, B. Sellers, and J. L. Hunerwadel, "Measurement of 200-400 nm Solar UV Fluxes at Altitudes up to 39 km on the Stratcom 7A Balloon Flight," Report PANA-AIR-3, Panametrics, Inc., Waltham, Mass. (Sept. 1977).
4. E. I. Reed, compiler, "Stratcom-8 Scientific Objectives and Mission Organization," Report GSFC-X-624-77-261, Goddard Space Flight Center, Greenbelt, MD (Oct. 1977).

Table 1

UVS Calibration Sensitivities  
for the Stratcom 8A Balloon Flight

Filter set average wavelength (nm)	Filter set bandwidth (nm)	Solar Calibration sensitivity (A/(W/(cm <sup>2</sup> -nm)))
220	10	5.034x10 <sup>-1</sup>
289.3	2	1.217x10 <sup>-2</sup>
291.8	2	7.213x10 <sup>-2</sup>
297.4	2	7.923x10 <sup>-2</sup>
302.0	2	2.253x10 <sup>-2</sup>
306.8	2	1.791x10 <sup>-2</sup>
311.7	2	1.144x10 <sup>-2</sup>
329.7	2	6.691x10 <sup>-3</sup>
371.6	28	3.574x10 <sup>-3</sup>
401.9	26	1.369x10 <sup>-3</sup>

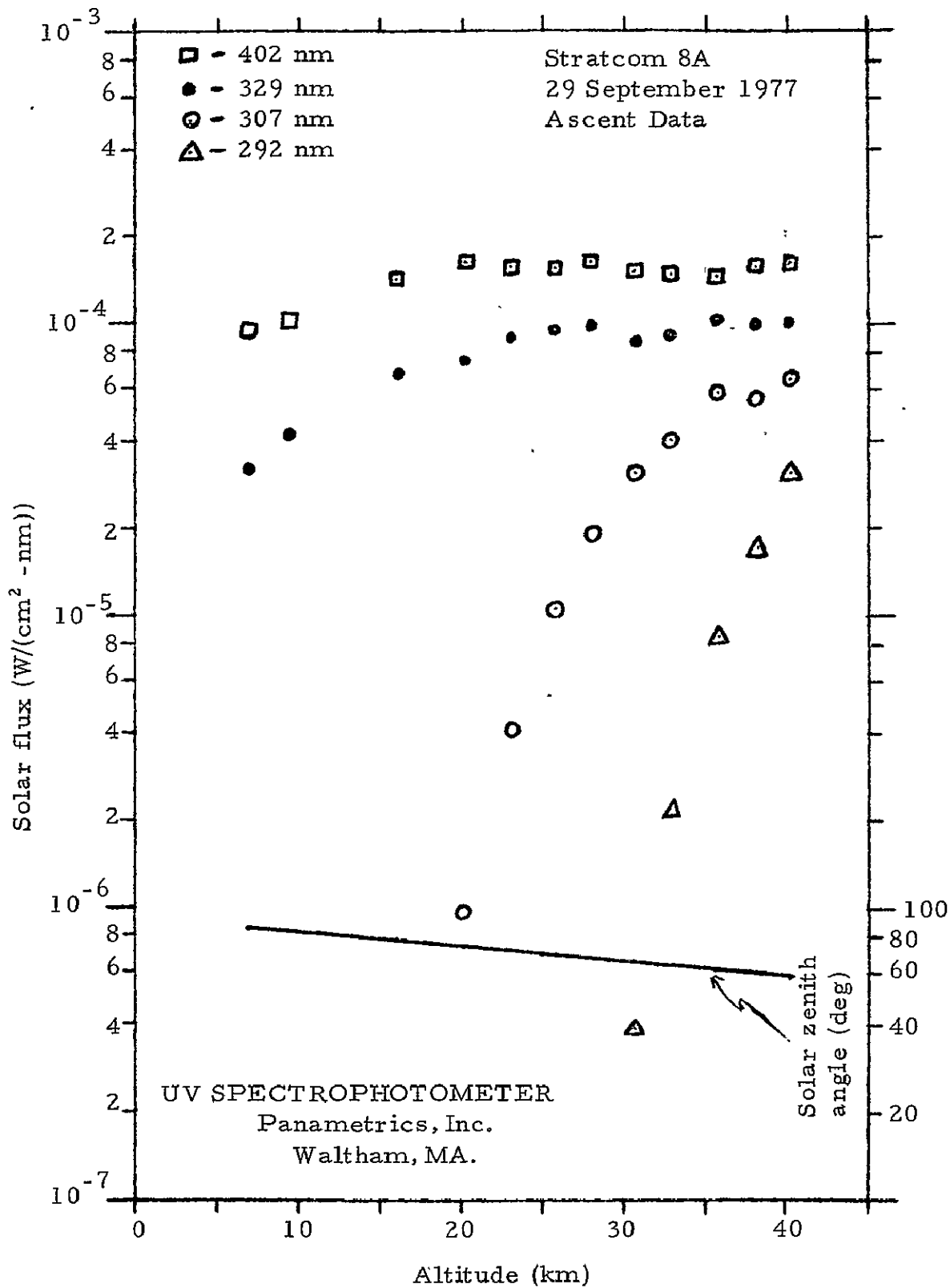


Fig. 1 Measured UVS Solar Fluxes during Ascent of Stratcom 8A.

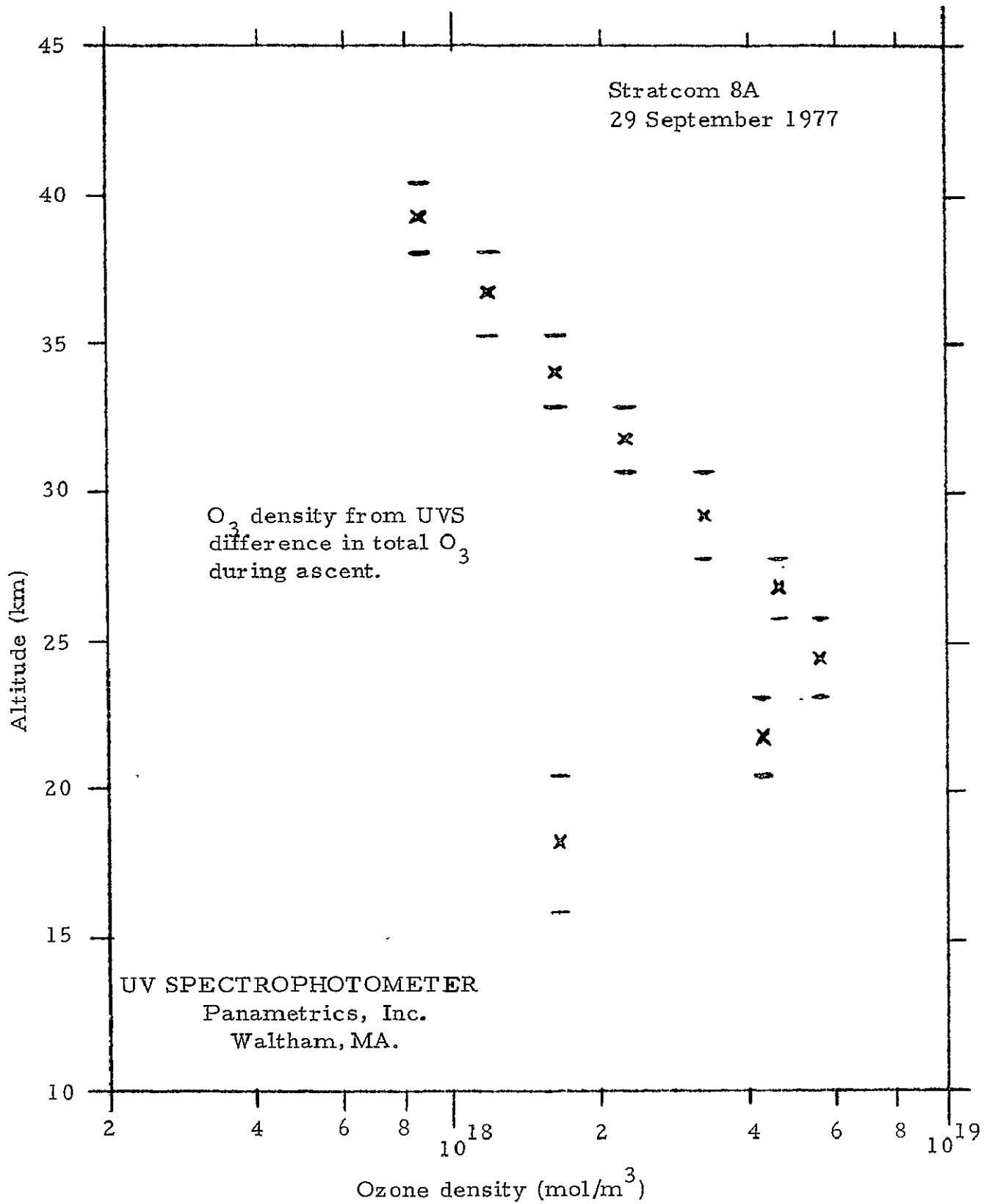


Fig. 2. Vertical Ozone Density Profile from UVS Data for Stratcom 8A Ascent.



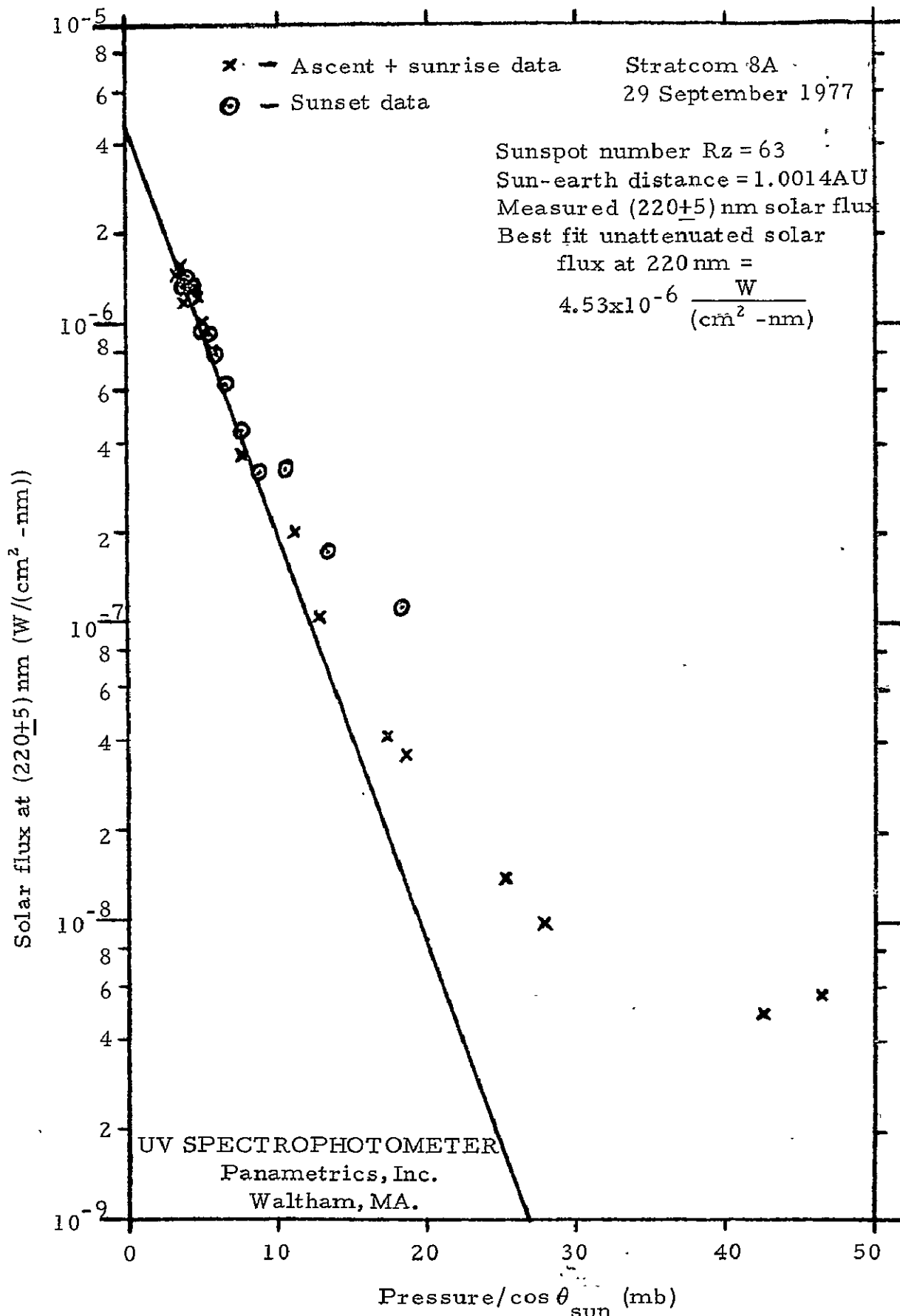


Fig. 3. Plot of UVS Measured 220 nm Solar Flux vs Attenuation Pathlength in Atmosphere.

## MEASUREMENTS OF ULTRAVIOLET FLUXES

L.R. Megill, Utah State University, Logan, Utah 84322

N 79-2346

U.S.U. flew a U.V. spectrometer on Stratcom VIII which measured the U.V. scattered light in the 2000 Å to 3000 Å range. These data were obtained at a variety of viewing angles. In addition data in 3000 Å to 4000 Å range were obtained using four photometers with filters approximately 300 Å wide. This instrument was downward viewing in order to obtain information on the variability of the albedo in this wavelength range. Another four channel instrument, looking upward, was designed to measure ozone overburden. This set of measurements will enable us to obtain data on the solar fluxes (from which the J value can be determined) and will cross check the filter technique for obtaining O<sub>3</sub> concentrations.

All instruments appeared to work well during the day, but did not work on the morning of the second day because of power problems. During a two hour period during the day the spectrometer was accidentally shifted to measure scatter to longer wavelengths, (limited to about 4000 Å because of the detector) and was reset after about two hours, intentionally, to the U.V. range. This gives the ability to determine the scattered light component in the entire 2000 Å to 4000 Å region for a portion of the day.

The instruments apparently worked well and all data are available on tape, unfortunately funding for data analysis has not been available. It is anticipated that analysis can be carried out during the summer under another project.

## MEASUREMENTS OF SOLAR UV FLUX IN THE STRATOSPHERE

J. E. Mentall/J. R. Herman, Goddard Space Flight Center,  
Greenbelt, Maryland 20771

B. Zak, Sandia Laboratories, Albuquerque, New Mexico 87115

## ABSTRACT

Solar uv flux measurements were obtained on STRATCOM-VIII from liftoff to sunset. Spectra cover the wavelength range from 1979Å to 2879Å and altitudes from ~25-42 km over a wide range of solar zenith angles. Good agreement is obtained between the observed spectra and synthetic spectra calculated using a two stream radiative transfer model.

## INTRODUCTION

Considerable attention has been focused on the stratosphere over the past few years. This attention has been the result of realizing that the ozone layer is fragile and the depletion of this protecting layer would have serious consequences for humanity. These facts are reflected by the number of experiments onboard STRATCOM-VIII which were concerned with the measurement of ozone directly or through measuring the attenuation of the solar radiation by the ozone layer.

For the study of the stratosphere, the wavelength region of interest is from ~1750Å to 3200Å. At wavelengths shorter than 1750Å solar radiation does not penetrate to the stratosphere due to strong absorption by O<sub>2</sub>. Above 3200Å, the atmosphere is essentially transparent. The 1750-3200Å region can be divided into three regions of interest determined by the dominant absorption process. From 1750-2000Å, absorption is predominantly via the O<sub>2</sub> Schumann-Runge bands. Between 2000 and 2200Å absorption results from the weak O<sub>2</sub> Herzberg continuum which allow uv radiation to penetrate to the lower stratosphere. The 2200-3000Å region is dominated by the strong O<sub>3</sub> absorption.

Since it was impossible for the flight spectrometer to cover the entire wavelength range of interest, the grating drive was set to cover as much of the 2000-3000Å interval as possible. Although the instrument was on at liftoff, the sensitivity of the instrument was such that no useful data was obtained below 25 km. Effectively, solar spectra were obtained as a function altitude and a low solar zenith angle (~60°) on the ascent portion of the flight and at a constant float altitude (~40 km) as a function of solar zenith angle. The data is compared with a theoretical model and can be used to obtain an ozone profile and ozone overburdens.

## MEASUREMENTS OF SOLAR UV FLUX IN THE STRATOSPHERE (Con't.)

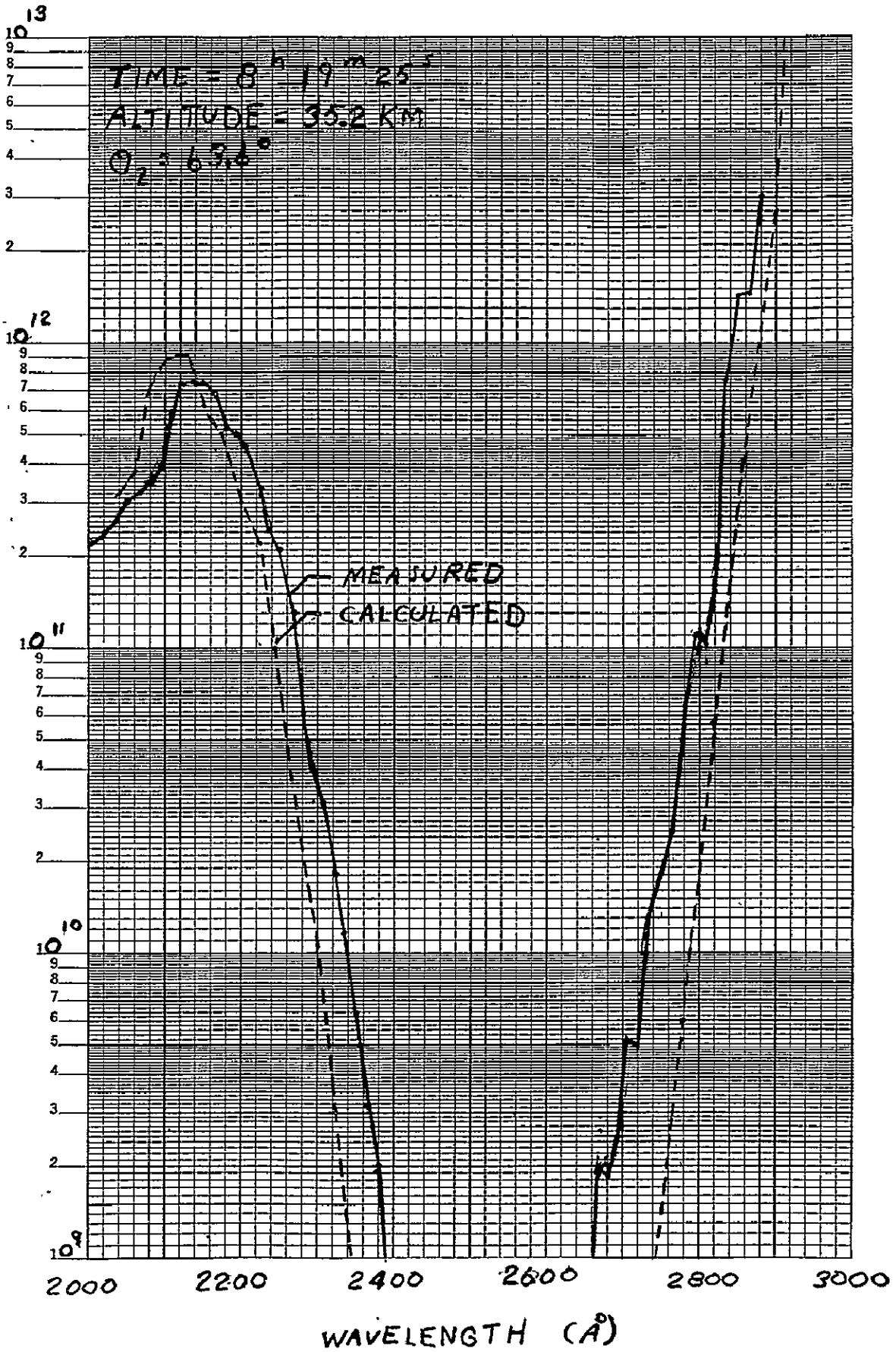
### EXPERIMENTAL

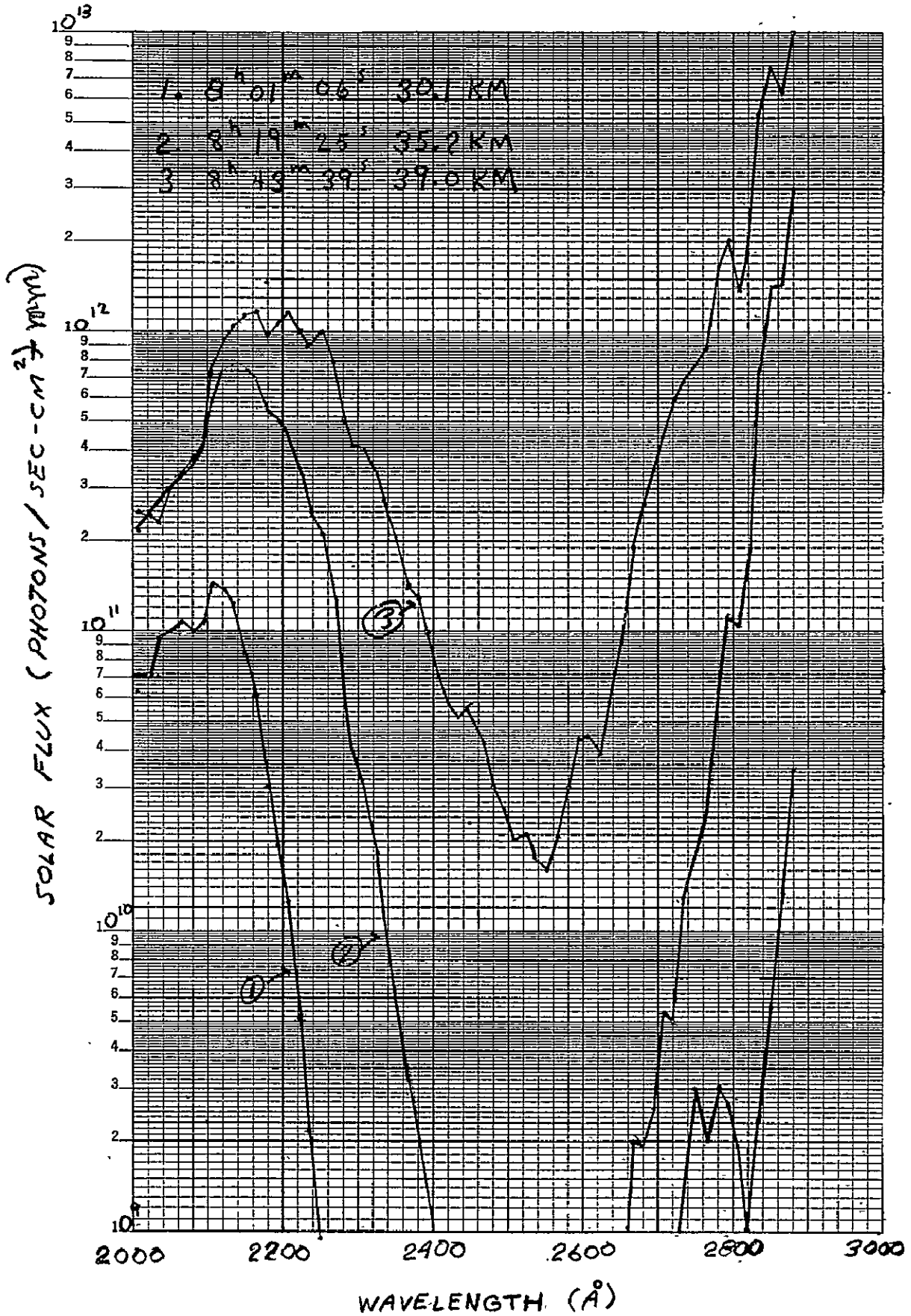
The flight spectrometer has been previously described in detail in the October 1977 STRATCOM-VIII report (E. I. Reed, GSFC X-624-77-261). In brief, the instrument consisted of an 0.125m scanning spectrometer preceded by a wide band interference filter to reduce scattered light in the system and a conical diffuser. The entire system was calibrated using a standard lamp at wavelengths above 2500Å and using a double monochromator technique to extend the calibration to below 2000Å. A relative accuracy of ±5% in the calibration was obtained with an additional ±10% error in the absolute flux. The variation of sensitivity with solar zenith angle is taken into account in the calibration.

### RESULTS

At this time, the experimental results have not been reduced to final form. A correction remains to be applied to the raw data at short wavelengths (<2100Å) and the effect of scattered light in the instrument has to be taken into account. Similarly, the model calculations are still in progress. A sample spectrum however is presented in Fig. 1. This particular spectrum was chosen because the altitude and solar zenith angle comes close to matching that for which a theoretical spectrum has been calculated. Reasonable agreement is obtained between the synthetic and observed spectra. This agreement is expected to improve when the calculations are refined.

SOLAR FLUX (PHOTONS / SEC - CM<sup>2</sup> - nm)





## MEASUREMENTS OF RADIATIVE ENERGY TRANSFER

## WITHIN THE ATMOSPHERE'S FIRST 40 KM

R. Rubio, USA Atmospheric Sciences Laboratory, WSMR, NM  
C. McDonald, University of Texas at El Paso, El Paso, TX  
M. Izquierdo, University of Texas at El Paso, El Paso, TX

## ABSTRACT

Measurements of solar shortwave irradiance and terrestrial infrared irradiance were made aboard the Stratcom VIII-a balloon on 29 September 1977 for respective periods of 3-1/2 hours and 23 hours. In addition solar shortwave irradiance measurements were made on 29 and 30 September at ground level. The measurement objectives and results are described in this report.

## INTRODUCTION

The ultimate objective of this experiment is to measure the amount of radiative energy transformed within the earth-atmosphere's heat budget as a function of other Stratcom measured parameters such as  $O_3$ ,  $H_2O$ ,  $CO_2$  and density. A secondary objective is to simultaneously determine earth albedo at balloon altitudes and on the earth's surface. By measuring the impinging solar shortwave irradiance, the corresponding shortwave irradiance reflected by the earth and atmosphere, and the longwave infrared irradiance escaping towards space on two successive cloudless days, the above objectives may be accomplished. Although two complete sets of irradiance data satisfying all the aforementioned requirements have not yet been obtained, progress towards that goal has been made and is the subject of this report.

To determine the earth-atmosphere's heat budget, two 0.28 to 2.8 micron pyranometers and one 4 to 50 micron Epply pyranometer were added onto the Stratcom VIII-a payloads and two additional shortwave pyranometers were operated at ground level. The experimental arrangement of the five pyranometers is depicted in Figure 1 in juxtaposition with a mean annual heat budget for the whole earth which was derived by G. D. Robinson (Advances in Geophysics, Vol 14, Chapter 10). Pyranometer 1 was mounted on the balloon's top plate and used to measure incoming solar flux while pyranometers 2 and 5 were located on the main instrumentation platform facing downward. Sensors 2 and 5, respectively, measured the total shortwave irradiance escaping into space and the total outgoing longwave irradiance. Pyranometers 3 and 4 were unobstructively located five feet above the desert floor and used to measure the shortwave irradiance impinging on the

ground and the amount of ground reflected radiation. As is illustrated in Figure 1, this arrangement of pyranometers will provide a measurement of those energy magnitudes entered in Robinson's diagram. For example, the radiation energy difference recorded with pyranometers 1 and 3 provide a measure of the amount of incoming radiation attenuated by the intervening atmosphere, while pyranometers 2 and 4 yield the same information about outgoing shortwave energy. These energy differences may be examined for quantitative dependence on atmospheric density,  $H_2O$ ,  $CO_2$  and  $O_3$ , provided the sky is devoid of clouds. Consequently, a Nikon camera, also illustrated in Figure 1, was attached to the main payload facing downward in order to detect the presence of clouds and photograph the terrain's reflective features. The combinations of pyranometers 1-2 and 3-4 should yield a measure of the earth's albedo at balloon altitudes and at ground level.

#### INSTRUMENTATION

The shortwave radiometers are Epply Precision Spectral Pyranometers (Epply Laboratory, Inc., 12 Sheffield Ave., Newport, RI), Model PSP, each with two concentric dome light filters which provide a  $180^\circ$  field of view and a wavelength transparency of 0.28 to 2.8 micrometers. The actual sensor comprises a circular multifunction thermopile<sub>1</sub> with a sensitivity in the order of 8 millivolts/cal  $cm^{-2}$   $min^{-1}$  and a one second time response. The expected performance accuracy of 8.5% for the zenith viewing PSP pyranometer is based on manufacturer specifications, payload calibration and accounts for solar zenith angle variations caused by top payload (balloon) wobble during the flight. The Nadir viewing PSP instrument performance accuracy was calculated to be 2.5%. An Epply Precision Infrared Radiometer (Pyrgeometer) with a  $180^\circ$  field of view and a wavelength transparency of 4 to 50 micrometers was the longwave radiation sensor. This pyranometer also has a thermopile<sub>2</sub> detector, but its sensitivity is approximately 5 mv/cal  $cm^{-2}$   $min^{-1}$  and its time response is two seconds. An overall expected performance accuracy of 3% was computed for this instrument and its associated electronics. The camera is a Nikon, model F2AS, with a DS-1 automatic aperture control. The lens was Nikon 16mm full frame fisheye providing a  $170^\circ$  viewing angle. Photographs were synchronized for exposure to occur at the beginning of each Stratcom data sample and the film transport was keyed to the telemetry clock such that the time between exposures was about five minutes.

#### ANALYSIS

Down-welling shortwave radiation data at balloon altitudes was obtained for a period of approximately 3-1/2 hours on the morning of 29 September 1977. These data, plotted on Figure 2, show that irradiance<sub>2</sub> magnitudes varied from 0.05 cal/ $cm^2$   $min^{-1}$  at 0615 to 1.41 cal/ $cm^2$   $min^{-1}$  at 0950 MST. After 0950, the telemetry

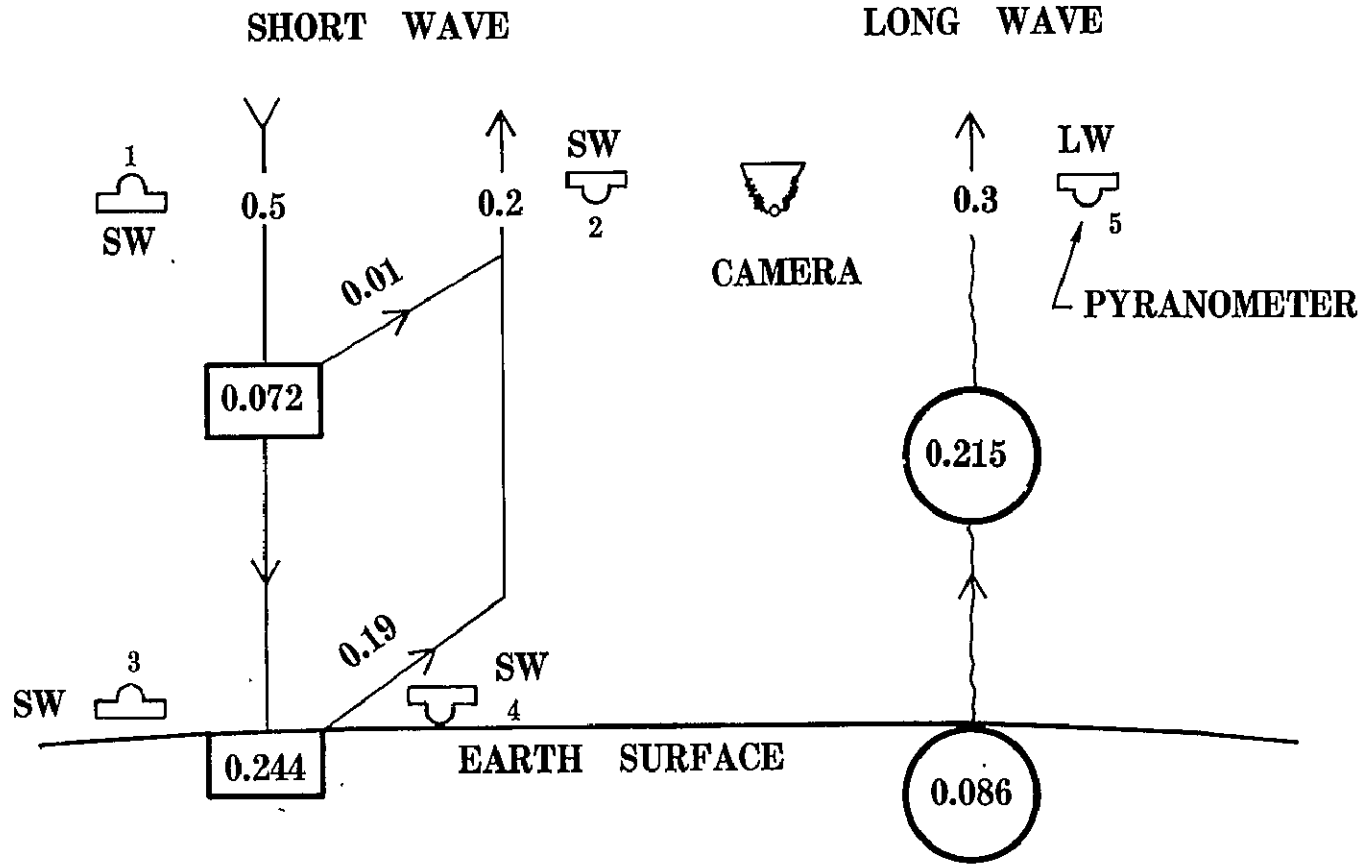


signal from the balloon's top payload transmitter expired and no additional data was collected. The Nadir viewing infrared pyranometer mounted on the balloons main payload frame sensed considerably more data. Up-welling longwave irradiance values were recorded from 0615, 28 September to 0530, 29 September. These values are shown in Figure 2 and on an expanded power density ordinate scale in Figure 3. Also included in Figure 3 is a graph of absolute temperatures at balloon altitudes as a function of time. Examination of the Figure 3 infrared irradiance and temperature plots reveals that this pyranometer primarily sensed the radiation of the atmosphere in the proximity of the radiometer. Longwave irradiance values recorded ranged from  $0.17 \text{ cal/cm}^2 \text{ min}$  to  $0.34 \text{ cal/cm}^2 \text{ min}$ . Up-welling shortwave irradiance data was not acquired because of payload malfunctioning throughout the flight.

Nadir viewing photographs, which are not included here, displayed a general absence of clouds throughout the flight except for a very few tenous cirrus that occurred on the morning of 29 September. The terrain features varied from forested terrain when above the Sacramento Mountains to desert type terrain when above the basin regions.

Surface measurements of both, down-welling and earth reflected, irradiances were successfully obtained for all daylight hours during which the balloon was aloft. Plots of these surface measurements are also entered in Figure 2. The maximum shortwave irradiance impinging upon the earth was found to be  $1.23 \text{ cal/cm}^2 \text{ min}$  while the magnitude of the maximum reflected irradiance was  $0.32 \text{ cal/cm}^2 \text{ min}$ . These magnitudes yield an earth surface albedo of 0.26 for desert type terrain. Figure 2 illustrates the shortwave radiation absorbed and reflected by the atmosphere between the balloon altitude and the earth surface. For instance, at 0900 MST and an approximate solar zenith angle of  $55^\circ$ , about  $0.38 \text{ cal/cm}^2 \text{ min}$  were dissipated within the intervening atmosphere. The lack of up-welling shortwave irradiance data precluded calculating earth albedo at balloon altitudes and construction of an earth-atmosphere heat distribution diagram for 29 September 1977.

# RADIATION



MEAN ANNUAL HEAT BUDGET FOR THE WHOLE EARTH.  
 UNITS IN  $\text{CAL CM}^{-2} \text{ MIN}^{-1}$  BY G. D. ROBINSON

# STRATCOM VIII A PYRANOMETERS

## EPPLY PRECISION SPECTRAL

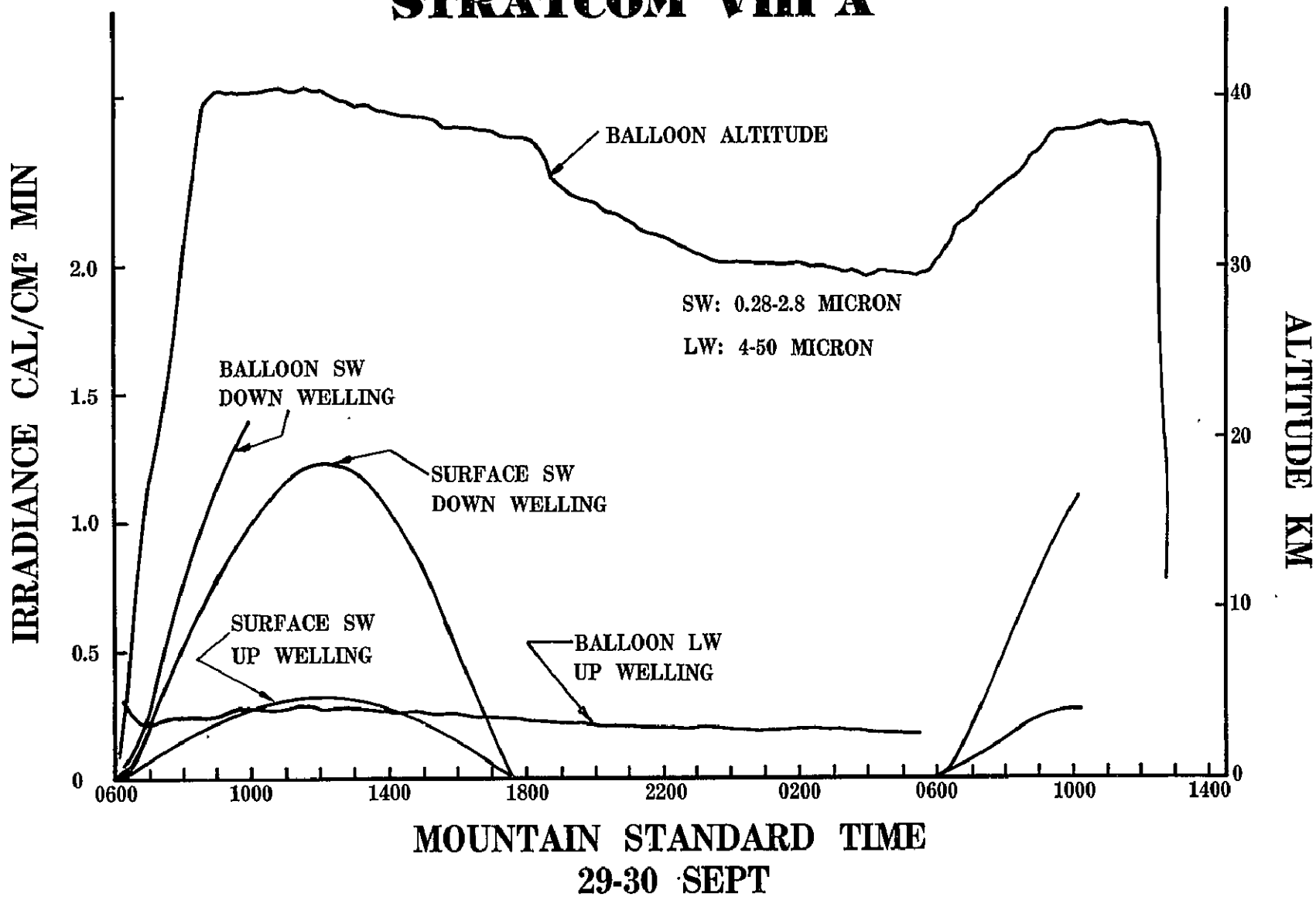
WINDOW	0.28 TO 2.8 MICRON
FIELD OF VIEW	180° (2 $\pi$ STERADIANS)
TIME RESPONSE	1 SEC
TEMPERATURE RANGE	-70 TO +50°C
EXPERIMENTAL ACCURACY	
SKYWARD	6.5%
EARTHWARD	2.5%

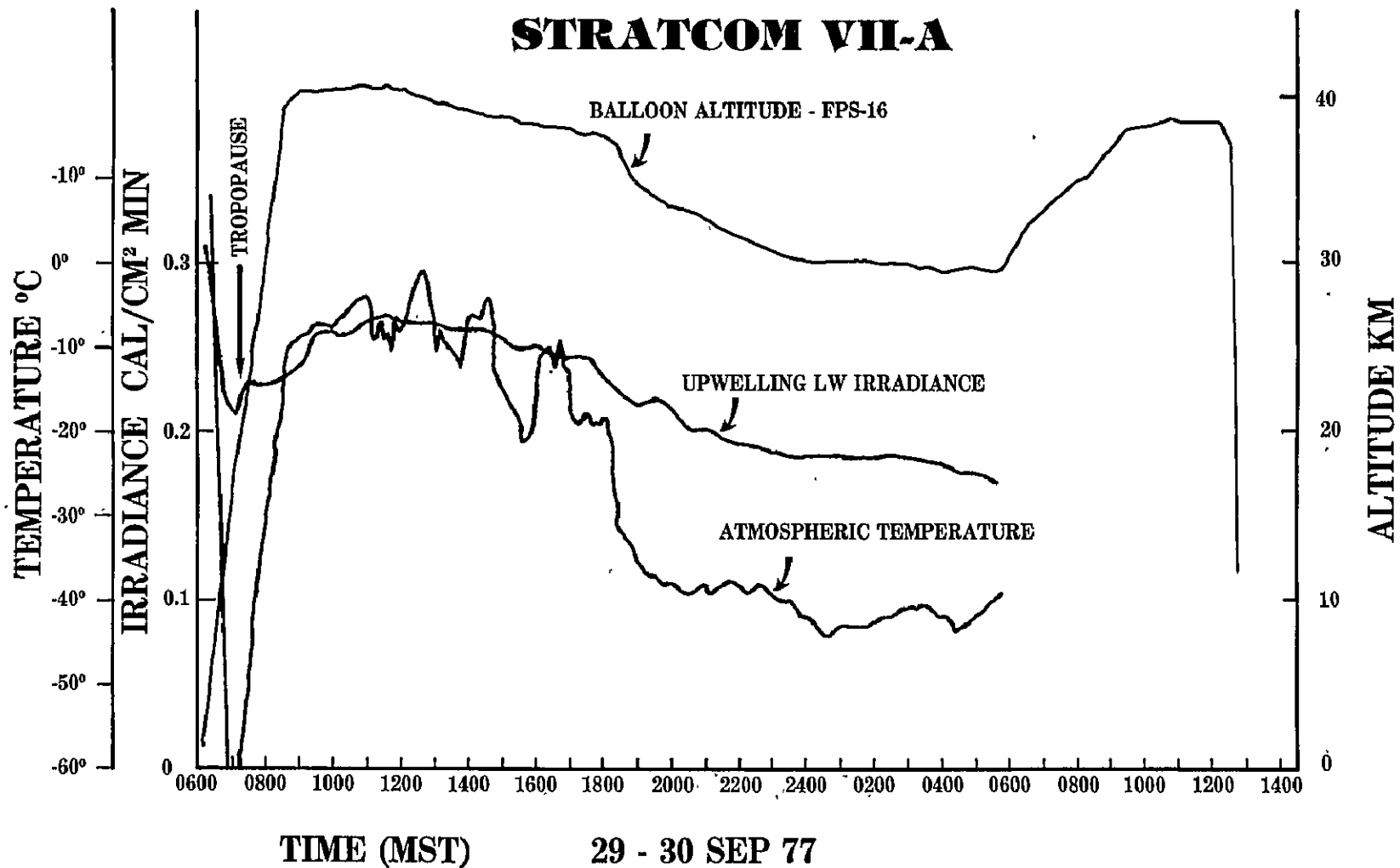
## EPPLY INFRARED RADIOMETER

WINDOW	4 TO 50 MICRONS
FIELD OF VIEW	180° (2 $\pi$ STERADIANS)
TIME RESPONSE	2 SEC
TEMPERATURE RANGE	-20 TO +40°C
EXPERIMENTAL ACCURACY	3%

# STRATCOM VIII A

-73-





Apex Plate Payload,  
Balloon VIII-A  
balloon-skin temperature  
air temperature  
water vapor  
Lyman-alpha radiation  
pyranometer

Carlos McDonald  
Electrical Engineering  
Department  
University of Texas at  
El Paso  
El Paso, Texas 79968

1. Description and Operation  
(Refer to NASA document, "STRATCOM VIII Scientific Objectives and Mission Organization", Edith Reed, GSFC-X-624-77-261, October 1977.)
2. Time Period and Altitude Range of Useful Data  
(Time Period: 6:13 to 9:43 MDT)  
Altitude Range: 3.6 to 40 km (ascent and initial float altitude range.)
3. Significant Events Affecting Data  
Telemetry of data limited to approximately three hours due to power supply failure.
4. Data
  - (a) Balloon-Skin Temperature  
Sensor: Bead Thermistor, .010 in diameter.  
Results: Balloon-skin temperature is shown tabulated and plotted as a function of Mountain Daylight Time (MDT) in Figures 1 and 2, respectively. For reference, the plot includes altitude and the average air temperature as measured on the main instrument platform. Data averaging was over 10 second intervals.  
  
As expected for daylight launchings, the balloon skin-temperature was generally warmer near and at float altitude due to radiation absorption.
  - (b) Air Temperature  
Sensor: STS film-mounted bead thermistor, .010 in diameter.  
Results: Data not obtained due to breakage of sensor during launch.
  - (c) Water Vapor  
Sensor: Al<sub>2</sub>O<sub>3</sub> Film Capacitance Sensor.  
(Panametrics, Inc.)  
Results: The frequency data obtained from this sensor is tabulated and plotted in Figures 3 and 4, respectively, as a function of time (MDT). Data was averaged over a 10 second interval. Frequency, an inverse function of water vapor, will be established from calibration data of

Panametrics, Inc.

(c) Water Vapor

Sensor: Radiosonde resistance type.

Results: This sensor was not included due to lack of channels.

(e) UV Radiation: Lyman-Alpha Range

Sensor: Mg-Fl. - No Ionization Chamber, 114.0-134.0 N.M. range.

Results: Based on the telemetered data, both the ionization gage and electronics worked satisfactorily. As expected, no appreciable current was detected. It was hoped to obtain measureable results during high noon, but data transmission was terminated earlier, at 9:43 MDT.

(f) IR Radiation

Sensor: Epply Precision Infrared Pyranometer (Pyrgeometer), Model PIR, 0.2-2.8 micron range (R. Rubio, ASL.)

Results: The data obtained is tabulated and plotted as function of time (MDT) in Figures 5 and 6, respectively. For reference, the balloon altitude is also included in Figure 6. Data averaging was over a 10 second interval. (Refer to Mr. Robert Rubio's analysis of this and other IR data).

(g) Levelness Indicator-Balloon Apex Plate

Sensor: Conductive Fluid Vessel.

Results: The frequency deviation, proportional to the angle of inclination from horizontal, is tabulated and plotted in Figures 7 and 8, respectively. Data was averaged over a 5 second interval.

The relation between frequency and inclination is approximately .01 degrees per Hz. Hence, the results indicate that the position of the apex plate is stable and remains essentially horizontal during descent and at float altitude, an ideal platform for experiments requiring an upward clear view and a stable horizontal platform.

STRATCOM VIII  
SKIN TEMPERATURE

TIME (MDT)	DEGREES (C)
6. 21667	27
6. 28333	5
6. 35	-5
6. 42333	-11
6. 5	-21
6. 56667	-31
6. 63333	-39
6. 7	-46
6. 76667	-54
6. 83333	-57
6. 91667	-59
6. 98333	-57
7. 05	-52
7. 11667	-49
7. 18333	-42
7. 25	-37
7. 33333	-35
7. 4	-31
7. 46667	-30
7. 53333	-28
7. 6	-27
7. 66667	-24
7. 73333	-23
7. 8	-21
7. 86667	-21
7. 93333	-18
8	-14
8. 06667	-18
8. 13333	-18
8. 21667	-15

Figure 1

ORIGINAL PAGE IS  
OF POOR QUALITY



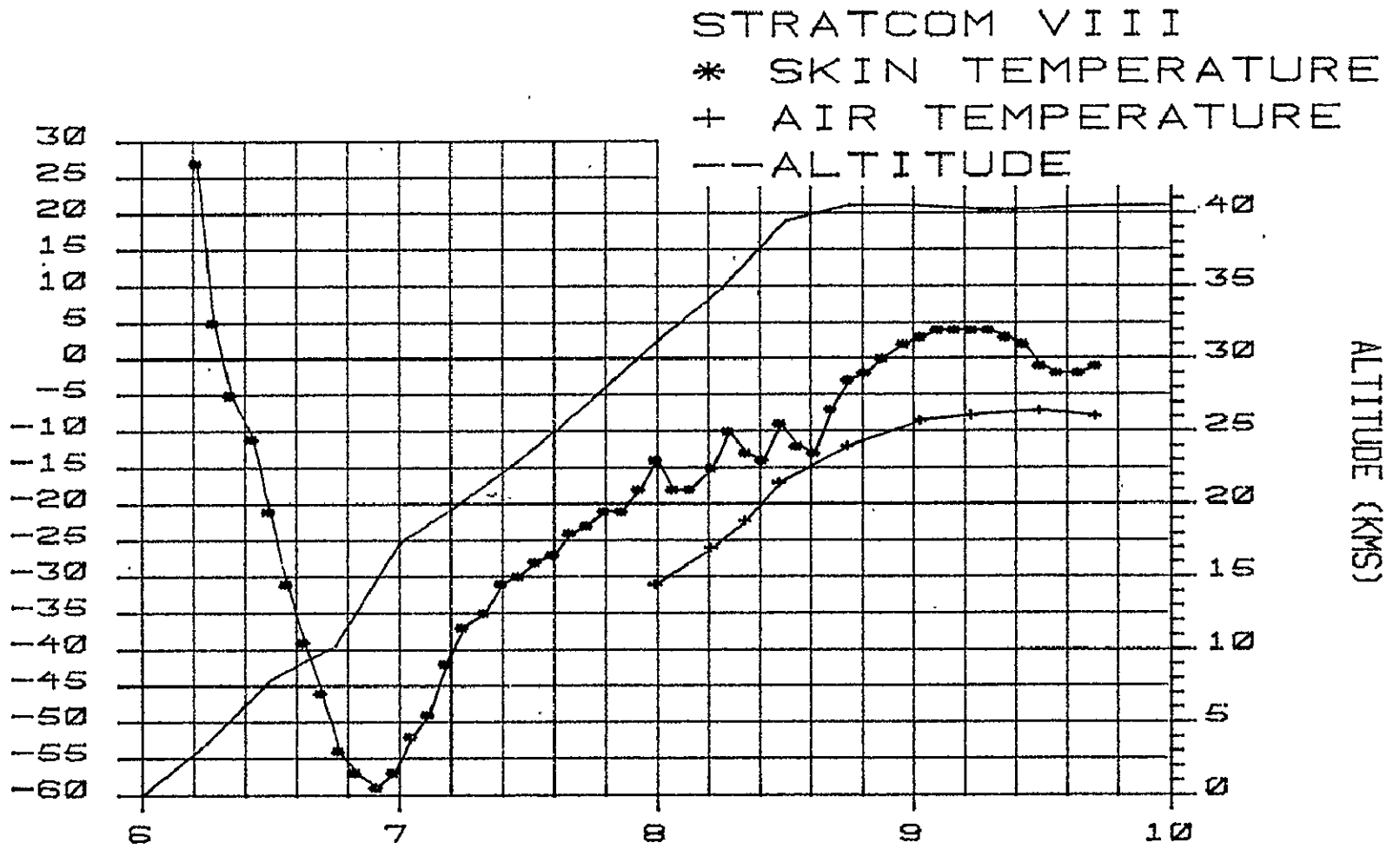
STRATCOM VIII  
SI.IN TEMPERATURE

TIME (MDT)	DEGREES (C)
8. 28333	-10
8. 35	-13
8. 41667	-14
8. 48333	-9
8. 55	-12
8. 61667	-13
8. 68333	-7
8. 75	-3
8. 81667	-2
8. 88333	0
8. 96667	2
9. 03333	3
9. 1	4
9. 16667	4
9. 23333	4
9. 3	4
9. 36667	3
9. 43333	2
9. 5	-1
9. 56667	-2
9. 65	-2
9. 71667	-1

Figure 1 continued

ORIGINAL PAGE IS  
OF POOR QUALITY

DEGREES CENTIGRADE



ALTITUDE (KMS)

M D T  
Figure 2

STRATCOM VIII TOP PACKAGE  
PANAMETRICS AL. OXIDE WATER VAPOR SENSOR

TIME (MDT)	FREQUENCY (HZ)
7:30	262.5
7:34	265.0
7:38	282.5
7:42	285.0
7:46	282.5
7:50	270.0
7:54	267.5
7:58	262.5
8:02	265.0
8:06	260.0
8:10	250.0
8:14	235.0
8:18	227.5
8:22	220.0
8:26	220.0
8:30	230.0
8:34	230.0
8:38	250.0
8:42	257.0
8:46	262.5
8:49	280.0
8:53	285.0
8:56	280.0
9:02	270.0
9:05	267.5
9:10	260.0
9:14	262.5
9:18	260.0
9:22	250.0
9:26	232.5
9:29	225.0
9:34	220.0
9:38	220.0
9:42	227.5
9:46	232.5
9:50	250.0
9:54	255.0

Figure 3

ORIGINAL PAGE IS  
OF POOR QUALITY

STRATCOM VIII TOP PACKAGE  
AL. O2 WATER VAPOR SENSOR  
+ SENSOR - ALTITUDE

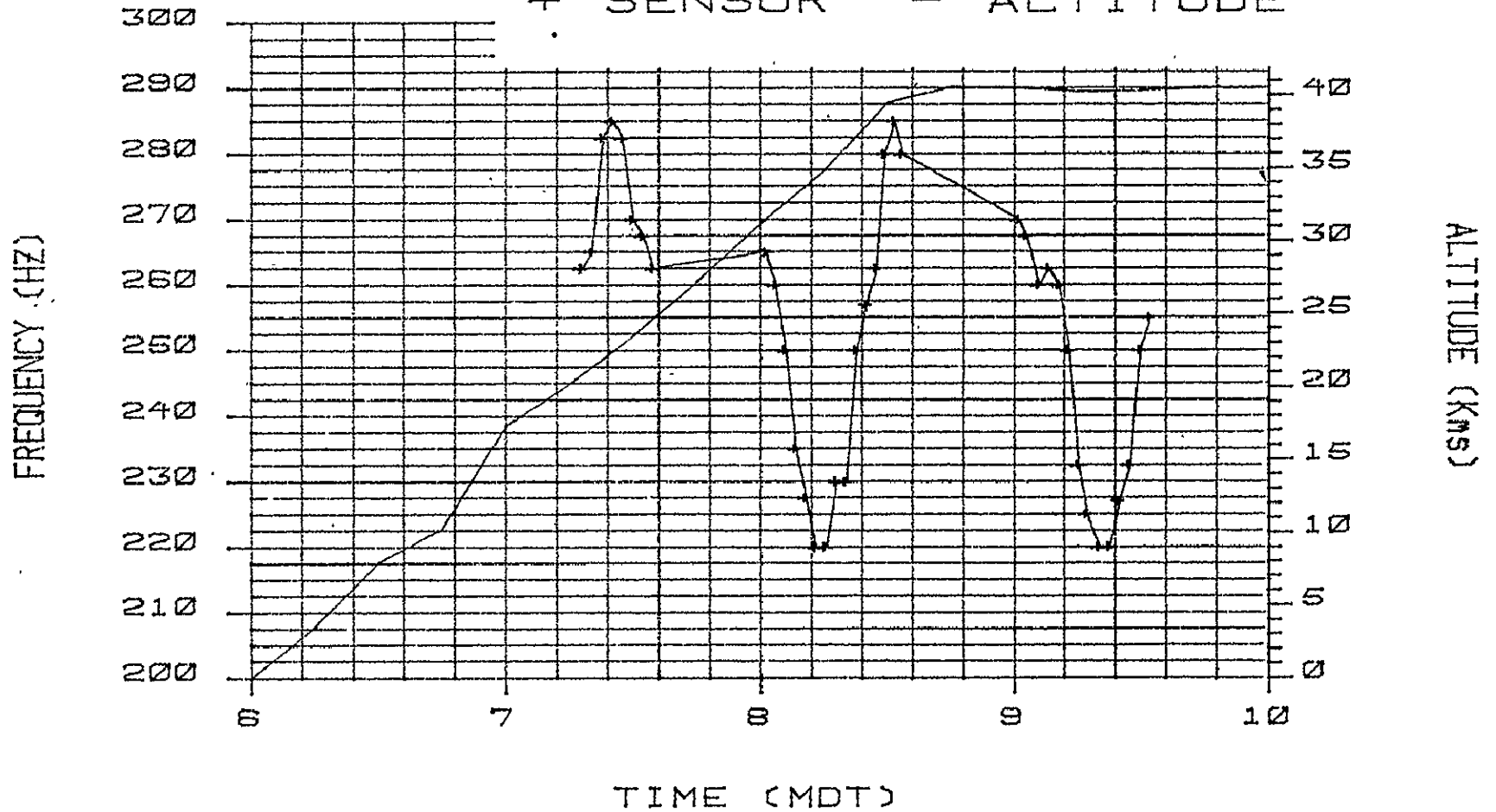


Figure 4

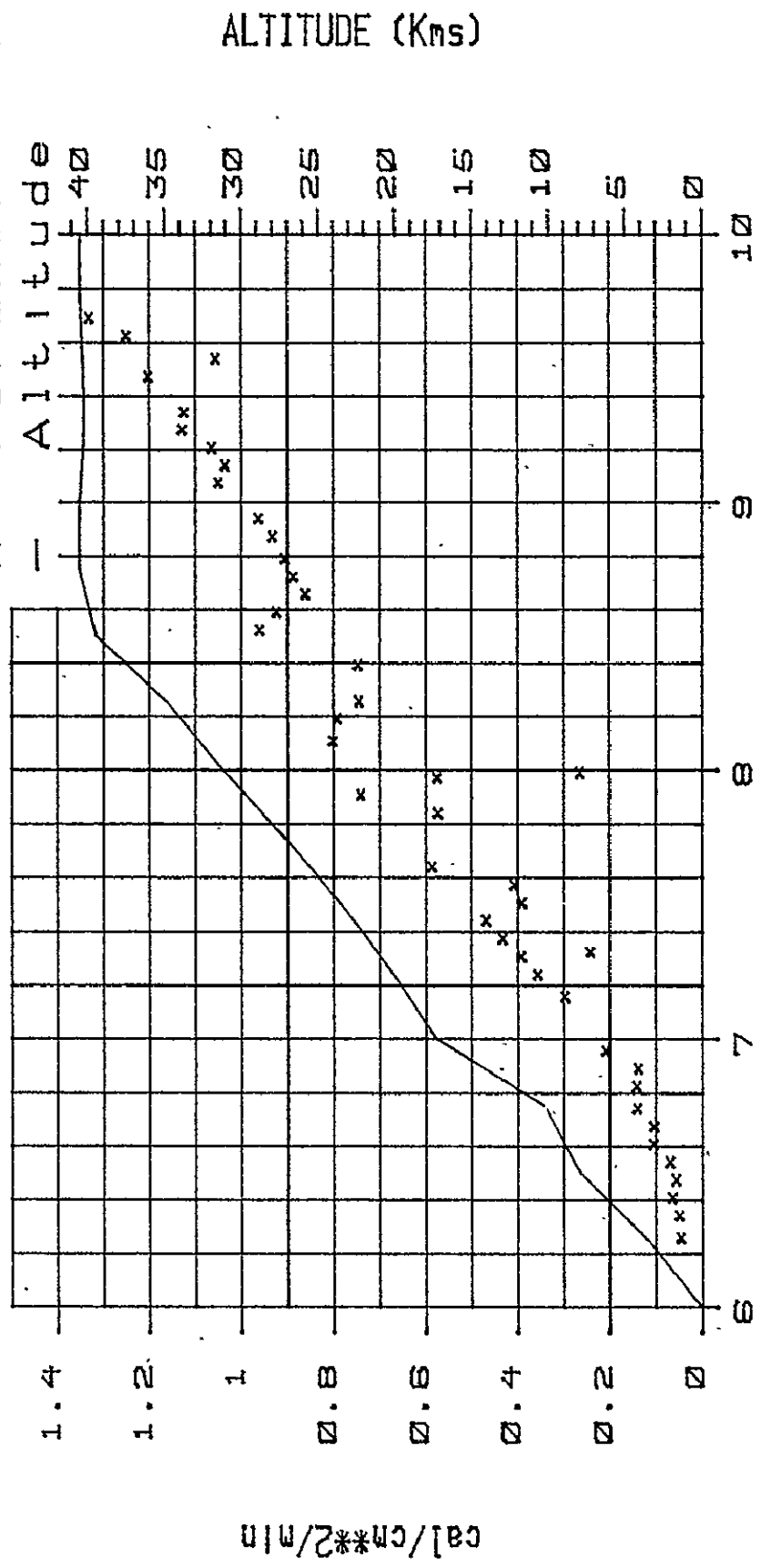
## STRATCOM VIII

## PYRANOMETER

TIME(MDT)	CAL/CM**2/MIN
6. 26667	. 05
6. 35	. 053
6. 41667	. 068
6. 48333	. 06
6. 55	. 073
6. 61667	. 109
6. 68333	. 108
6. 75	. 145
6. 83333	. 147
6. 9	. 143
6. 96667	. 213
7. 16667	. 302
7. 25	. 361
7. 31667	. 396
7. 33333	. 247
7. 38333	. 437
7. 45	. 473
7. 51667	. 395
7. 58333	. 412
7. 65	. 591
7. 85	. 578
7. 91667	. 745
7. 98333	. 58
8	. 27
8. 11667	. 806
8. 2	. 796
8. 26667	. 749
8. 4	. 751
8. 53333	. 964
8. 6	. 928
8. 66667	. 866
8. 73333	. 892
8. 8	. 91
8. 88333	. 937
8. 95	. 967
9. 08333	1. 054
9. 15	1. 04
9. 21667	1. 07
9. 28333	1. 133
9. 35	1. 129
9. 48333	1. 207
9. 55	1. 06
9. 63333	1. 255
9. 7	1. 335
9. 83333	1. 414

Figure 5

STRATCOM VIII  
TOP PACKAGE  
X - Pyranometer



M D T  
Figure 6

STRATCOM VIII TOP PACKAGE  
INCLINATION DATA

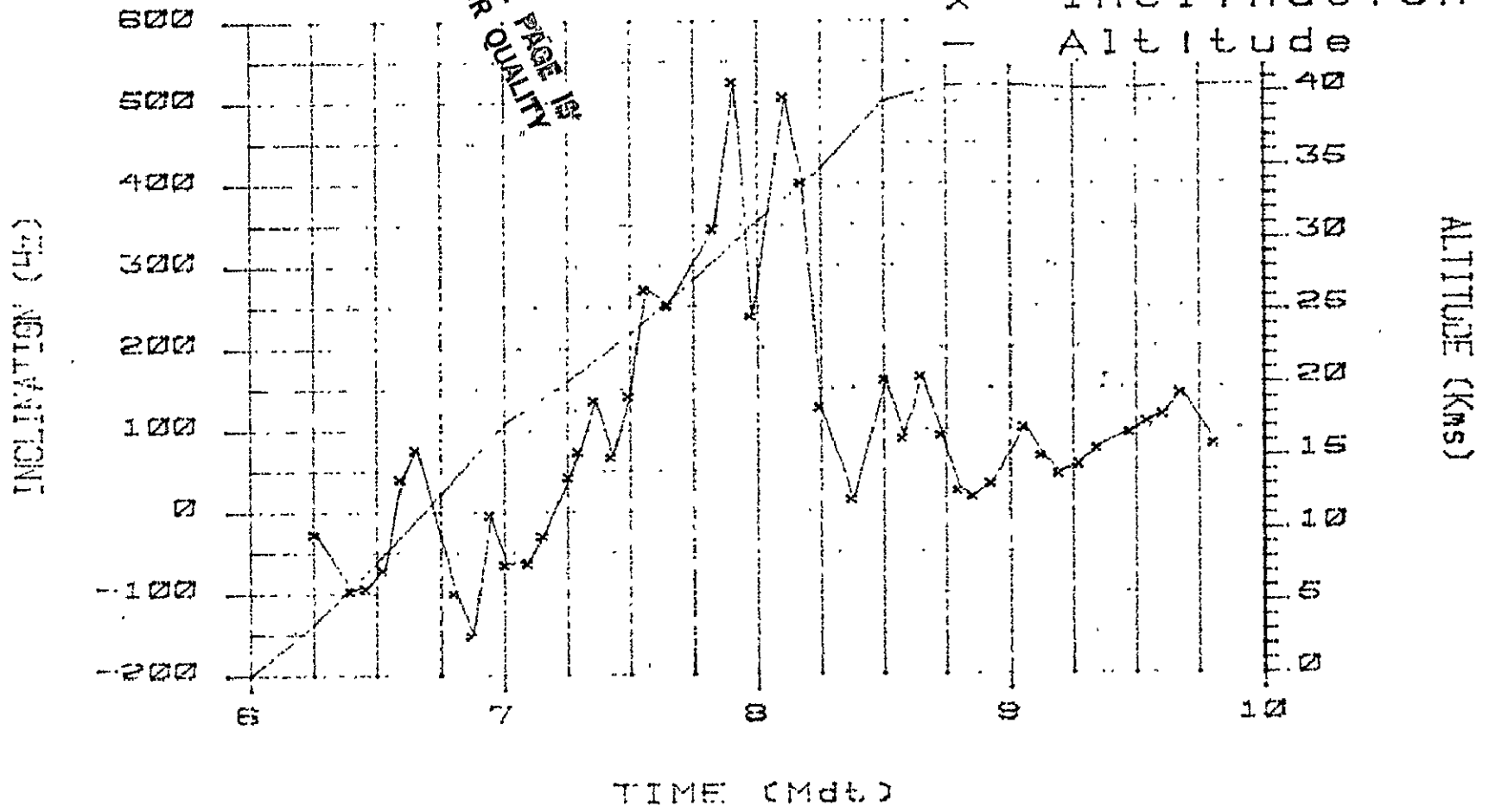
TIME(ZULU)	AVG. INCLINATION
13:16:10	-25
13:24:20	-94
13:28:30	-90.8333
13:32:40	-68.8333
13:36:50	42.8333
13:40:00	78.6667
13:45:10	1456
13:49:20	-97.5
13:53:30	-149.667
13:57:40	-1.33333
14:01:50	-62.5
14:06:00	-61
14:10:10	-27.5
14:14:20	44.1667
14:18:30	75.5
14:22:30	137.833
14:26:40	69
14:30:50	143
14:34:50	273.333
14:39:00	254.167
14:50:50	347.833
14:55:00	527
14:59:10	240.833
15:07:20	509
15:11:30	404.167
15:15:40	192.167
15:23:40	16.1667
15:31:30	162
15:35:40	90.5
15:39:50	165.833
15:44:00	95
15:48:00	27.3333
15:52:20	19.5
15:56:20	35.1667
16:04:30	103.667
16:08:40	68.8333
16:12:50	46.3333
16:17:02	58.5
16:21:10	77.6667
16:29:10	97
16:33:20	110.333
16:37:30	119.667
16:41:40	145.333
16:49:40	83

Figure 7

ORIGINAL PAGE IS  
OF POOR QUALITY

ORIGINAL PAGE IS  
OF POOR QUALITY

STRATCOM VIII  
TOP PACKAGE  
x Inclination  
— Altitude



TIME (Mdt.)

Figure 8

0-9



Anemometers  
STRATCOM  
VIII-A

Carlos McDonald  
Electrical Engineering Department  
University of Texas at El Paso  
El Paso, Texas 79968

### 1. Description and Operation

The wind anemometer is based on the use of bead thermistors (.011 n. diameter) exposed to the air flow and operated in a constant temperature mode. Matched thermistor pairs operating at different temperatures are used to eliminate the dependence on ambient temperature and pressure. Air density dependence is accounted for by the use of an enclosed reference pair of thermistors. At pressures lower than 10 mm Hg, the reference pair may serve as a densitometer. Calibration is based on the measurement of the difference in thermistor power as a function of Reynolds number by varying wind speed and density.

### 2: Objectives

Four of these instruments were arranged as a 3-axis wind anemometer for monitoring the horizontal and vertical wind components of air flow relative to the instrument platform. These measurements may provide information regarding the Lagrangian characteristics of the balloon and on boundary layer phenomena.

### 3. Time Period and Altitude Range of Useful Data

Useful data was obtained throughout the flight, starting from 7:21 AM (MDT) on the first day of flight.

### 4. Significant Events Affecting Data

Due to a circuit malfunction, data was not obtained from one of the horizontal and one of the vertical (downward component) anemometers. In addition, data was not obtained from the high sensitivity channels. However, useful data was obtained from the remaining anemometers which measured the horizontal and upward vertical wind components.

### 5. Data

The frequency deviation, corrected for both temperature and density effects, is tabulated and plotted as a function of time (MDT) in Figures (1) and (2), respectively. Ten second averaging of data was used, and only the ascent and initial float altitude is shown. Although the relation between frequency deviation and wind speed has not been definitely established at this time, the maximum relative wind speed should be less than 0.5 m/sec at float altitudes, as has been established in previous STRATCOM flights.

STRATCOM VIII  
WIND ANEMOMETERS

TIME MDT	VX (HZ)	VZ (HZ)
7. 36611	-74	-2
7. 39556	-217	-109
7. 42333	-252	-199
7. 45194	-221	-93
7. 47944	-77	-127
7. 50806	-129	-68
7. 53611	-270	-135
7. 56417	-79	-108
7. 59333	-141	-126
7. 62167	-33	-103
7. 64972	-30	-89
7. 67806	-36	-139
7. 70583	-156	-108
7. 73528	-44	-100
7. 76306	-20	-124
7. 79139	-39	-160
7. 81972	-54	-121
7. 84806	-70	-126
7. 87639	-27	-61
7. 90417	4	-93
7. 9325	-22	-92
7. 96083	-3	-77
7. 98917	-7	-89
8. 01917	-26	-73
8. 04528	-9	-77
8. 07583	-17	-64
8. 10111	-20	-61
8. 12917	8	-61
8. 15861	-153	-81
8. 18722	-29	-53
8. 21528	-24	-64
8. 24306	-28	-57
8. 27111	-19	-85
8. 29917	-47	-81
8. 3275	-57	-77
8. 35556	-44	-74
8. 38361	-109	-75
8. 41194	-34	-70
8. 44028	-13	-73
8. 46851	-10	-68

Figure 1

ORIGINAL PAGE IS  
OF POOR QUALITY

STRATCOM VIII  
WIND ANEMOMETERS

TIME MDT	VX (HZ)	VZ (HZ)
8 49639	0	-74
8 52472	0	-70
8 55361	-37	-65
8 58332	-78	-77
8 60972	-46	-50
8 63806	-63	-56
8 66667	-67	-80
8 69444	-36	-58
8 72194	-49	-34
8 75111	-61	-62
8 77917	-68	-62
8 8075	-70	-70
8 83583	-39	-68
8 86417	-38	-66
8 8925	-49	-77
8 92028	-75	-67
8 94861	-31	-54
8 97667	-14	-56
9 06139	-41	-51
9 09	-82	-12
9 11832	-34	-50
9 14583	-52	-67
9 17556	-19	-39
9 20332	-55	-53
9 23139	-56	-57
9 25972	-45	-50
9 28806	-74	-6
9 31611	-67	-30
9 34444	-53	-40
9 37278	-53	-24
9 40083	-67	31
9 42889	-85	-26
9 4575	-70	-60
9 48554	-71	-68
9 51383	-112	69
9 54167	-111	69
9 57028	-138	55
9 59833	-100	-17
9 62667	-114	-12
9 655	-88	-19

Figure 1 continued

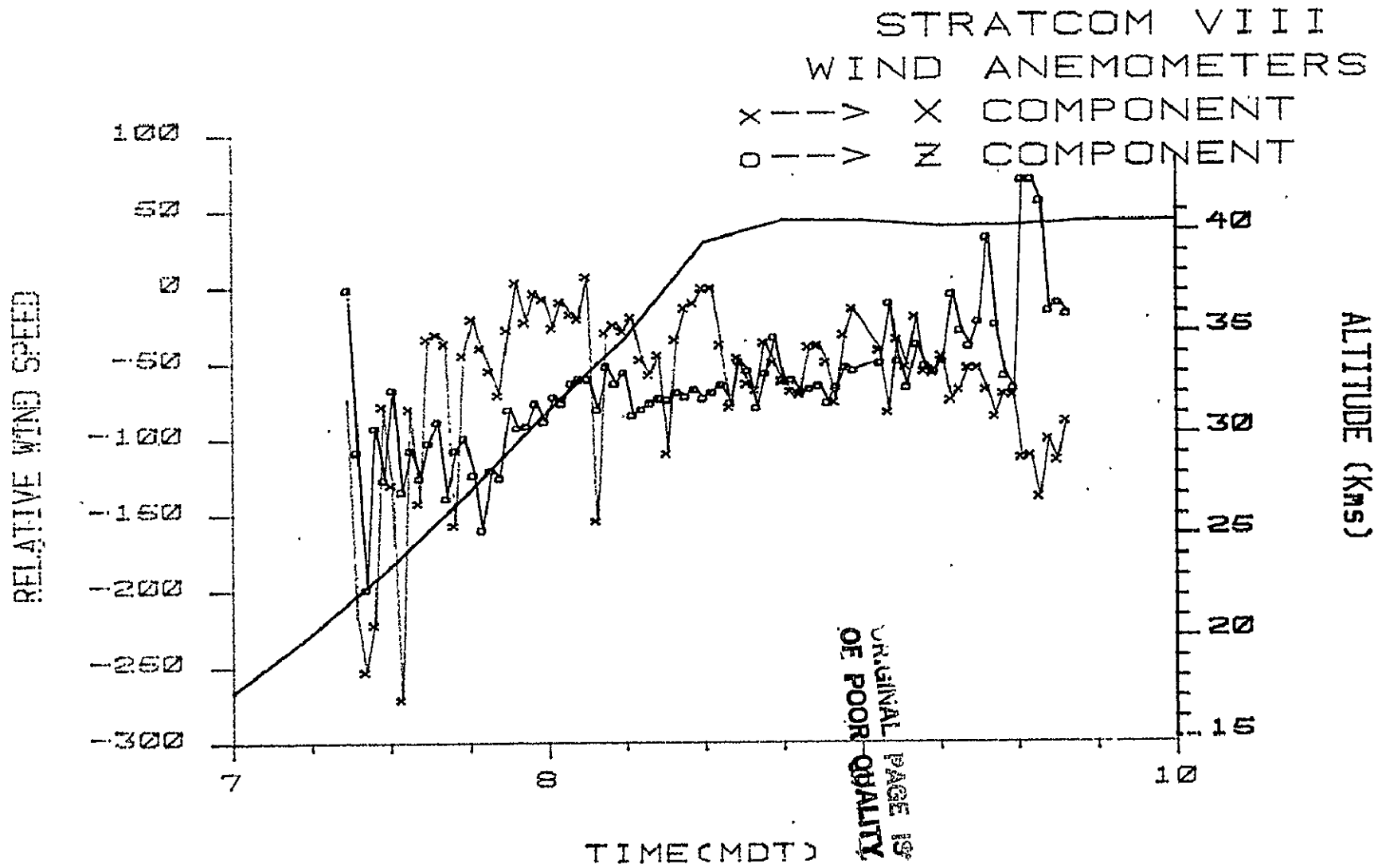


Figure 2

omit

U-2 Aircraft

MEASUREMENT OF INFRA-RED SPECTRA, NITROGEN OXIDES AND AEROSOLS

The U-2 aircraft flew in the vicinity of the STRATCOM-VIII effort on September 28 and 29. Aboard were the SAS-II chemiluminescent NO, NO<sub>2</sub>, and O<sub>3</sub> sensors (Loewenstein and Starr), the infrared spectrometer for thermal emission (Murcray), and the aerosol collectors (Farlow, Ferry, and Snetsinger). Data were obtained from all three types of instruments.

(Since all of the invitations to the Workshop that were sent to Ames Research Center went astray, a more detailed report could not be prepared for inclusion in this publication.  
Edith Reed)

Partial-Reflection Sounder

Ground Based

MEASUREMENT OF D-REGION ELECTRON DENSITY  
BY PARTIAL REFLECTIONS

R. O. Olsen, USA Atmospheric Sciences Laboratory, WSMR, NM  
D. L. Mott, Physical Science Laboratory, NMSU, Las Cruces, NM  
B. G. Gammill, Physical Science Laboratory, NMSU, Las Cruces, NM

## ABSTRACT

Measurements of electron density in the lower ionosphere were made at White Sands Missile Range throughout the STRATCOM VIII launch day using a partial-reflection sounder. Information regarding the sounder's antenna pattern was gained from the passage of the balloon over the array.

## INTRODUCTION

The Atmospheric Sciences Laboratory (ASL), White Sands Missile Range (WSMR), currently operates a partial-reflection sounder at the Range. The sounder provides measurements of free-electron density in the D-region of the ionosphere (below 100 kilometers). Measurements were made throughout the day on 29 September 1977, the launch day for STRATCOM VIII, and results are included herein.

## APPARATUS

The ASL sounder is a monostatic radar operating at 2.24 MHz, pulse width 20 microseconds, PRF 17 pulses per second. Pulses are transmitted vertically, and the received echoes, partially reflected from the lower ionosphere, are digitally recorded. Reflections from altitudes between 56 and 114 kilometers are recorded at 2 kilometer increments. The antenna array, used for both transmitting and receiving, consists of five pairs of crossed dipoles, strung between wooden poles. Four of the pairs are located at the corners of a square area of dimension 440 feet per side, and the fifth pair is located at the center of the square.

Pulses are transmitted and received in circular polarization, alternating between left and right hand polarization. This provides signals in the ordinary and extraordinary modes---terms that are associated with differing indices of refraction in the ionosphere. As is well known (see, for example, Belrose and Burke, *J. Geophys. Res.*, pp 2799-2818, 1 Jul 64), the ratio of echo amplitudes for the two modes provides a determination of electron density as a function of altitude.

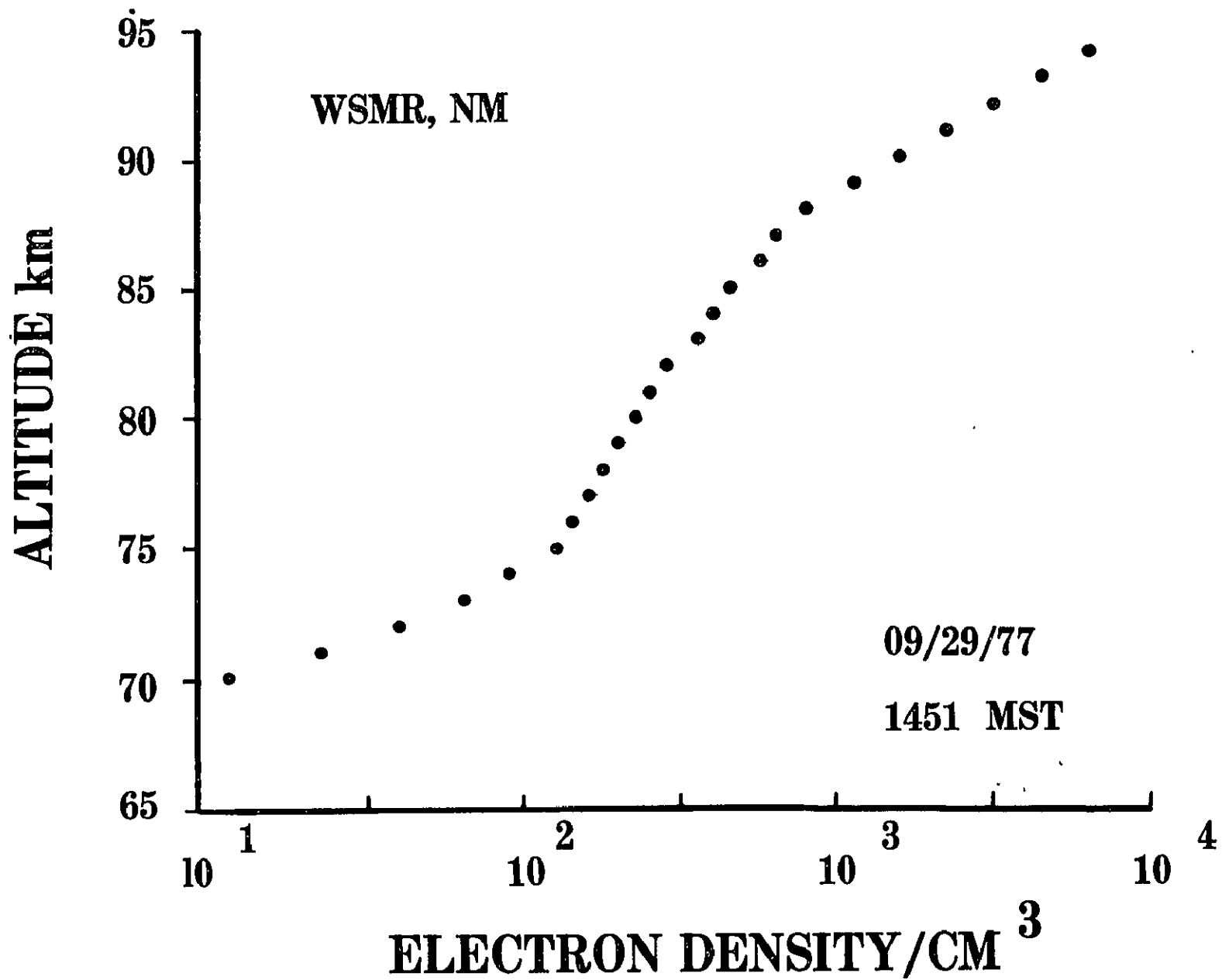
## ANALYSIS

In our data-processing procedure, the amplitude ratio is used only to provide a system-calibration constant. This constant along with corrections for the echo altitude and for signal attenuation below the altitude of interest, is then used to transform the ordinary-mode echo profile into an electron-density profile. Details of the data-processing procedure will be published at a later date.

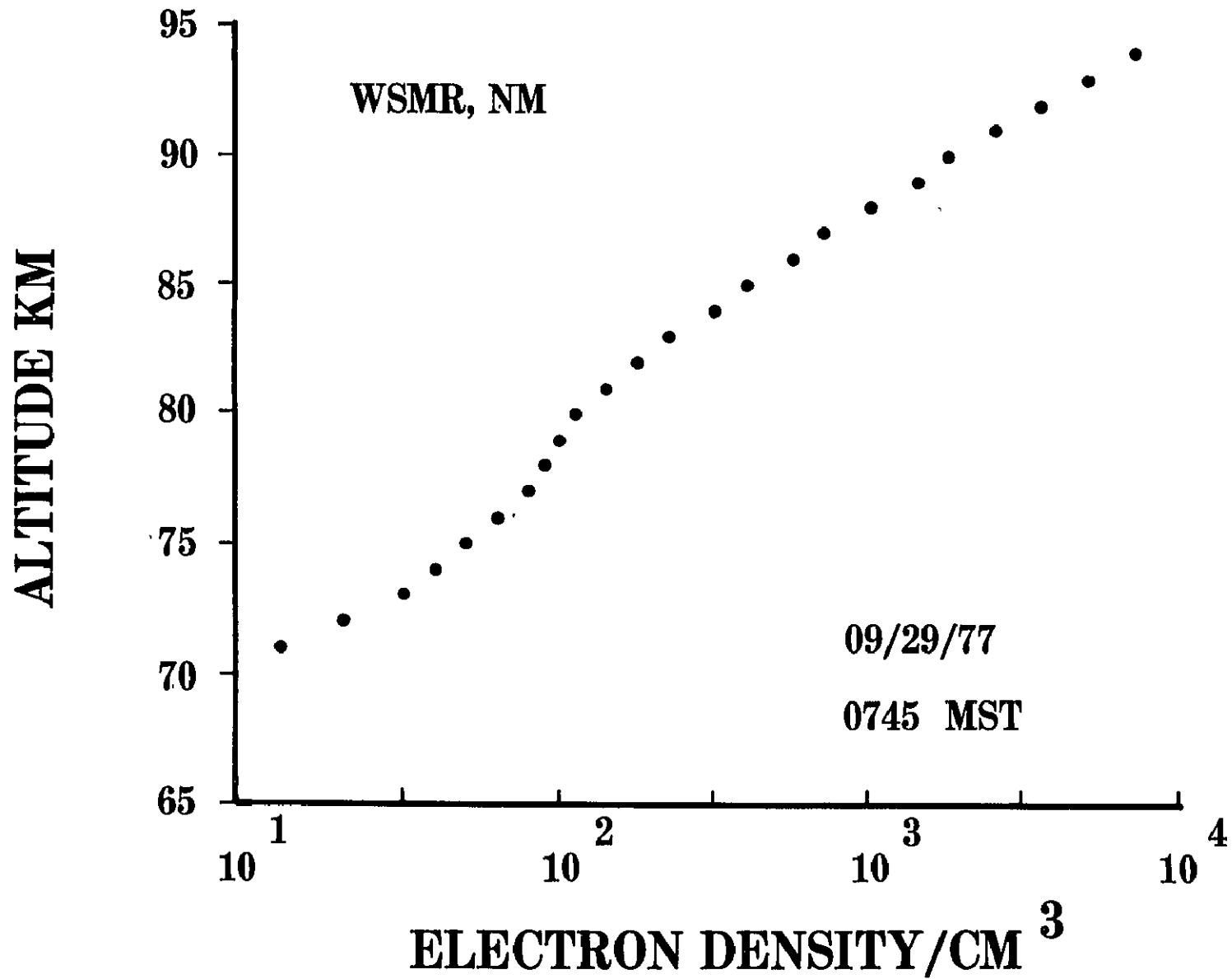
Fourteen runs were recorded on 29 September. Within each run, data was collected for approximately 10 minutes. Figures 1-3 show results for four of the runs. The starting time of the run, Mountain Daylight Savings Time (MDT), is noted in the figure. The two columns of numbers at the left show altitude in kilometers (relative to the radar) and electron density in free-electrons per cubic centimeter. The graph then displays electron density vs. altitude on a semi-log scale between  $10^1$  and  $10^4$  electrons/cm<sup>3</sup>. In each case, the result is average density over the run.

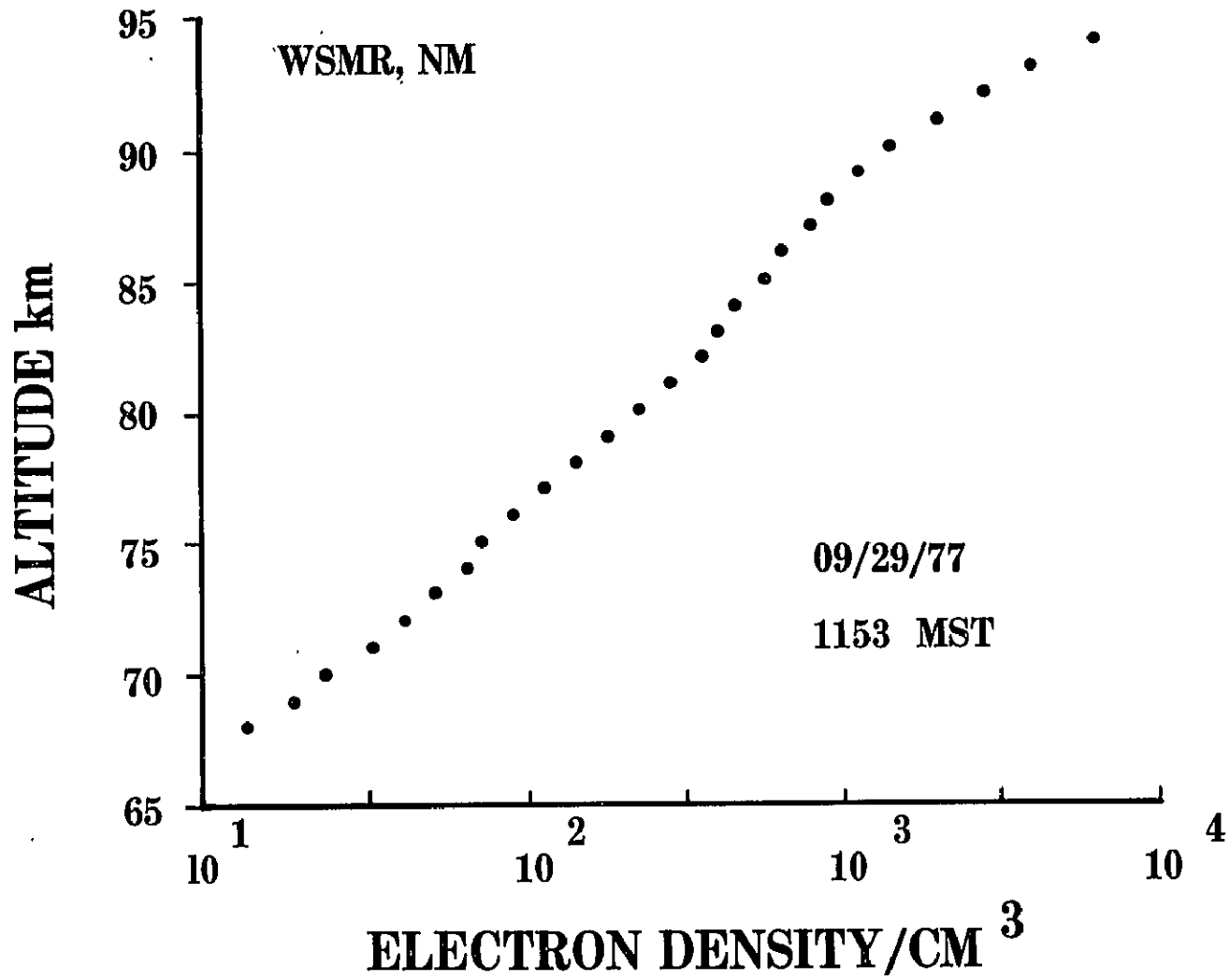
## BALLOON TRANSIT

During the day of 29 September, the balloon passed over the partial-reflection sounder site, providing a unique opportunity for checking our antenna pattern. An observable reflection from the balloon was noted on the radar's A scope from shortly before 1100 MDT until shortly after 1500 MDT. From balloon position data, it was found that, during this period the sub-balloon point moved from approximately 30 km south east of the sounder site to approximately 30 km north west, with the balloon altitude approximately 40 km throughout. (Sounder coordinates are 32°39' north, 106°21' west.) This data verifies the symmetry of our antenna pattern, and indicates that the main, vertical lobe of the antenna array has a cone half-angle of approximately 37 degrees. A theoretical calculation of the antenna pattern places the null-limit of the main lobe at 34 degrees, which agrees favorably with the observation. According to the calculation, the half-power point on the main lobe would occur at a cone half-angle of approximately 15 degrees.









~~D#~~  
D13

ELECTRICAL CONDUCTIVITY MEASUREMENTS FROM THE STRATCOM VIII  
EXPERIMENT

J. D. Mitchell and K. J. Ho, Electrical Engineering Department,  
The University of Texas at El Paso, El Paso, TX 79968  
L. C. Hale and C. L. Croskey, Ionosphere Research Laboratory,  
The Pennsylvania State University, University Park, PA 16802  
R. O. Olsen, Atmospheric Sciences Laboratory, US Army Electronics  
Command, White Sands Missile Range, NM 88002

ABSTRACT

A blunt probe experiment for measuring electrical conductivity was flown with the STRATCOM VIII-a instrument package. Data were obtained by the instrument throughout the entire measurement period (approximately 23 hours). A preliminary analysis of the data indicates an enhancement in conductivity associated with the krypton discharge ionization lamp (1236 Å), particularly in negative conductivity. The conductivity values and their altitude dependence are consistent with previous balloon and rocket results.

INTRODUCTION

The blunt probe is a two-electrode instrument for measuring the polar electrical conductivity of the atmosphere [Hale (1967); Hale, Houtt and Baker (1968); Mitchell (1973)]. When flown with balloon systems, it is preferable to place the probe at a nominal distance from the rest of the package, thereby reducing possible effects other instruments might have on the probe's collection of charged particles. For this particular flight, the instrument was extended horizontally on an arm approximately one meter from the main instrument package. (A picture of the probe configuration is given in Figure 2 of "STRATCOM VIII Scientific Objectives and Mission Organization" [Reed (1977)]).

The electrical conductivity experiments included a blunt probe and a Gerdien condenser mounted parallel to each other with their collectors directed vertically downward. The collection voltage waveform was common to both instruments. Positioned between the two instruments was a krypton discharge ionization lamp (1236 Å) which was cycled on and off such that the probes could measure the enhancements in conductivity associated with the lamp.

Ionization Lamp Off

Ten-minute, time-averaged values of electrical conductivity obtained with the krypton discharge lamp off are shown versus local time (MST) in Figure 1. The plus and minus signs represent positive and negative conductivity values, respectively, and the dots represent time intervals during which no distinct differences were observed between the positive and negative conductivity measurements. The upper curve in the figure shows the balloon's altitude as a function of local time.

The conductivity values measured on this balloon flight are in good agreement with previous balloon [Mitchell, Hale and Groskey (1978); Mitchell and Hale (1976)] and rocket [Cipriano, Hale and Mitchell (1974)] flights. In general, the differences observed between the positive and negative conductivity values for the same altitude are relatively small, and are thought to be associated with differences in the respective ion mobility values.

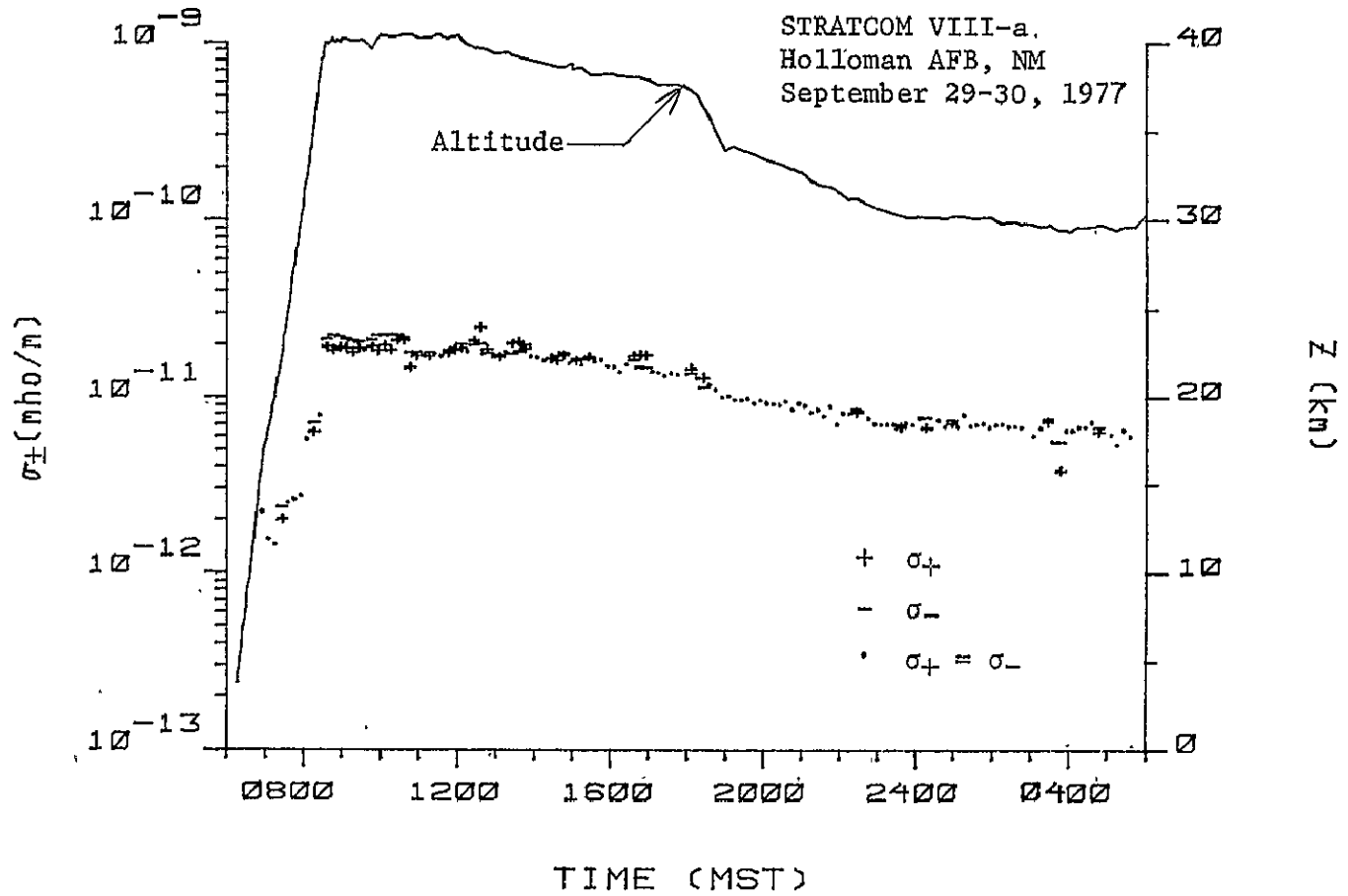
A noticed altitude dependence for electrical conductivity was observed during the complete measurement period of the flight. The altitude dependence in this region typically is inversely proportional to that for neutral number density [Mitchell and Hale (1973)]. This is better demonstrated in Figure 2 where electrical conductivity values for the descent phase of the flight (1200 MST on September 29 to 0400 MST on September 30) are plotted for the balloon's altitude. The notation for the conductivity values in this figure is consistent with Figure 1.

Ionization Lamp On

As discussed previously, a krypton discharge lamp was used as an ionization source with the blunt probe during designated periods of the flight. The enhanced positive and negative conductivity values (averaged over ten-minute intervals) are represented by the x's in Figures 3 and 4, respectively. In addition, the plus signs in Figure 3 and the minus signs in Figure 4 represent the respective positive and negative conductivity values for the lamp off as shown in Figure 1.

The enhanced positive conductivity values are typically a factor of 1.5 to 2.0 larger than the respective conductivity values measured with the lamp off. In contrast, the Gerdien condenser dropsonde (with an ionization lamp) measured considerably larger positive conductivity enhancements during its relatively faster descent [Hale (1978)]. The smaller positive conductivity enhancements measured by the balloon instrument would indicate a flow dependence for the collection of positive ions associated with the lamp.

Excluding the initial ascent, the enhancements in the blunt probe negative conductivity measurements for the lamp on are at



ed electrical conductivity values (lamp off).

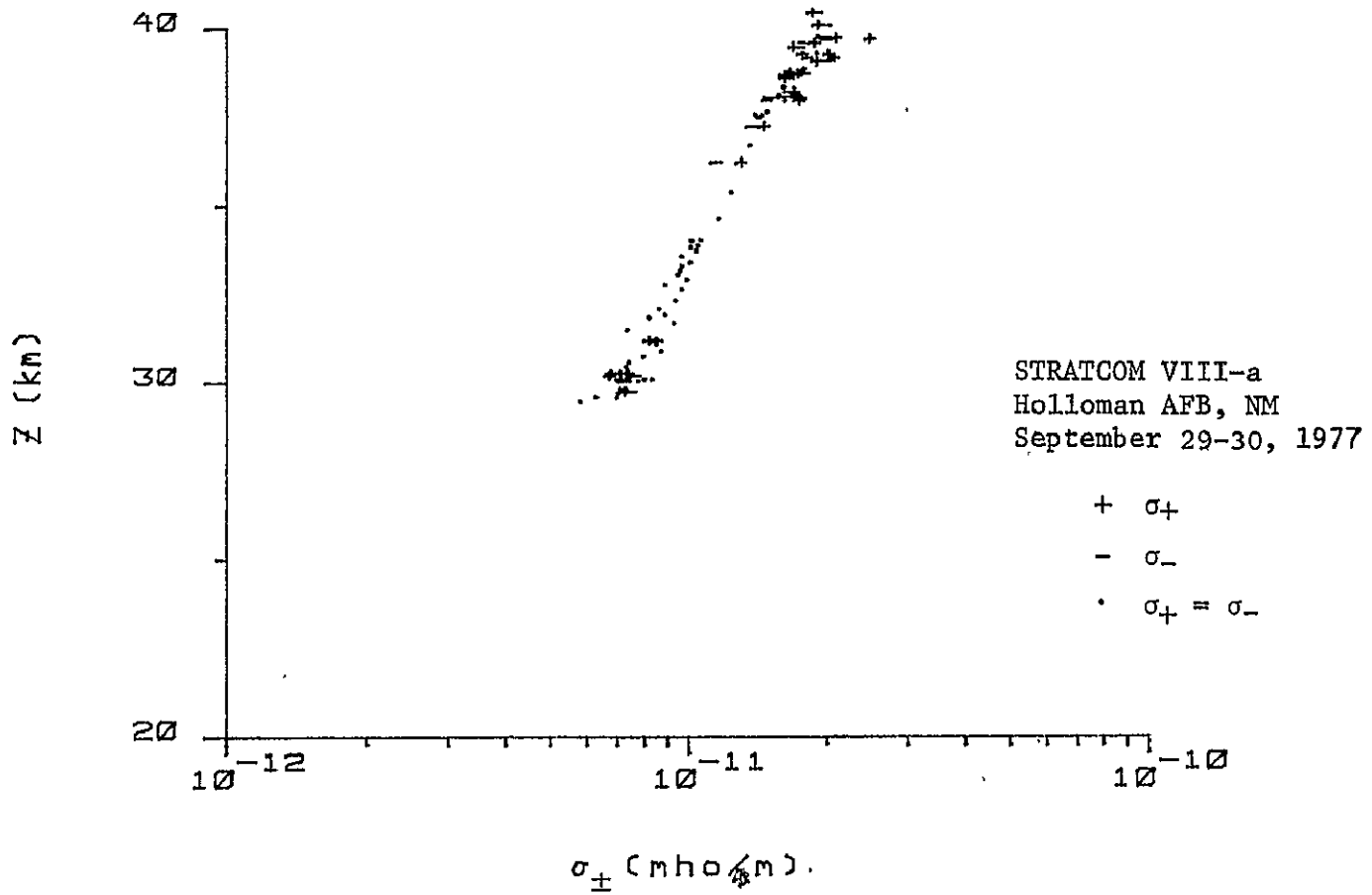
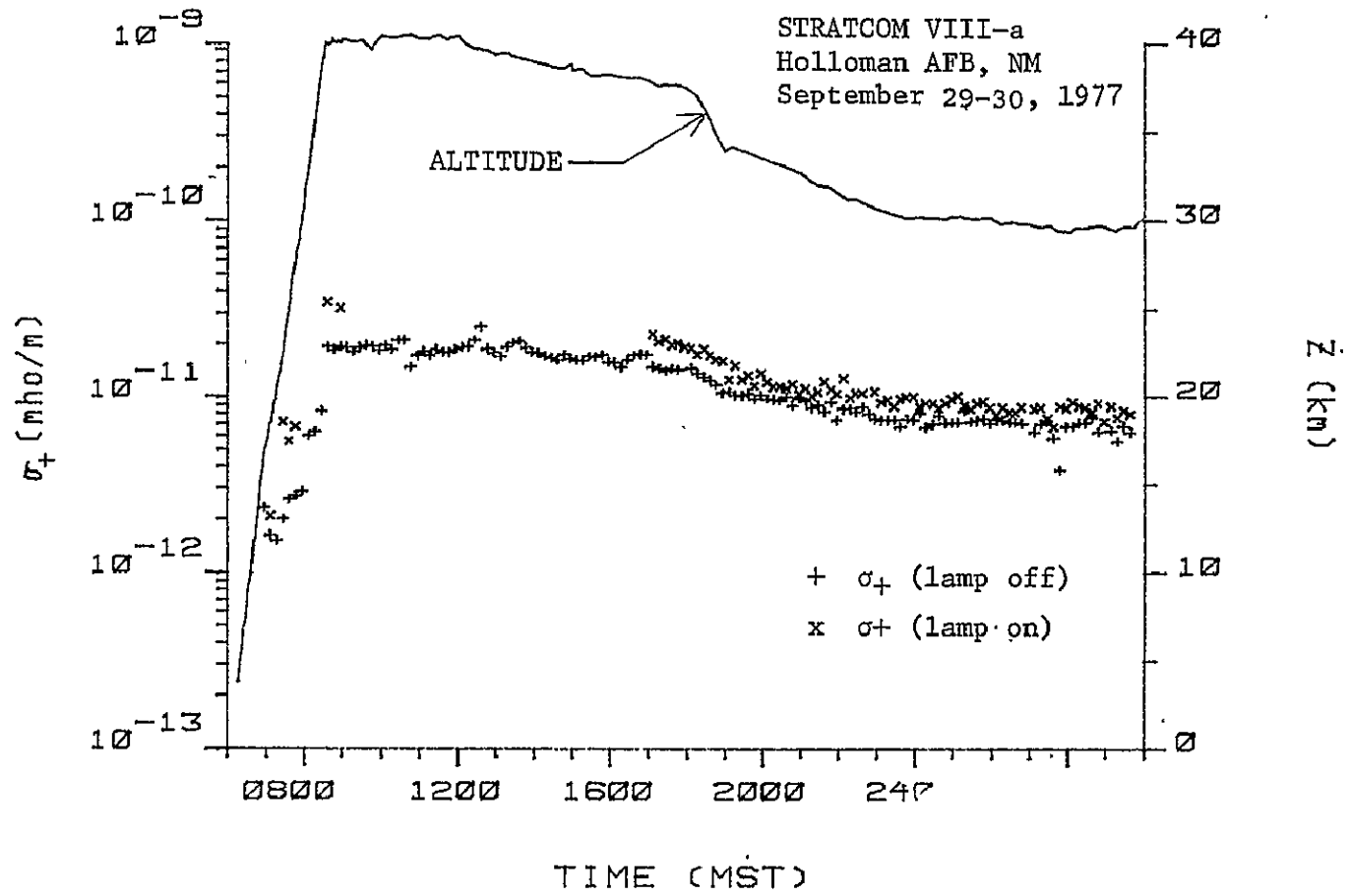


Figure 2. Altitude dependence of electrical conductivity during descent (lamp off).



re 3. Time-averaged positive electr:

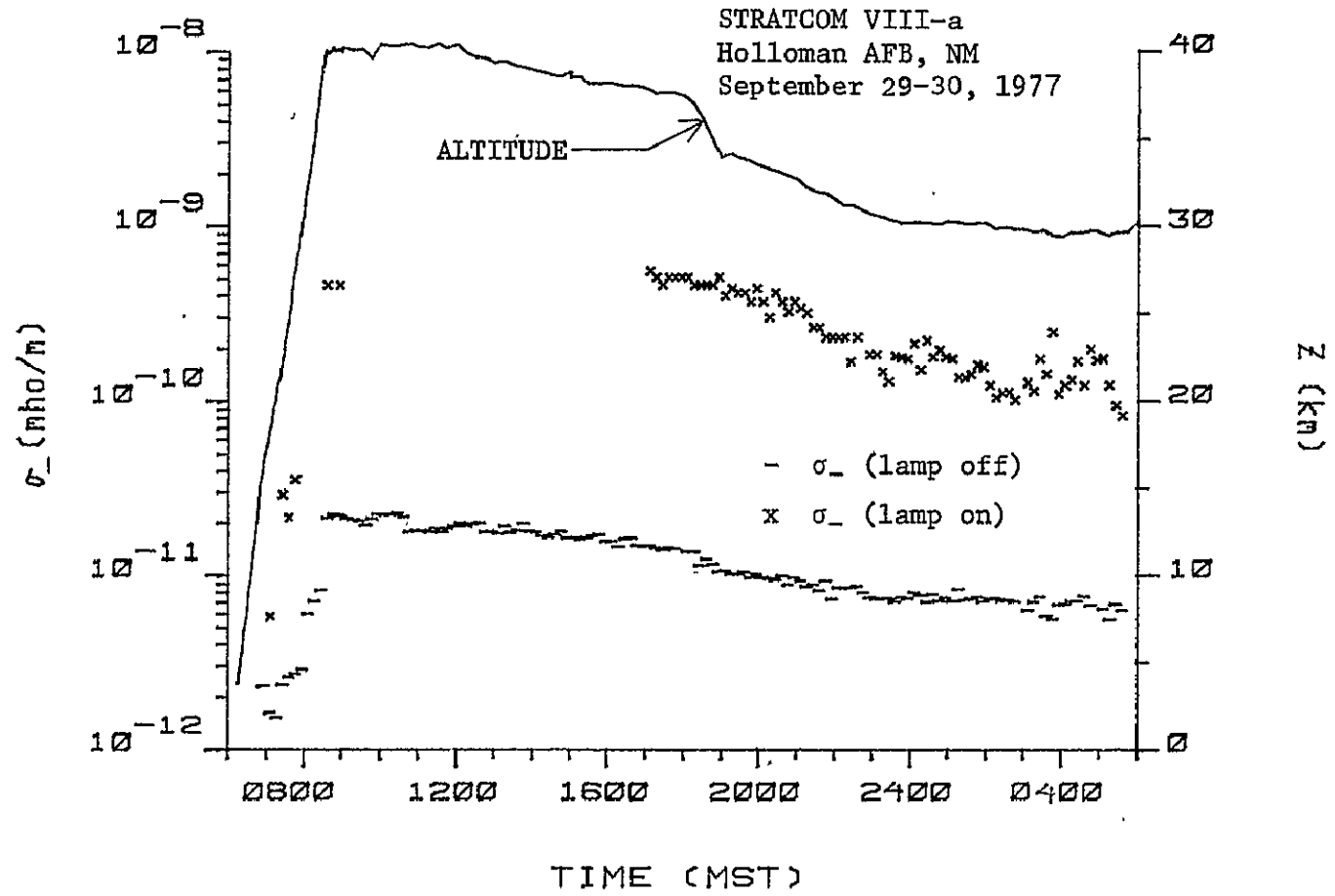


Figure 4. Time-averaged negative electrical conductivity values.



least an order of magnitude larger than the respective values with the lamp off. This would suggest that the negative charge species associated with the krypton lamp are generally more mobile than the positive ions.

#### CONCLUSIONS

A preliminary analysis of the blunt probe electrical conductivity data indicates that the instrument operated successfully throughout the entire measurement period of the flight. Positive and negative conductivity measurements for the same altitude and with the lamp off are generally comparable, and are observed to have an altitude dependence consistent with previous data. Enhancements in both positive and negative conductivity were observed during the times when the krypton discharge lamp was operating. The relatively smaller positive conductivity enhancements would indicate a flow dependence for the collection of positive ions associated with the ionization lamp.

#### REFERENCES

- Cipriano, J. P., L. C. Hale and J. D. Mitchell, *J. Geophys. Res.* 79, 2260-2264 (1974).
- Hale, L. C., Space Research VII, North-Holland, Amsterdam, 140-151 (1967).
- Hale, L. C., Private Communication (1978).
- Hale, L. C., D. P. Hoult and D. C. Baker, Space Research VIII, North-Holland, Amsterdam, 320-331 (1968).
- Mitchell, J. D., Ionosphere Research Laboratory Scientific Report No. 416, The Pennsylvania State University (1973).
- Mitchell, J. D. and L. C. Hale, Space Research XIII, Akademie-Verlag, Berlin, 471-476 (1973).
- Mitchell, J. D. and L. C. Hale, Air Force Geophysics Laboratory Report No. AFGL-TR-76-0306, 425-439 (1976).
- Mitchell, J. D., L. C. Hale and C. L. Croskey, Space Research XVIII, in press.
- Reed, E. I., NASA Goddard Space Flight Center Report No. X-624-77-261, 77 (1977).

## ELECTRICAL STRUCTURE AND IONIZABLE CONSTITUENT MEASUREMENTS

L. C. Hale and C. L. Croskey, Ionosphere Research Laboratory,  
Pennsylvania State University, University Park, PA 16802

## ABSTRACT

In-situ stratospheric ions showed typical characteristics. A Krypton lamp created large numbers of additional ions of remarkably high mobility with a product of number density and ionization cross section of the ionizable constituent(s) ( $N\sigma$ ) greater than  $10^9 \text{ cm}^{-1}$ .

A parachute-borne Gerdien condenser dropsonde was used for measuring the electrical properties of the stratosphere, including polar conductivities and ion mobility and number densities. Both in-situ ions and ions created by a Krypton lamp with a MgF window to ionize low IP species were analyzed. The total lamp output was about  $4 \times 10^{13}$  photons/sec. in a  $38^\circ$  beam. (Ref. October 1977 Stratcom VIII Document and PSU-IRL Scientific Report No 442, 1976).

The conductivities are shown in the first figure, both with and without the lamp on. The Stratcom VIII conductivities in the stratosphere are similar to what has been observed previously with rocket deployed payloads, but of course do not show the unusual variability observed above 42 km between 18 JAN '76 (an "anomalous" winter day) and 23 JAN '76 (a "normal" winter day) at Wallops Flight Center. The stratospheric "in-situ" conductivities show the normal exponential altitude dependence. The enhancement produced by the lamp in the positive conductivities below 40 km. is quite large, much greater than expected. (The negative lamp-on data is very much more difficult to analyze because of the creation of large numbers of free electrons by the lamp, and is not included here.)

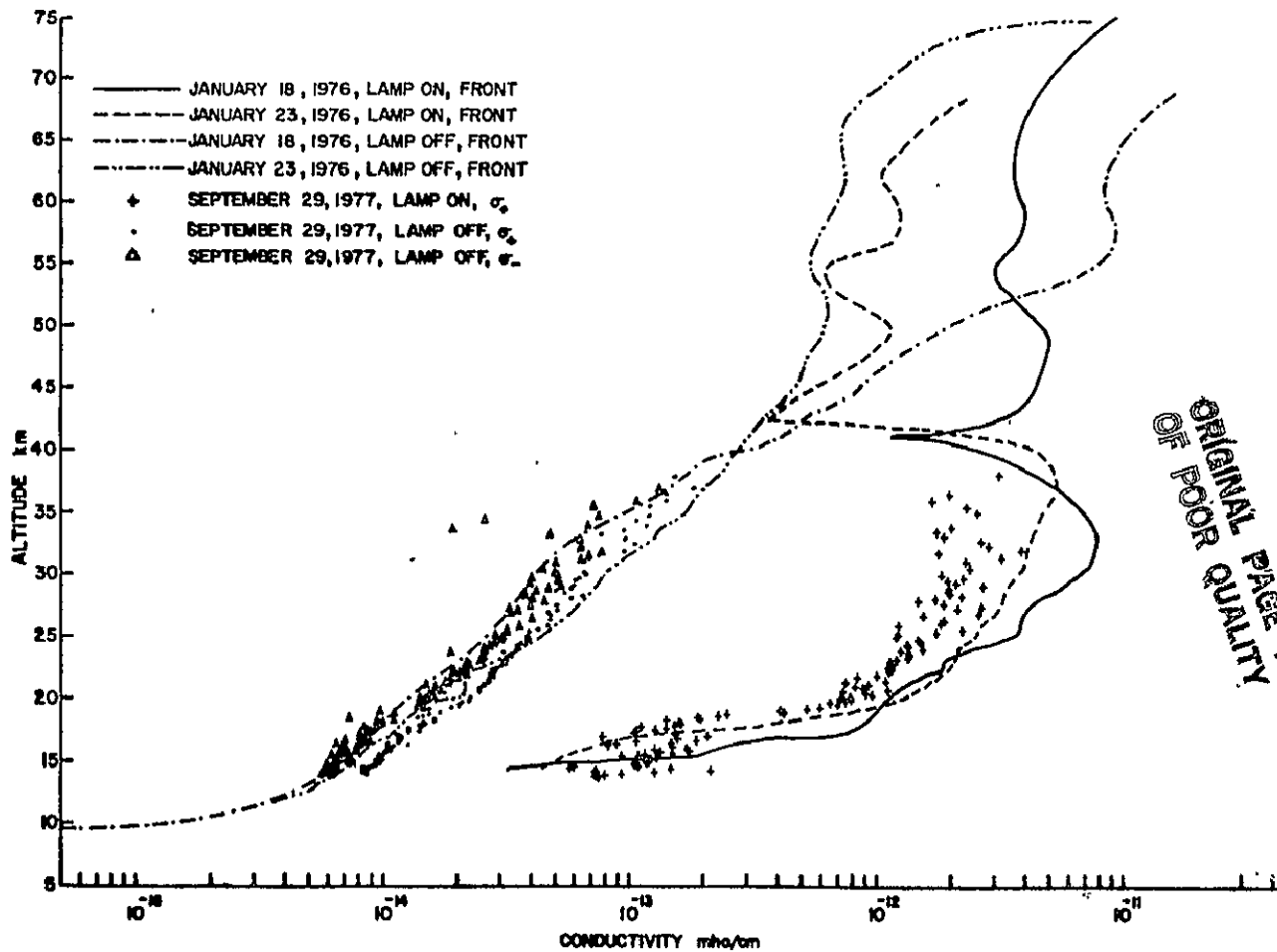
Wind tunnel tests of this type of instrument conducted at the von Karman Institute for Fluid Dynamics showed a positive conductivity increase due to NO and not to other tunnel air constituents or photoelectron effects. The dropsonde data indicate that the product of ionizable constituent density and ionization cross section is of order  $2 \times 10^9 \text{ cm}^{-1}$ . If interpreted as NO density, this yields  $10^9 \text{ cm}^{-3}$ , which is probably too high. From this (and the mobility data, see below) we conclude that large quantities of a low ionization potential constituent exist in the stratosphere that do not

occur in (fairly dirty) tropospheric air. This constituent is unknown, but tentative possibilities are addressed below.

The data on the in-situ ions are not remarkable, except perhaps that the principal negative and positive ions seem to have precisely the same mobility over the entire stratosphere. A narrow layer of higher mobility positive and negative ions appears below 20 km. An analysis of the number densities and mobilities of ions created by the lamp shows that the ions created by the lamp are of very much higher mobility than the in-situ ions. Apparently three mobility groups are formed, all with mobilities at least one order of magnitude greater than the in-situ ions and approximately in the ratio of  $2/3:1:3/2$ . These mobilities are so high that we are forced to consider the following possibilities:

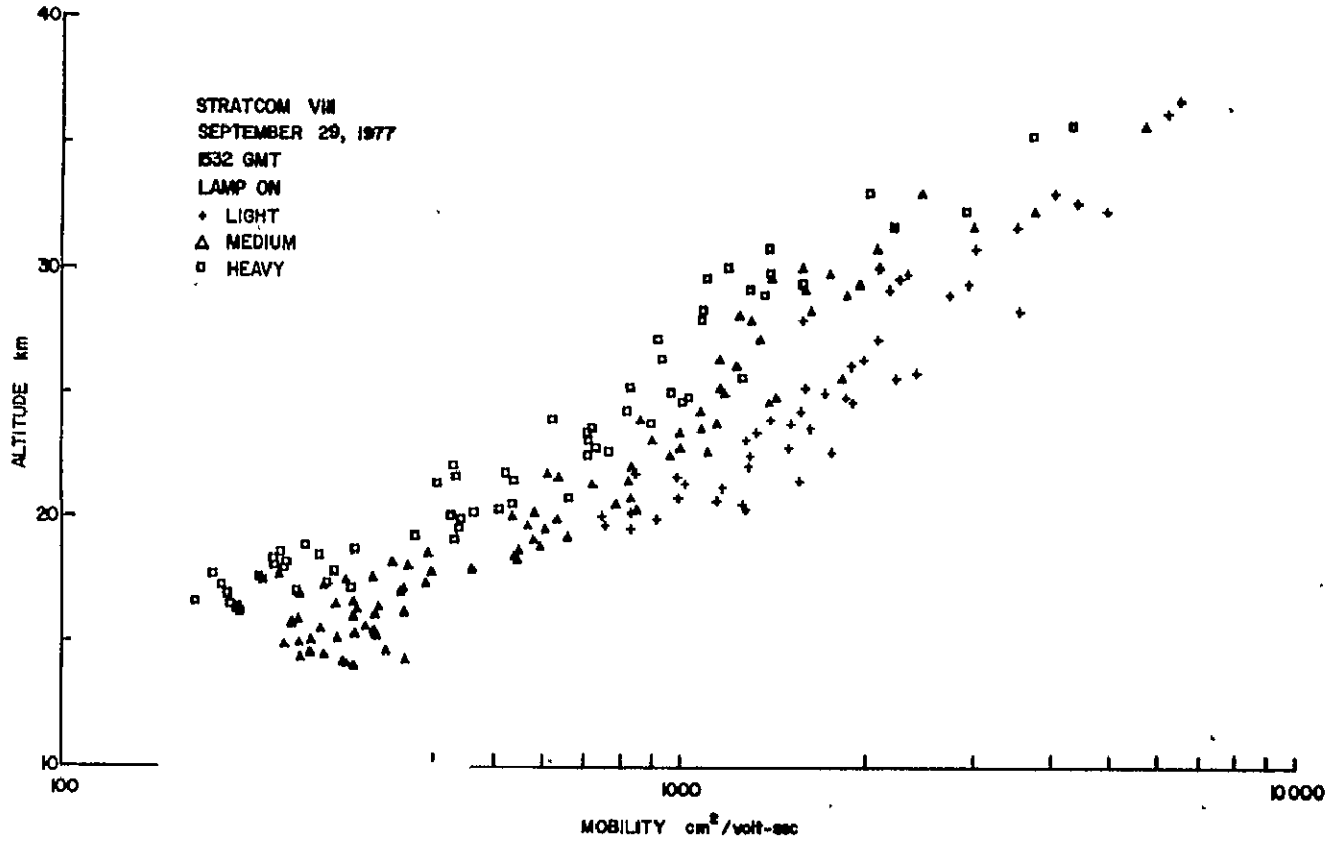
- 1) The particles are effectively much smaller than ordinary molecules.
- 2) They are multiply charged.

Alternative (1) requires the presence of three groups of positive particles with mobilities greater than protons, which is outside the realm of ordinary chemical constituents. (2) requires that many electrons be emitted in a single photon interaction, which is perhaps possible with a tenuous particulate which is demolished by the interaction, leaving a multiply charged nucleus.

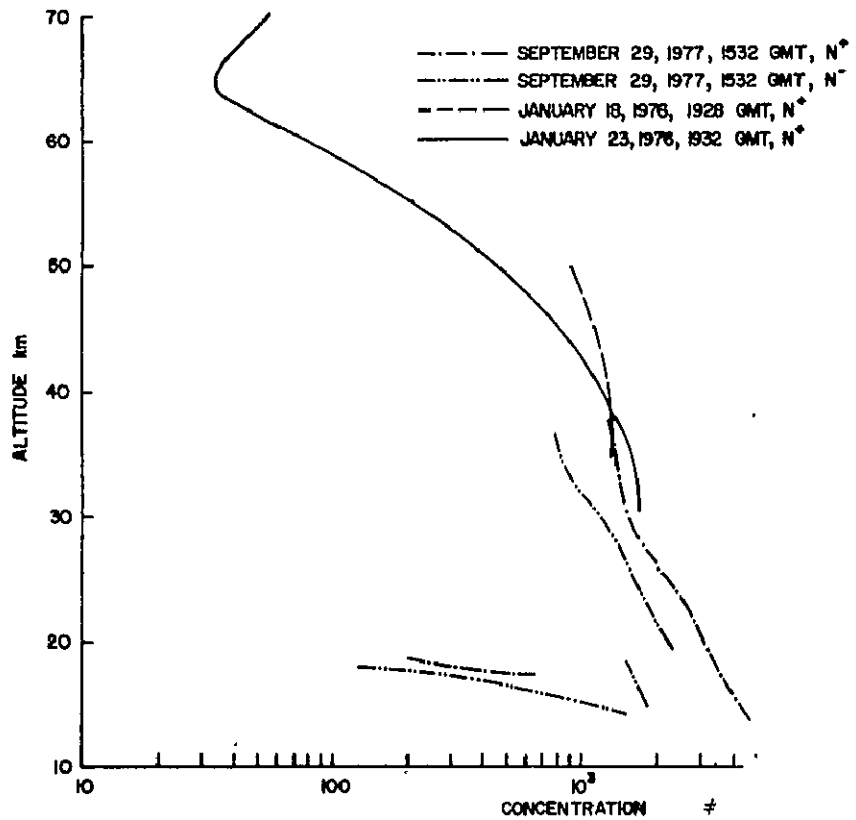


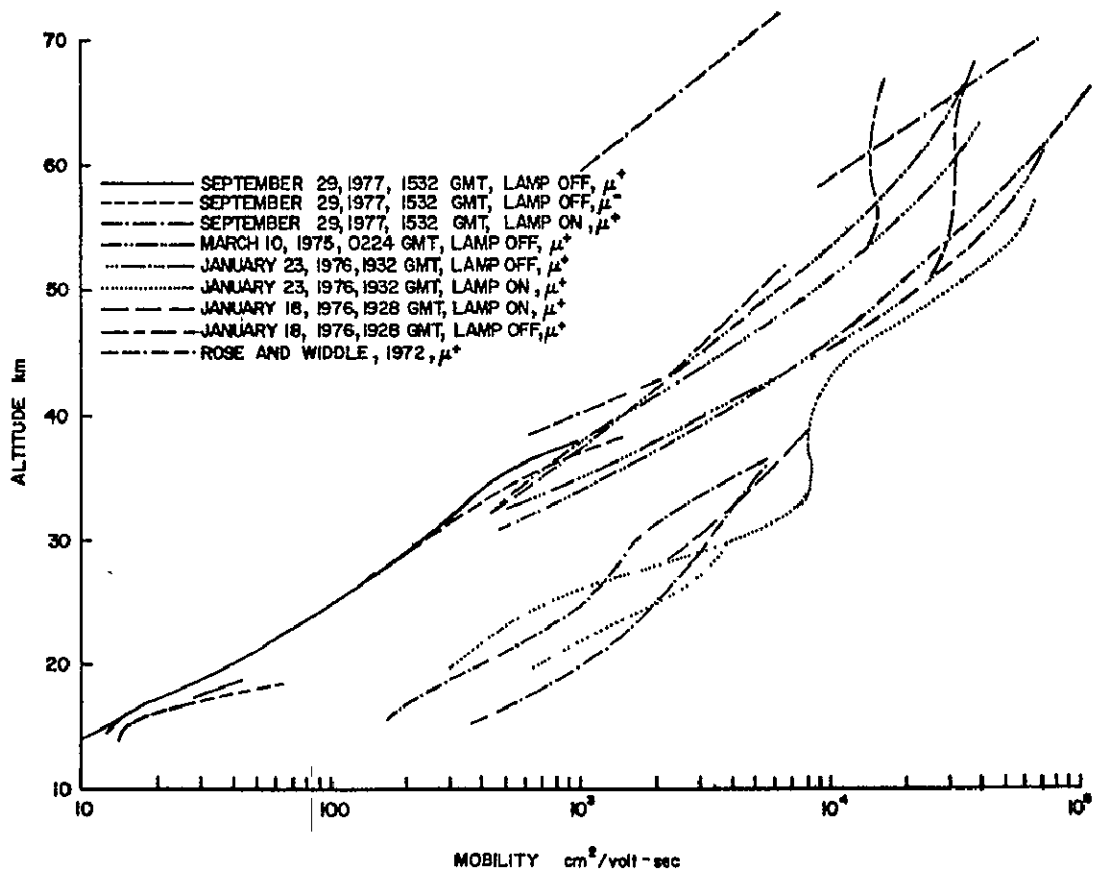
ORIGINAL PAGE IS  
OF POOR QUALITY

ORIGINAL PAGE IS  
OF POOR QUALITY



ORIGINAL PAGE IS  
OF POOR QUALITY





ORIGINAL PAGE IS  
OF POOR QUALITY

# BIBLIOGRAPHIC DATA SHEET

1. Report No.	2. Government Accession No.	3. Recipient's Catalog No.	
4. Title and Subtitle STRATCOM-VIII DATA WORKSHOP April 13-14, 1978		5. Report Date April 1978	
		6. Performing Organization Code	
7. Author(s) Edith I. Reed (compiler)		8. Performing Organization Report No. n/a	
9. Performing Organization Name and Address Stratosphere Physics and Chemistry Branch NASA/Goddard Space Flight Center Greenbelt, Maryland 20771		10. Work Unit No.	
		11. Contract or Grant No. n/a	
12. Sponsoring Agency Name and Address  Same as 9		13. Type of Report and Period Covered Conference Publication	
		14. Sponsoring Agency Code	
15. Supplementary Notes			
16. Abstract  The STRATCOM-VIII effort took place at Holloman Air Force Base and White Sands Missile Range, New Mexico, on September 28-30, 1977. The prime emphasis was on the study of stratospheric photochemistry involving ozone, with secondary objectives including a study of the balloon environment, comparison of independent techniques for the measurement of O <sub>3</sub> and NO, and the development of new sensor systems. More than forty sensors were included on the two large balloons, a U-2 aircraft, and several rockets and small balloons, in addition to meteorological balloons and rockets. Most of the systems performed as expected. This report consists of material available at a Data Workshop held April 13-14, 1978, and serves both to distribute information among the experimenters and to give some indication as to the extent to which the original objectives can be realized.			
17. Key Words (Selected by Author(s)) Stratcom, scientific balloons, stratosphere, ozone, nitrogen oxides, water vapor, conductivity, aerosols, ultraviolet spectrometry, infrared spectrometry, cryogenic sampler, chemiluminescent detector		18. Distribution Statement	
19. Security Classif. (of this report) Unclassified	20. Security Classif. (of this page) Unclassified	21. No. of Pages	22. Price*